SwRI 03.10415

2007 DIESEL PARTICULATE MEASUREMENT RESEARCH

Prepared by

Imad A. Khalek, Ph.D.

Final Report
Project E-66-Phase 1

Prepared for

Coordinating Research Council
3650 Mansell Road, Suite 140
Alpharetta, GA 30022

May 2005

SOUTHWEST RESEARCH INSTITUTE®
P.O. Drawer 28510 6220 Culebra Road
San Antonio, Texas 78228-0510

2007 DIESEL PARTICULATE MEASUREMENT RESEARCH

Prepared by

Imad A. Khalek, Ph.D.

Final Report
Project E-66-Phase 1

Prepared for

Coordinating Research Council
3650 Mansell Road, Suite 140
Alpharetta, GA 30022

May 2005

Prepared by:

Imad A. Khalek, Project Leader

Approved:

Daniel W. Stewart,
Director of Research

Reviewed by:

Terry L. Ullman,
Assistant Director of Research

DEPARTMENT OF ENGINE AND EMISSIONS RESEARCH
ENGINE, EMISSIONS AND VEHICLE RESEARCH DIVISION

FOREWORD

This work was funded by the Coordinating Research Council (CRC), Department of Energy National Renewable Energy Laboratory (DOE/NREL), Environmental Protection Agency (EPA), Engine Manufacturers Association (EMA), and California Air Resources Board (CARB). The SwRI Principal Investigator and Project Manager was Dr. Imad Khalek, Principal Engineer. Technical staff members who contributed to this work were Mr. Kevin Hohn, Technician, Mr. Richard Cortez, Laboratory Assistant, Mr. Joe Sosa, Senior Technician, Mr. Robert West and Mr. Daryl Krenmueller, Staff Technicians, Ms. Kathy Jack, Research Assistant, Mr. Keith Echtle, Laboratory Supervisor, and Mr. Ernest Kruger, Laboratory Assistant Manager.

Mr. Brent Bailey from CRC was the Project Manager representing the sponsors. This work was initiated and reviewed by the E-66 Panel members who are listed below in alphabetical order:

Mr. Adewale Aoshinuga Aoshinuga, SCAQMD
Dr. Ewa Bardasz, Lubrizol
Dr. Nick Barsic, John Deere
Mr. Mike Bogdanoff, SCAQMD
Dr. Steve Cadle, General Motors
Dr. Bruce Cantrell, EPA
Mr. King Eng, Shell Global Solution (U.S.), Inc.
Mr. Tim French, EMA
Mr. Rob Graze, Caterpillar
Dr. Doug Lawson, NREL
Mr. Hector Maldonado, CARB
Dr. Matti Maricq, Ford
Dr. Mani Natarajan, Marathon Ashland Petroleum Co.
Dr. Shirish Shimpi, Cummins, Inc.
Mr. Matt Spears, EPA
Mr. Joe Sucheki, EMA
Mr. Bill Trestrail, Navistar-International
Mr. Ken Wright, ConcoPhillips

ACKNOWLEDGMENTS

SwRI would like to recognize DOE/NREL additional funding in support of Task 1 of Project E-66. SwRI would also like to recognize EPA additional funding in support of Task 1 and for providing the Sunset Laboratory OC/EC instrument and the humidity sensor. SwRI thanks Lubrizol for providing the engine oil and ConcoPhillips, ExxonMobil, and British Petroleum for fuel chemical analysis.

SwRI thanks TSI, Dekati and Mr. Ville Niemela from Dekati for his extended stay at SwRI, Sensors, and Horiba for their support in providing the EEPS, DMM-230, QCM, and the MEXA 1370-PM, respectively. SwRI would also like to thank Donaldson for providing the Teflon filters with Teflon rings.

EXECUTIVE SUMMARY

This report covers work under Phase 1 of Project E-66. The objectives of Phase 1 of Project E-66 are to:

- Minimize volatile and semi-volatile gas phase adsorption, onto the filter used for particulate matter (PM) collection during PM sampling from a dilute diesel exhaust stream, by using a carbon denuder,
- Investigate the effect of filter media on PM emissions,
- Investigate the effect of filter face velocity on PM emissions,
- Investigate the performance of different particle measurement instruments such as the engine exhaust particle sizer (EEPS), scanning mobility particle sizer (SMPS), Dekati mass monitor (DMM-230), and the quartz crystal microbalance (QCM) relative to the filter-based method that meets the 2007 PM sampling protocol.

All work was performed using a 1998 DDC Series 60, heavy-duty diesel engine equipped with a continuously regenerative technology diesel particulate filter (CRT-DPF), with and without a partial exhaust bypass. The fuel was an ultra low sulfur fuel that meets 2006 specifications. The fuel sulfur level was 7 ppm. The engine oil was a 15W-40 viscosity grade with low sulfated ash, phosphorous, and sulfur. The PM sampling methodology utilized the EPA 2007 sampling protocol.

The carbon denuder developed in this project did not yield consistent performance in removing gas phase semi-volatile compounds from upstream of the filter used for PM collection. The performance of the denuder continued to deteriorate even after regeneration using inert gas such as helium or nitrogen at 400 °C. The use of the carbon denuder was abandoned early in this program. Future work will require more detailed development and characterization of the carbon denuder before it can be used in a sampling train for PM measurement.

The Whatmann Teflo filter media, a Teflon membrane with a Polymethypentene ring, gave the lowest positive artifact mass and the lowest coefficient of variation in comparison to TX-40 and other Teflon membrane filters. As a result of these experiments, the use of the Teflo filter was recommended for future measurements of PM. The Donaldson Teflon membrane filter with a Teflon ring gave similar and acceptable performance to that of the Teflo, but was not as easy to handle due to its tendency to curl. This filter may be useful for chemical analysis due to its inert nature (all Teflon); however, work is needed to investigate whether or not such a filter can be used for solvent extraction of the soluble organic fraction (SOF) or other methods to support PM characterization.

Changes in filter face velocity showed a significant influence on PM emission measurement. At a filter face velocity of 120 cm/sec, the PM emission was about 25 percent lower than at a filter face velocity of 24 cm/sec for the federal test procedure (FTP) transient cycle. For light load engine operation, the filter face velocity affected measured PM in a similar manner to that observed for the FTP transient cycle, but the reduction in measured PM emission when the filter face velocity was changed from 60 cm/sec to 120 cm/sec was more than 60 percent. Gas phase adsorption on the filter and filter saturation may be responsible for such changes. To minimize such variations, it is recommended that the acceptable range for filter face velocity be narrowed to 90 cm/sec ± 10 cm/sec rather than the current acceptance of filter face velocity of below 100 cm/sec.

The DMM-230 and the EEPS data correlated well with the filter-based method; having a linear correlation coefficient, R^2, of better than 0.95. This correlation was only demonstrated for a PM emission level at 70 percent of the 2007 PM standard using a diesel engine equipped with a CRT-DPF with a bypass around it. It is not clear whether or not the same correlation will hold using a CRT-DPF without a bypass, where the PM emission is expected to be at 5 to 10 percent of the 2007 PM standard, and be dominated by only volatile and semi-volatile material. The DMM-230 and EEPS have an advantage over the filter-based method because of their high sensitivity to low particle concentration and their real-time particle measurement capability. It is recommended that these two instruments be used for the remainder of Project E-66.

Due to improved particle measurement, capability to measure very low brake-specific PM mass emission rates, below 0.001 g/hp-hr or 10 percent of the 2007 PM standard, were demonstrated in this program using a CRT-DPF. In order to perform testing at a PM emission level near the 2007 standard, a partial exhaust ceramic honeycomb bypass around the CRT-DPF was used to increase the PM emissions to 0.007 g/hp-hr or 70 percent of the 2007 PM standard. The CRT-DPF with bypass or less efficient DPF may be used to adjust engine emissions to near the 2007 PM standard. Such an exhaust configuration may help lower engine back pressure and frequent DPF regeneration that may result in better DPF durability and improved fuel economy.

Phase 1 of Project E-66 was successful in meeting most of the objectives. Future tasks will include investigating the influence of primary and secondary dilution ratio and residence time, and engine and dilution tunnel conditioning on PM measurement. It will also include investigating the performance of partial flow sampling system relative to the CVS method. It may also include PM measurements for a natural gas engine and possibly a gasoline engine. Although gasoline PM measurement is not officially part of the E-66 current scope, it is important to verify that the measurement process is satisfactory for other internal combustion engine PM sources.

Building on the completed work, the planned work in this program is expected to lead to improved PM emission measurements and characterization of particles from different engine sources that exist today as well as in the future.

TABLE OF CONTENTS

LIST OF FIGURES

LIST OF TABLES

1.0 BACKGROUND

The Environmental Protection Agency (EPA) defines diesel exhaust particulate matter (PM) as the material that collects on a filter in a stream of exhaust that is cooled and diluted to a temperature of less than 52 °C. Gravimetric filter analysis, following EPA definition of PM collection specified in 40 CFR, Part 86, has been the basis for determining PM emissions from heavy-duty diesel (HDD) engines for certification and other research and testing activities targeting the quantification of PM mass emitted from engines for the purpose of engine, fuel, oil, and instrument development and research.

Although PM emissions from on-highway HDD engines were reduced by more than 83 percent, from 0.6 g/hp-hr in 1988 to 0.1 g/hp-hr in 1998, the current EPA definition and procedures for PM collection were sufficiently manageable to produce repeatable results. For engines at or near the 0.1 g/hp-hr level, the PM composition is generally dominated by solid particles that are not strongly affected by changes of the dilution parameters such as dilution ratio, dilution temperature, residence time, in addition to other phenomenon such as gas phase adsorption of filter media, and other factors.

In 2007, however, on-highway heavy-duty diesel engines are required to meet a PM emission level of 0.01 g/hp-hr, a 90 percent reduction from the current emission level. In addition, the exhaust PM composition is expected to change because most engines will require catalyzed particulate filters to meet the stringent standard. PM composition is expected to mainly consist of volatile and semi-volatile hydrocarbon and sulfate derived from unburned and partially burned fuel and lubricating oil. This low level of volatile PM mass poses a technical challenge for the accurate mass measurement of PM using the current sampling protocol, particularly relative to lab-to-lab variability. Measuring a low quantity of PM mass deposited on a filter is a major challenge, but several other factors including filter handling, filter media, artifact, sampling system conditioning, and good monitoring of the dilution parameters also affect the measurement significantly.

Recognizing some of the PM measurement challenges for 2007, EPA adjusted the definition of PM by narrowing the filter face temperature from below 52 °C to a range between 42 °C and 52 °C (47 °C ± 5 °C). EPA also implemented several changes to the secondary dilution tunnel of the constant volume sampler (CVS) as well as to the filter media, filter handling, and weighing chamber in order to improve the quantification of PM mass emissions from engines that meet the 2007 standards [1].

Although the new PM measurement procedures, specified by EPA for 2007 were demonstrated by EPA to achieve less than a 10 percent Coefficient of Variance (COV) at the 0.004 g/hp-hr [2], recent preliminary data produced by SwRI for EPA, using the 2007 procedures, gave a COV of 23 percent for four hot-start FTP transient tests at the 0.0034 g/hp-hr level. Although difference in the COV between SwRI and EPA may not be comparable due to differences in the sampling methodology, background particulate level, and the difference in engine and aftertreatment systems used, it is useful to demonstrate the level of variability that can be in PM measurement expected for engines equipped with traps.

While the new 2007 sampling methodology is expected to improve the quantification of PM mass and reduce variability in comparison to the current sampling methodology, several factors of the 2007 sampling methodology are still loosely defined and it is not clear how these factors will influence the results of PM mass measurement. For example, EPA does not specify secondary dilution tunnel geometry and residence time. It allows for a wide range of filter face velocities and does not give a detailed descriptive requirement on how the 47 °C ± 5 °C filter face temperature should be achieved. It does not address any issues relative to combining primary dilution ratio and secondary dilution ratio. The 2007 procedures allow more than one filter media to be used and accept a wide equilibration time ranging from 30 minutes to 60 hours. It also allows the use of a HEPA filter in the primary tunnel with a maximum penetration of 0.02 or lower but it specifies a much more stringent filter penetration factor of the secondary air with a penetration factor of 0.0003, a two order of magnitude difference than the penetration for the primary tunnel filter.

In light of these new changes in PM regulations and procedures, Project E-66, titled, "2007 Diesel Particulate Measurement Research," was initiated by the CRC Real World Vehicle Emissions and Modeling Committee to investigate different factors that may affect and help improve future PM measurement.

2.0 INTRODUCTION

Project No. E-66 focuses on four main objectives. Objective 1 is to improve particulate matter (PM) emissions measurement from low emitting diesel engines that meet the 2007 EPA standard of 0.01g/hp-hr. Objective 2 is to investigate and identify a potential real time PM method that may serve as an alternative to the currently prescribed filter-based method. Objective 3 is to investigate and improve the correlation between PM measured using partial flow sampling systems and the full flow constant volume sampler (CVS). Objective 4 is to develop and implement a quality assurance quality control QA/QC plan for this work, and to provide a QA/QC plan that defines QA procedures to support the 2007 PM measurement method.

SwRI has developed an approach that uses eleven Tasks with two Subtasks to address Project E-66 objectives in a technically sound and efficient manner. A summary of each Task is listed below. The work covered in this report covers Phase 1 of Project E-66 that included Tasks 1, 2, 3, and 4, and other support tasks whenever applicable. The remainder of the Tasks has not yet started and will be covered in future reports.

Task 1 was to design, build, and characterize a ceramic honeycomb substrate denuder coated with a carbon sieve for removal of semi-volatile hydrocarbon. The carbon denuder was used to study the influence of gas phase semi-volatile organics on PM collection during sampling.

The objective of SwRI Task 2 is to investigate five different filter media using a heavy-duty diesel (HDD) engine that meets the EPA 2007 PM standard. Filter media, depending on their characteristics, may lead to PM measurement artifact due to its ability to adsorb or desorb gas phase species, particularly hydrocarbons. The aim of this work was to identify a filter media that minimizes gas phase adsorption (positive artifact) and desorption of volatile droplets or particle bound volatile material (negative artifact), for use during the rest of this program.

SwRI Task 3 addressed the effect of filter face velocity and filter loading on PM collection. This information was crucial in identifying whether there is a linear relationship between the increase in filter face velocity and the PM loaded on a filter.

Task 4 addressed the use of different real time PM sampling instruments, including the TSI scanning mobility particle sizer (SMPS), TSI engine exhaust particle sizer (EEPS), Dekati Mass Monitor (DMM-230), and the Sensors quartz crystal microbalance (QCM), aimed at establishing either an alternative or a surrogate method for the filter-based method. The technique that best correlates with the filter method will be utilized for further study on this program. This task also included filter-based measurement using a filter face temperature of 47°C ± 5°C in parallel to a filter face temperature of 25°C ± 5°C to provide information for comparison of ambient PM measurement to EPA prescribed PM measurement.

The successful accomplishment of Task 4 in identifying a real time PM mass measurement method will provide the means, as part of Task 5, to study the effect of a wide range of dilution parameters, such as CVS primary dilution ratio, secondary dilution ratio, and residence time, on PM mass measurement.

After finishing with Task 5, Task 6 will include variation in engine and CVS dilution conditioning operations to study their impact on PM measurement.

Task 7 will include two subtasks. Subtask 7.1 will address the effect of dilution geometry on PM measurement using five commercially available partial flow sampling systems provided by Horiba, AVL, Sierra, Sensors, and Cummins. Each partial flow sampling system will sample PM from the full flow CVS, operated as an individual secondary dilution tunnel, in parallel to the EPA-defined secondary tunnel of the CVS. The PM measurements will be taken by all systems using a set of comparable dilution parameters, such as dilution ratio, residence, filter face temperature, and filter face velocity. Ideally, the only difference will be the mixing, or dilution geometry.

Subtask 7.2 will compare the performance of the partial flow sampling systems with the full-flow CVS, using the wealth of information gained from previous work and tasks performed on this program, to optimize variables associated with the partial flow sampling systems to improve the correlation between the full-flow CVS and partial flow systems.

Task 8 will compare results from the real time PM measurement technique selected in Task 4 with the filter method, using a natural gas engine. Such information should be useful in determining whether the instrument of choice is only applicable to diesel engine or it can be applied to different engine technologies.

Task 9 is a support task for the entire project designated for chemical analysis of gas phase material that may interfere with PM mass measurement. It is assumed that the E-66 Work Group will participate in deciding when and what additional chemical analyses are needed.

Task 10 is another support task of the entire project dedicated to quality assurance and quality control (QA/QC). SwRI will use their existing structure for QA/QC and extend it to cover some of the new activities to be performed on this program. SwRI will also provide a standard operating procedure (SOP) for PM collection experiments under the constraint of the 2007 PM sampling procedures. It was agreed that SwRI will propose a QA/QC implementation plan prior to performing a specific task.

Task 11 will be dedicated for the final report. A draft final report will be submitted to CRC. After review by CRC, appropriate changes will be made and a final report will be submitted.

3.0 EXPERIMENTAL SETUP

This section covers the experimental setup applicable to Tasks 1, 2, 3, and 4.

3.1 Engine

The engine used in this program, shown in Figure 1 and described in Table 1, was a 1998 DDC Series 60, turbo-charged, heavy-duty on-highway diesel engine. The engine is owned by SwRI and has more than 1500 hours of operation on various projects prior to using it in Project E-66. The engine exhaust was equipped with a CRT diesel particulate filter (CRT-DPF) and a ceramic honeycomb (600 cells per square inch) bypass.

For Task 1, the engine was used with the CRT-DPF without an exhaust bypass. For Tasks 2, 3, and 4, the bypass was necessary to increase the PM emission from below 10 percent (without a bypass) to about 70 percent (with bypass) of the 2007 PM standard, during a hot-start FTP transient cycle. It was decided that a PM emission level at 70 percent of 2007 PM standard may be representative of what the emission level might be in 2007 and beyond.

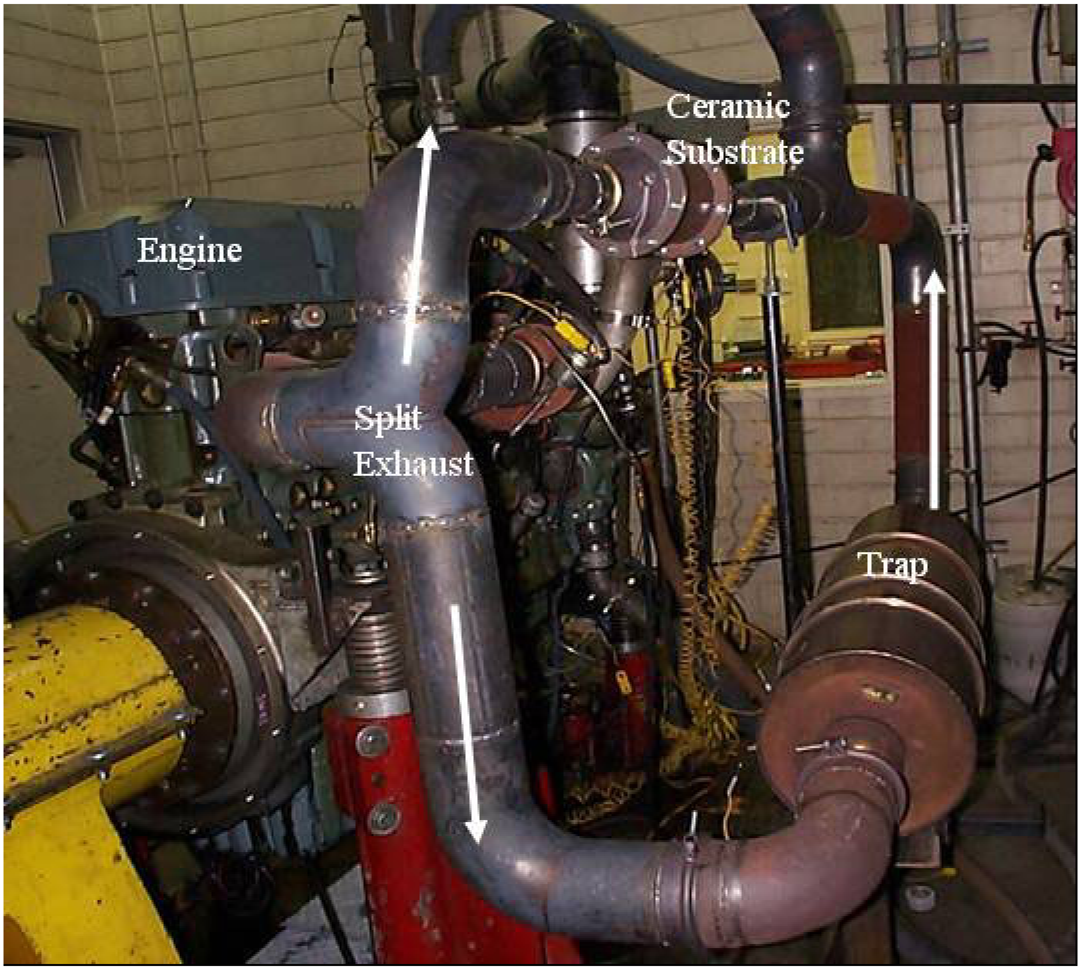

FIGURE 1. ENGINE EXHAUST CONFIGURATION WITH A CERAMIC SUBSTRATE BYPASS

TABLE 1 ENGINE IDENTIFICATION INFORMATION

Item	Description	Value
1	Engine Serial Number	06R0422316
2	Engine Model	6067TK60
3	Engine Family	Series 60
4	Model Year Designation	1998
5	Type of Electronic Control Module (ECM)	DDEC-III
6	EPA Certification Number	874
7	Power Rating	400 hp at 1,810 rpm
8	Torque Rating	1,550 lb-ft at 1200 rpm
9	Injection System	Electronically Controlled Unit Injectors
10	Induction System	Turbocharged-Waste Gated-Aftercooled

3.2 Diesel Particulate Filter (DPF)

The CRT-DPF is made by Johnson Matthey. It was acquired from Johnson Matthey on an EPA sponsored project. The CRT-DPF was used previously on three different EPA projects at SwRI using the 1998 DDC Series 60 used in Project E-66. The CRT-DPF experienced more than 250 hours of engine operation prior to using it in Project E-66.

The CRT-DPF consists of a platinum loaded ceramic honeycomb substrate (oxidation catalyst) followed by a bare ceramic substrate wall-flow particle filter. The purpose of the catalyst is to facilitate trap regeneration at low temperature. The catalyst oxidizes NO typically present in diesel engine exhaust to NO_2. NO_2 is more reactive than oxygen and helps oxidize soot on the surface of the soot filter at a relatively low temperature of about 300 °C, compared to an oxidation temperature of about 550 °C to 650 °C with oxygen and non-catalyzed DPF.

3.3 Fuel and Oil

The fuel used in this program was an ultra low sulfur diesel (ULSD) with selected properties shown in Table 2. This fuel was a refinery fuel that was supplied by Sinclair. This ULSD fuel meets EPA 2006 fuel specifications that require a sulfur level of less than 15 ppm. The fuel sulfur level was 7 ppm with a Cetane number of 45. The boiling point profile and the carbon number distribution are also shown in Figures 2 and 3, respectively.

The engine oil was 15W-40 viscosity grade, supplied by Lubrizol. It was chosen to closely resemble what is expected for 2007 engines. The oil contained 1 percent of sulfated ash, 0.1 percent of phosphorus, and 0.4 percent of sulfur.

TABLE 2. FUEL PROPERTIES

Property	ASTM	
API Gravity (60F)	D287	34.5
Cetane number	D613	45.4
Distillation IBP, F	D86	382
10% recovery, F	D86	441
50% recovery, F	D86	511
90% recovery, F	D86	608
FBP	D86	654
Cloud point, F	D2500	2.3
Pour point, F	D97	-27
Flash point, PMCC, C	D93	80
Sulfur, ppm	D5453	6.9
Aromatics	D5186	
1 Ring Aromatics, wt%		23.8
2 Ring Aromatics, wt%		9.8
3+ Ring Aromatics, wt%		2.2
Total Aromatics		35.8
Non-aromatics, wt. %		64.2

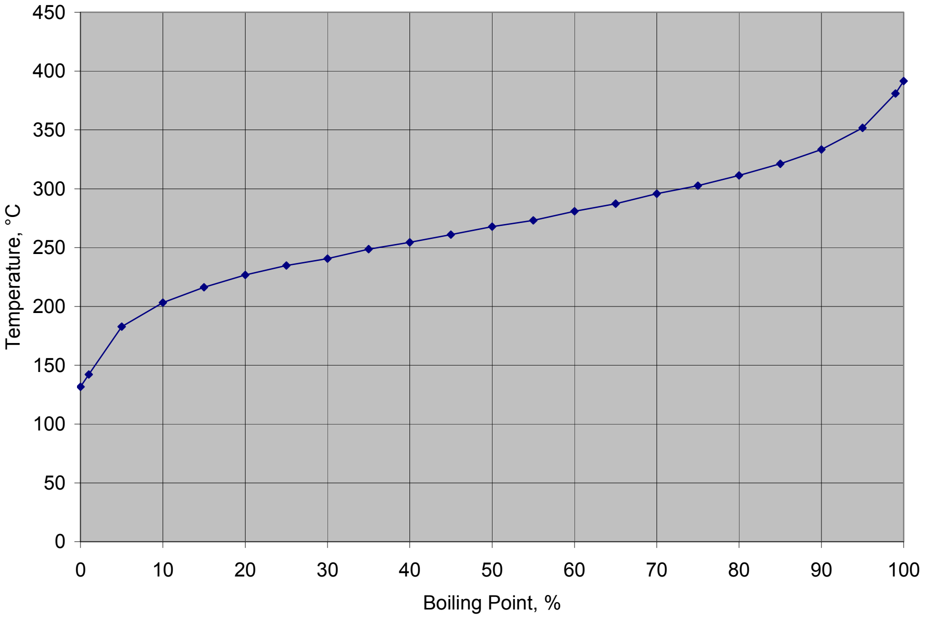

FIGURE 2. FUEL BOILING POINT TEMPERATURE PROFILE

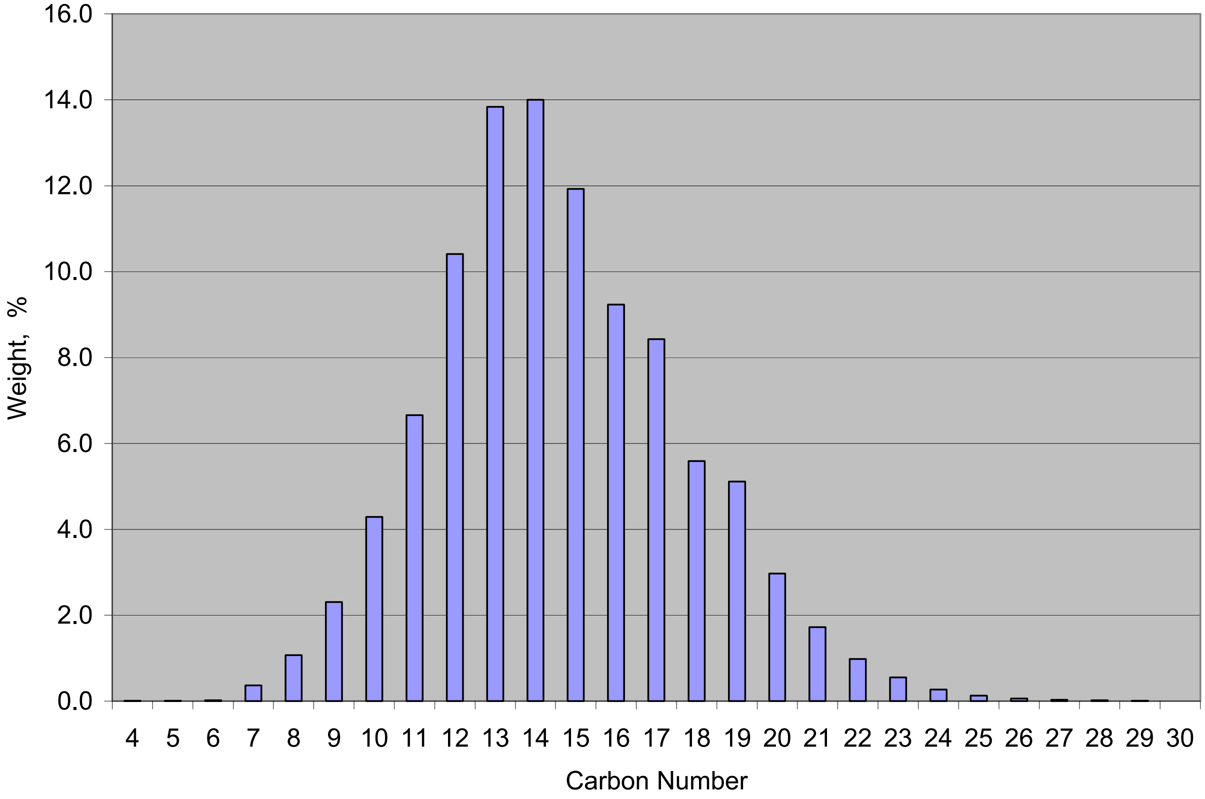

FIGURE 3. FUEL CARBON NUMBER DISTRIBUTION

3.4 Carbon Denuder Development

This section describes the development of a carbon denuder for semi-volatile gas phase adsorption.

3.4.1 Carbon Molecular Sieve

SwRI received the carbon molecular sieve, Carboxen-1000, from Supleco. This material was recommended for the honeycomb ceramic substrate denuder coating due to its high surface area of 1200 m²/g. SwRI performed scanning electron microscopy (SEM) and energy dispersive spectroscopy analysis on the Carboxen-1000, as received. Figures 4 and 5 show the size and chemical analysis of the Carboxen 1000, as received. The original shape of the Carboxen-1000 consisted of uniform spheres, 250 μm in diameter. They were mainly composed of sulfur and carbon with a small quantity of aluminum and oxygen, likely in the form of aluminum oxide.

The original Carboxen-1000 spheres were milled down to a size of about 2 μm. This size was recommended to achieve smooth coating of the denuder. Figures 6 and 7 are similar to Figures 4 and 5, but they were taken after the milling process was completed. The final size was close to 2 μm in diameter and no contamination was recognized after milling, as observed in Figure 5.

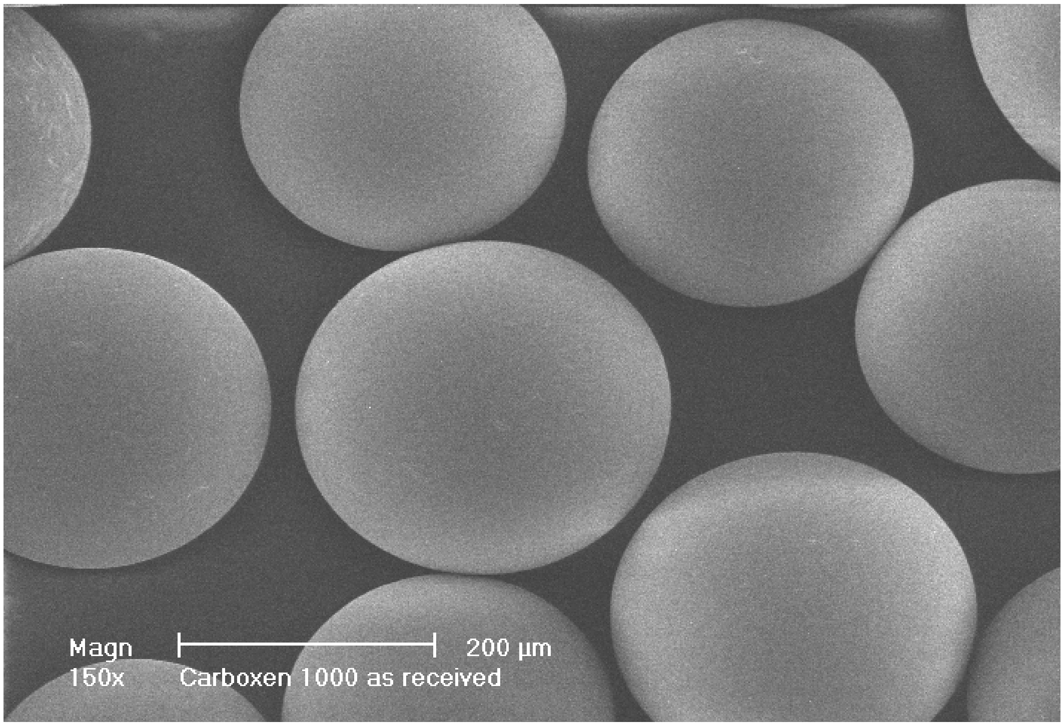

FIGURE 4. SCANNING ELECTRON MICROSCOPE IMAGING OF CARBOXEN-1000 AS RECEIVED

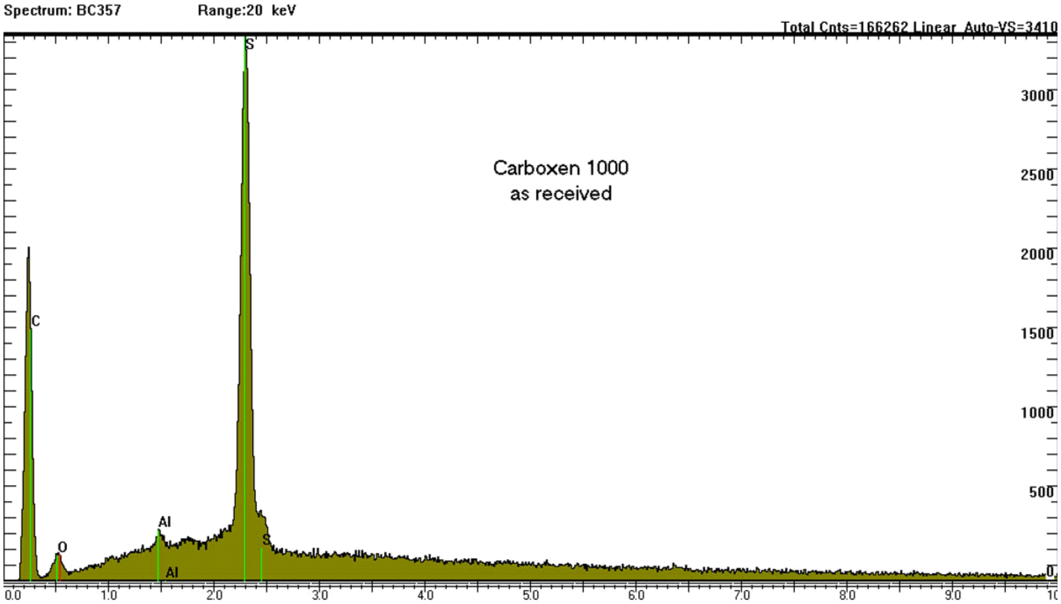

FIGURE 5. CHEMICAL COMPOSITION OF CARBOXEN-1000 AS RECEIVED

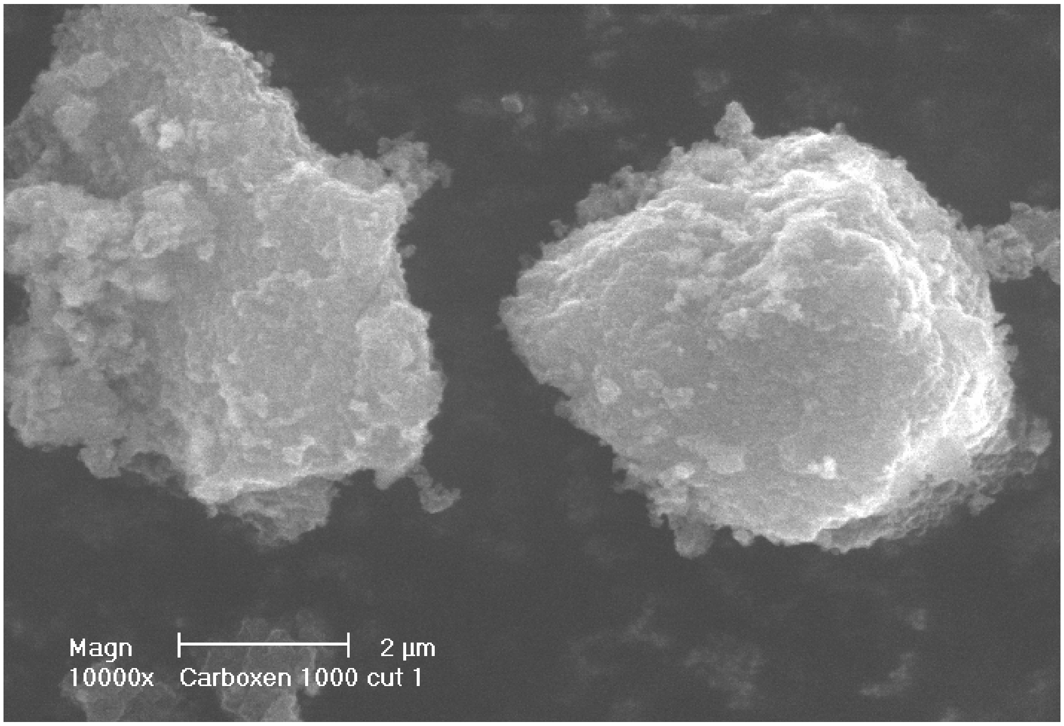

FIGURE 6. SCANNING ELECTRON MICROSCOPE IMAGE OF CARBOXEN-1000 AFTER MILLING

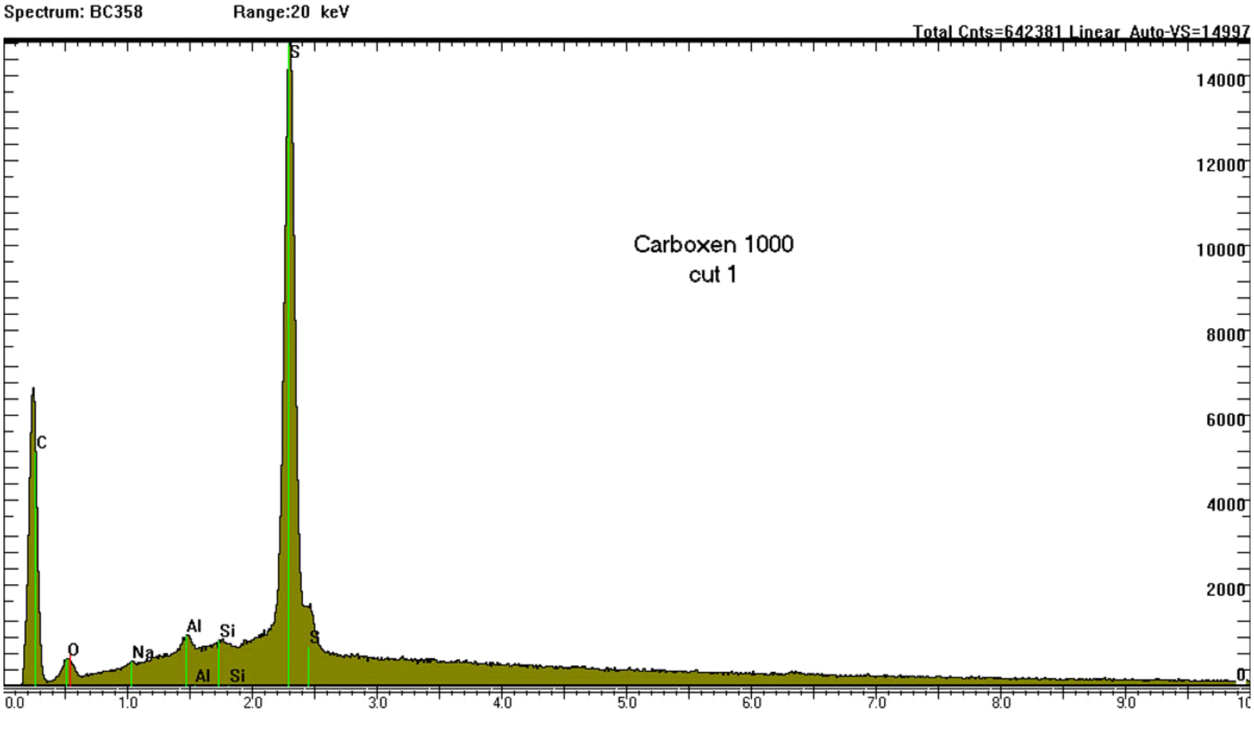

FIGURE 7. CHEMICAL ANALYSIS OF CARBOXEN-1000 AFTER MILLING

Unfortunately, during the first trial of the milling process, the yield was very small, on the order of 25 percent. This means that only 25 percent of the original mass of the Carboxen-1000 was recovered after milling due to losses to internal surfaces of the milling machine. The recoverable quantity was not sufficient for denuder coating and more Carboxen-1000 was needed to be milled. Because the milling machine was coated during the first milling process, a higher yield of about 80 percent was achieved during the second round of milling.

A Corning honeycomb ceramic substrate with a cell density of 62 cells per square centimeter and cell thickness of 165 µm was sized to give a high efficiency for diffusing semivolatile compounds to the internal surfaces of the substrate square channels and low efficiency for diffusing particles. Details on the final size of the ceramic substrate are given in Table 3. The flow rate chosen for the analysis represented the expected flow rate through the denuder during engine testing. Figures 8 through 10 show the diffusion efficiency of different size molecules ranging from CH_4 to $C_{40}H_{82}$. Based on the theory, it was expected that more than 75 percent of the heaviest molecule used, namely the $C_{40}H_{82}$, would interact with the substrate wall.

TABLE 3. CARBON DENUDER CERAMIC SUBSTRATE

Material:	Ceramic Monolith
Geometry:	Square Channels
Overall Length, cm	9.3
Overall Diameter, cm	8.6
Cell Density, number of cells per cm²	62.0
Square Channel Wall Thickness, cm	0.0165
Square Channel Length, cm	9.3
Square Channel Open Width or Height, cm	0.096

Figures 11 through 13 show the particle losses at different flow rates. Generally, more than 30 percent of particles in the sub-0.01 size range were lost by diffusion. In the size range between 0.01 µm and 0.04 µm, particle loss ranged from 30 percent to less than 5 percent. In the size range between 0.04 µm and 1 µm, particle loss ranged from 5 percent to 1 percent. For particles between 1 µm and 10 µm, particle loss was between 1 percent and 70 percent. The high losses for particles above 1 µm was due to sedimentation.

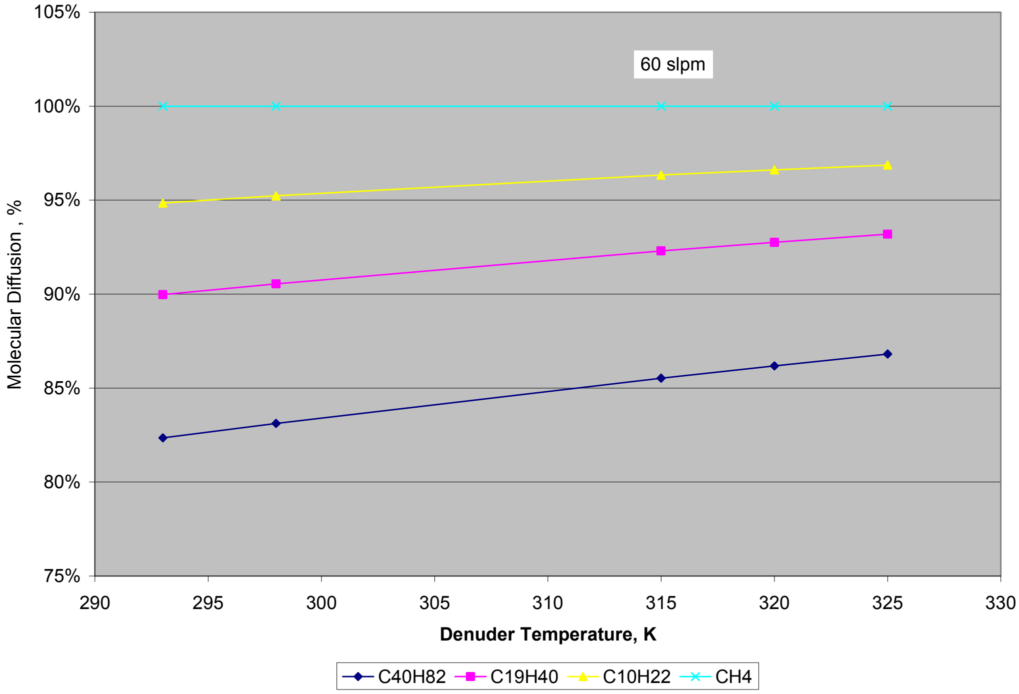

FIGURE 8. MOLECULAR DIFFUSION IN DENUDER AT 60 SLPM

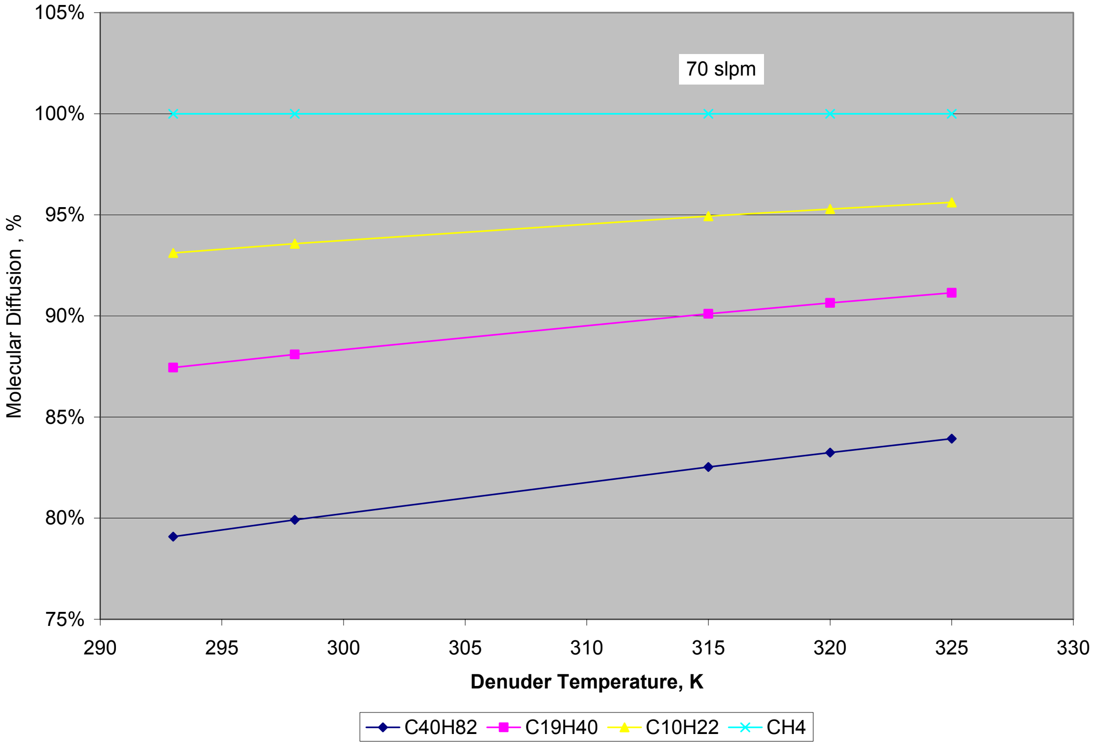

FIGURE 9. MOLECULAR DIFFUSION IN DENUDER AT 70 SLPM

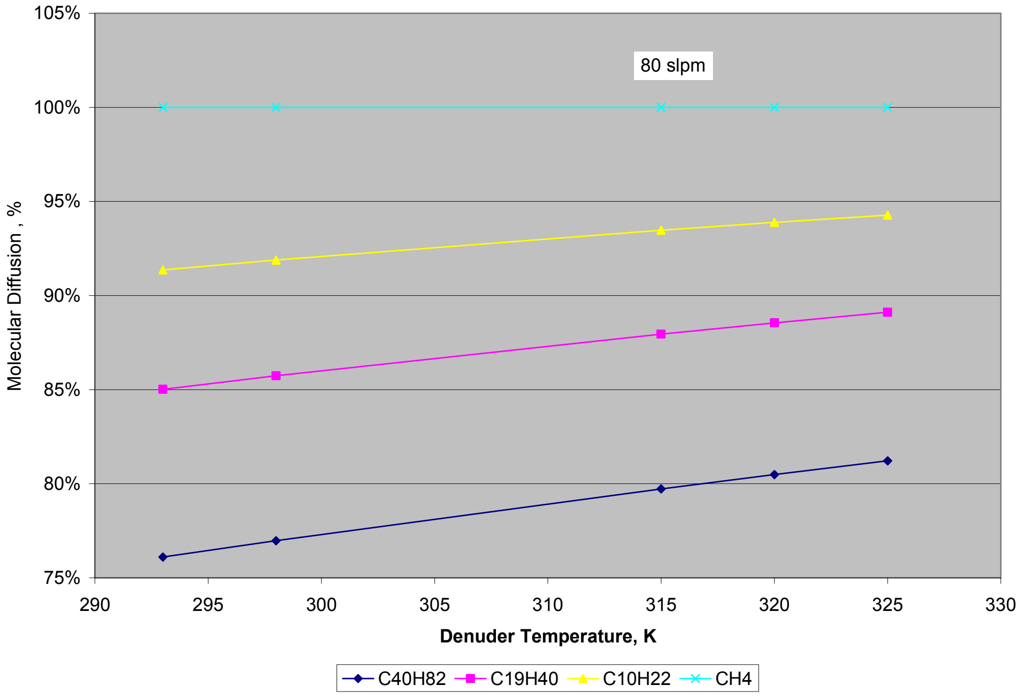

FIGURE 10. MOLECULAR DIFFUSION IN DENUDER AT 80 SLPM

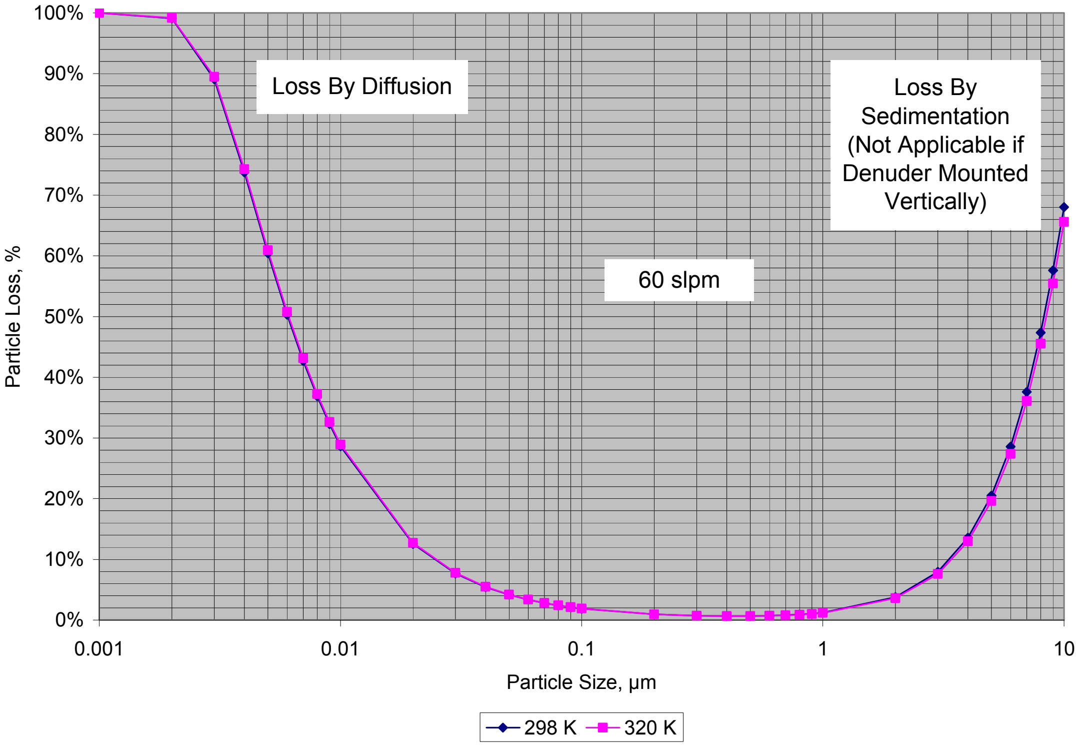

FIGURE 11. PARTICLE LOSSES IN DENUDER AT 60 SLPM

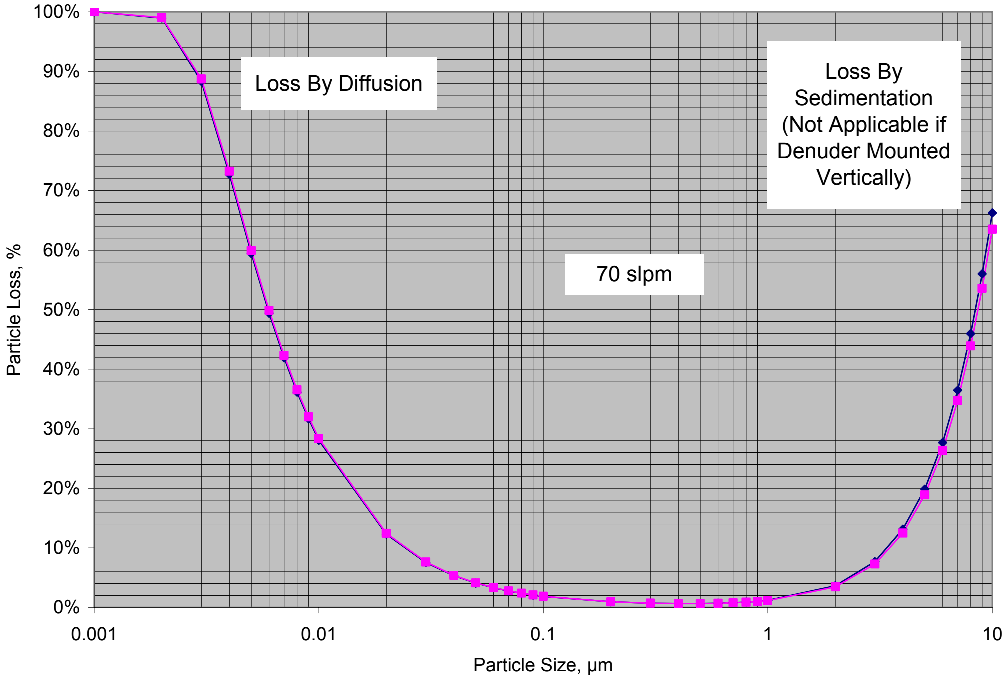

FIGURE 12. PARTICLE LOSSES IN DENUDER AT 70 SLPM

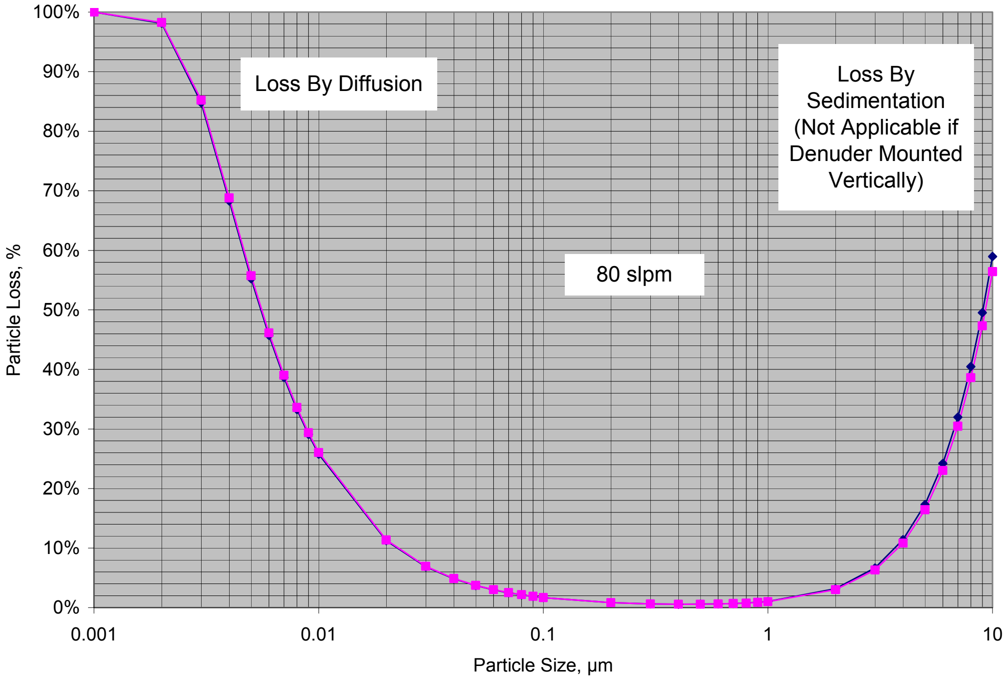

FIGURE 13. PARTICLE LOSSES IN DENUDER AT 80 SLPM

3.4.2 Carbon Denuder Coating

Two honeycomb ceramic substrates were coated with carbon molecular sieve at SwRI. The coating mixture consisted of 40 grams of milled carbon molecular sieve, 60 grams of pentane, 70 grams of methanol, and 360 grams of methylene chloride. A bonding reagent that consisted of 83.2 grams of triethoxysilane and 24 grams of dimethyldimethoxysilane, two highly toxic compounds, and 18 grams of acidified water was also added to the original mixture to form the coating slurry.

The bonding reagent was prepared separately before it was mixed with the rest of the mixture. The 18 grams of water were acidified to a pH level of 1, using hydrogen chloride (HCl). The bonding reagent was supposed to react exothermically when water is added and stay in a liquid phase. However, due to the high water acidity, the bonding reagent went from a liquid phase to a solid phase, shown in Figure 14, as the acidified water was added. Later, it was discovered that only 60 percent of the acidified water was needed in order for the bonding reagent to stay in a liquid phase. When all components of the slurry were mixed together, the slurry was put in a beaker and was continuously stirred for good mixing, as shown in Figure 15.

FIGURE 14. SOLIDIFICATION OF BONDING REAGENT

FIGURE 15. CARBON COATING SLURRY IN BEAKER

Safety measures such as wearing gloves and using a hood in a well ventilated area were practiced during the preparation of the slurry and coating of the ceramic substrate.

The ceramic substrate was dipped and removed from the beaker many times, as shown in Figure 16, for a period of two hours before the coating was complete. It was discovered that dipping the substrate into the slurry, removing it to dry, then dipping it again, achieved much better results than repeatedly dipping and removing the substrate while still wet.

The final coated ceramic substrates, known as carbon denuders, are shown in Figure 17.

FIGURE 16. CERAMIC SUBSTRATE COATING PROCESS

FIGURE 17. COATED HONEYCOMB CERAMIC SUBSTRATE (CARBON DENUDER)

3.4.3 Carbon Denuder Assembly

Carbon Denuder

The carbon denuder was wrapped with a 0.32 cm thick heat-expandable ceramic mat (Unifrax, 3M) and tightly fitted inside stainless steel housing, shown in Figure 18. The whole carbon denuder assembly was put in a 400°C oven for four hours to expand the mat to adhere to the external surface of the denuder and to the internal surface of the housing to provide a proper seal and fix the denuder inside the housing. One thermocouple was installed in the denuder housing to measure the surface temperature of the denuder and another thermocouple was mounted to measure the exit temperature of the flow stream.

A conical inlet and outlet with a 12.5° angle was adapted to the carbon denuder assembly, shown in Figure 19, to provide an undisturbed entry and exit from the denuder and prevent flow circulation that may lead to particle deposition. The entire denuder assembly is shown in Figure 20.

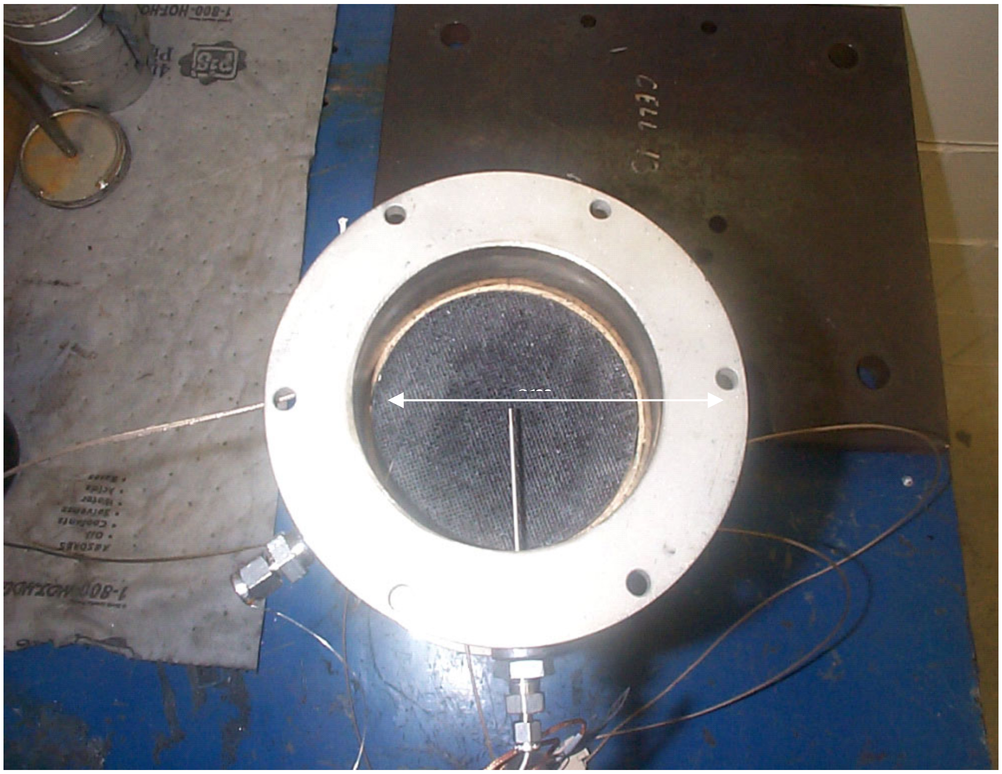

FIGURE 18. CARBON DENUDER AND HOUSING

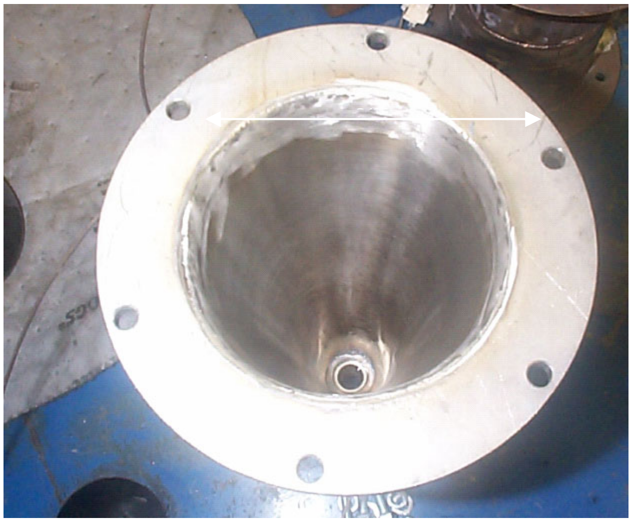

FIGURE 19. INLET AND OUTLET CONE

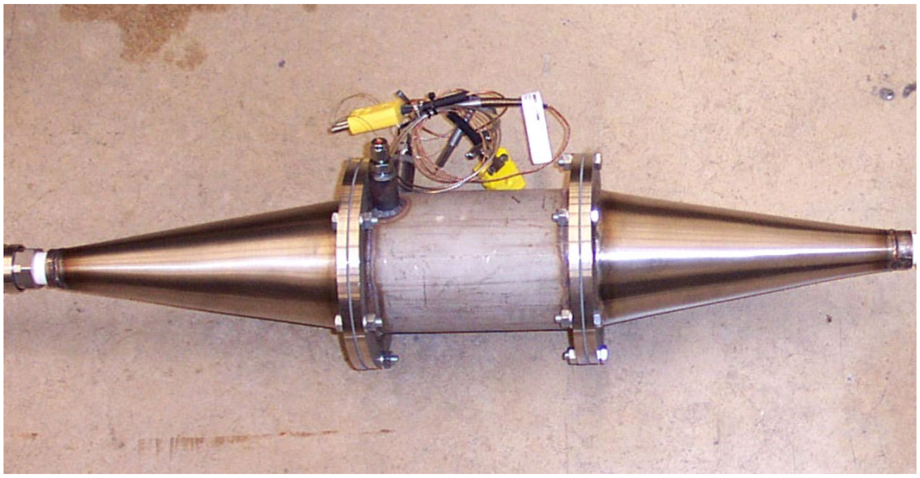

FIGURE 20. CARBON DENUDER ASSEMBLY

3.5 Dilution System

3.5.1 Secondary Dilution Construction

The secondary dilution tunnel was built to accommodate the 2007 sampling protocol and to provide easy access for other particle measurement instruments upstream of the filter used for PM collection.

The Code of Federal Regulations, 40 CFR Part 86 or Part 1065, mandates that the measurement of PM be performed downstream of a secondary dilution tunnel that is coupled to the full flow CVS. A secondary dilution system (SDS), shown in Figure 21, was designed and

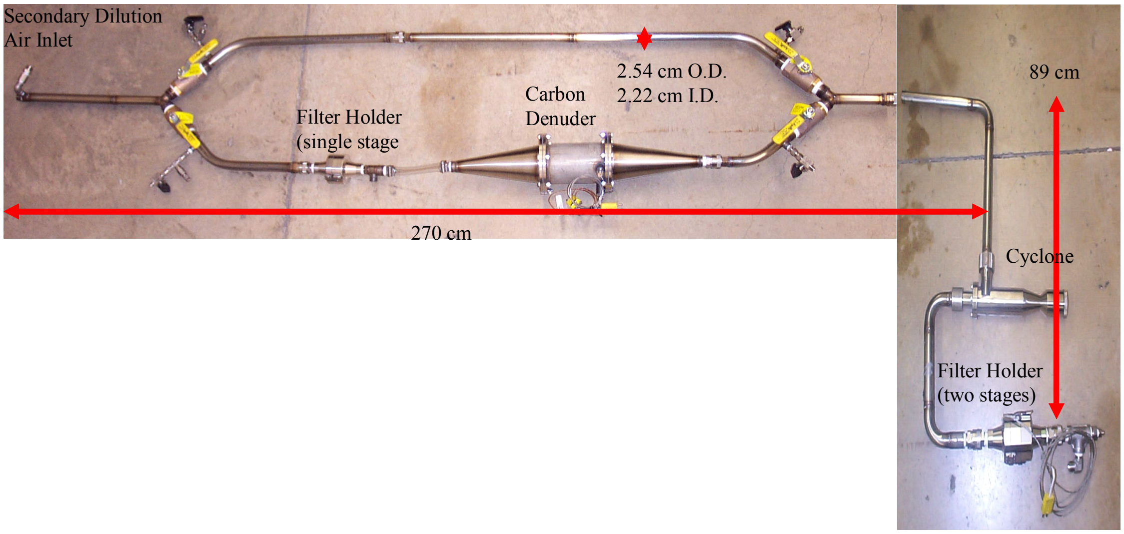

FIGURE 21. SECONDARY DILUTION SYSTEM

fabricated at SwRI to satisfy the requirements specified in the EPA 2007 PM sampling procedures and to satisfy the requirements to meet project objectives. The SDS consisted of two parallel flow paths, with and without the carbon denuder, that ran sequentially through a common two-stage filter holder downstream of a PM-2.5 cyclone. The single stage filter placed upstream of the carbon denuder was specific to testing denuder performance. The SDS was wrapped with heating tapes that were connected to a bank of temperature controllers along with feedback thermocouples to maintain a dilute exhaust and a filter face temperature of 47 °C ± 5 °C. The SDS was coupled to the sample zone of the full flow CVS as shown in Figure 22.

3.5.2 Secondary Tunnel Theoretical Particle Losses

Figure 23 shows the particle losses in the secondary dilution tunnel sampling system with and without the carbon denuder. Losses for particles between 0.1 µm and 1 µm for both with and without denuder were less than 2 percent. Particle losses between 0.01 µm and 0.1 µm ranged from 33 percent to less than 2 percent with the denuder and from 6 percent to less than 2 percent without the denuder. The losses for particles larger than 1 µm were typically due to inertial impaction in tube bends of the sampling system and normally will be removed by the $PM_{2.5}$ to PM_{10} cyclone required for 2007 PM measurement. For the sub-0.01 µm particles, the losses were less than 30 percent for particles larger than 0.003 µm, the 50 percent lower detection limit of the condensation particle counter (CPC), and less than 90 percent for the system with the denuder.

For this work, the calculated average particle losses for particles between 0.01 µm and 0.3 µm that are expected to contribute to particle mass and number was less than 2 percent for the dilution system without the denuder and less than 7 percent for the system with the denuder.

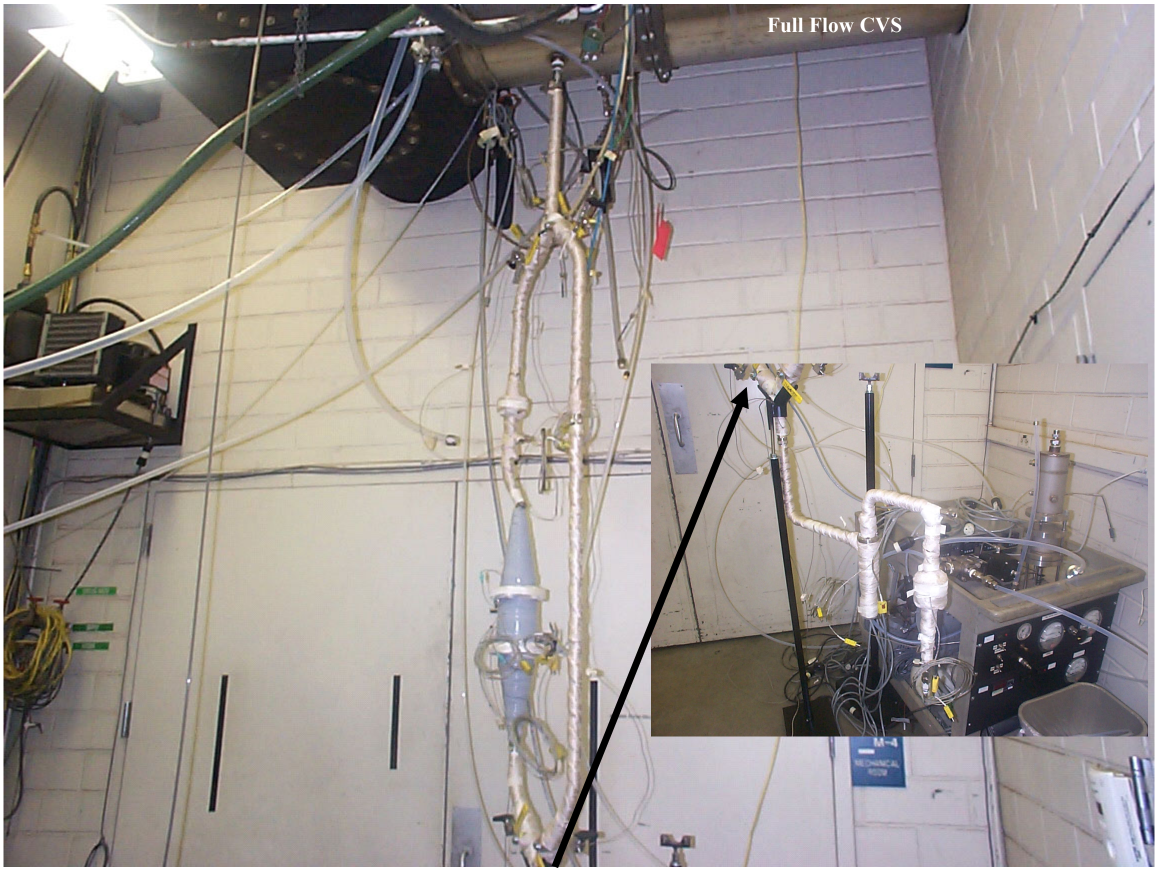

FIGURE 22. SECONDARY DILUTION SYSTEM COUPLED TO FULL FLOW CVS

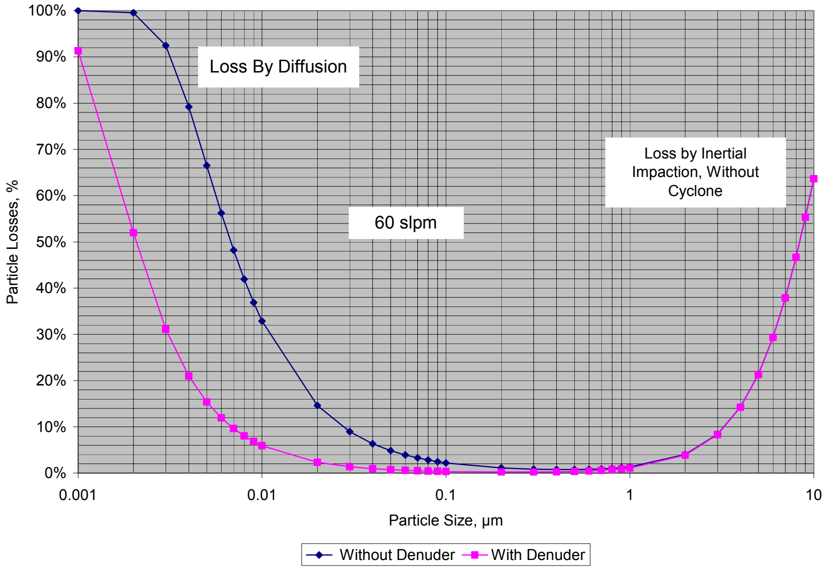

FIGURE 23. PARTICLE LOSSES IN SECONDARY DILUTION TUNNEL SAMPLING SYSTEM

3.5.3 *Primary and Secondary Sampling System*

Figure 24 shows the primary full flow CVS tunnel and the secondary sampling system. The primary tunnel was operated at a nominal flow rate of 3000 cfm for all experiments. The total flow through the secondary tunnel ranged from 2.2 cfm to 0.7 cfm, depending on the filter face velocity setting.

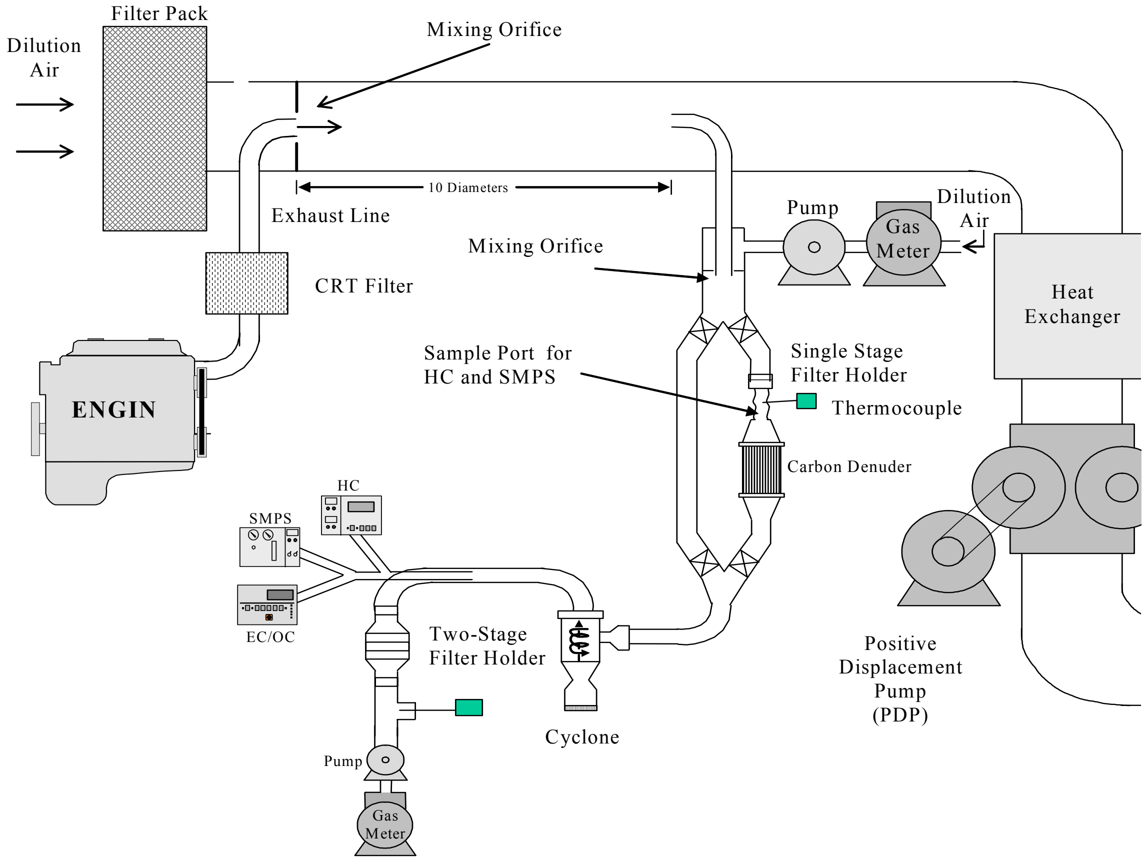

FIGURE 24. SCHEMATIC OF PARTICULATE MATTER SAMPLING SYSTEM

3.6 Particle Instruments

During Phase 1 of the E-66 program six different particle instruments were used. The Sunset Laboratory organic carbon (OC)/elemental carbon (EC) analyzer and the Horiba MEXA 1370-PM were used in Tasks 1 and 2 to characterize the OC and EC portion of the PM. The TSI engine exhaust particle sizer (EEPS) and scanning mobility particle sizer (SMPS), Sensors quartz crystal micro-balance (QCM), and the Dekati mass Monitor (DMM-230) were used in Task 4 to compare their performance with the filter method. Below is a brief description of each of the instruments used.

3.6.1 Sunset Laboratory Semi-Continuous OC/EC

The Sunset Laboratory semi-continuous OC/EC analyzer, shown in Figure 25, measures the organic carbon fraction and elemental carbon fraction of particulate matter collected on a quartz filter placed in a quartz oven inside the instrument. The OC/EC analysis is performed on-line in about 8 minutes after PM collection is complete. After the OC/EC analysis is finished, the same quartz filter is used again. The same quartz filter can be used for a few days with continuous use of the instrument.

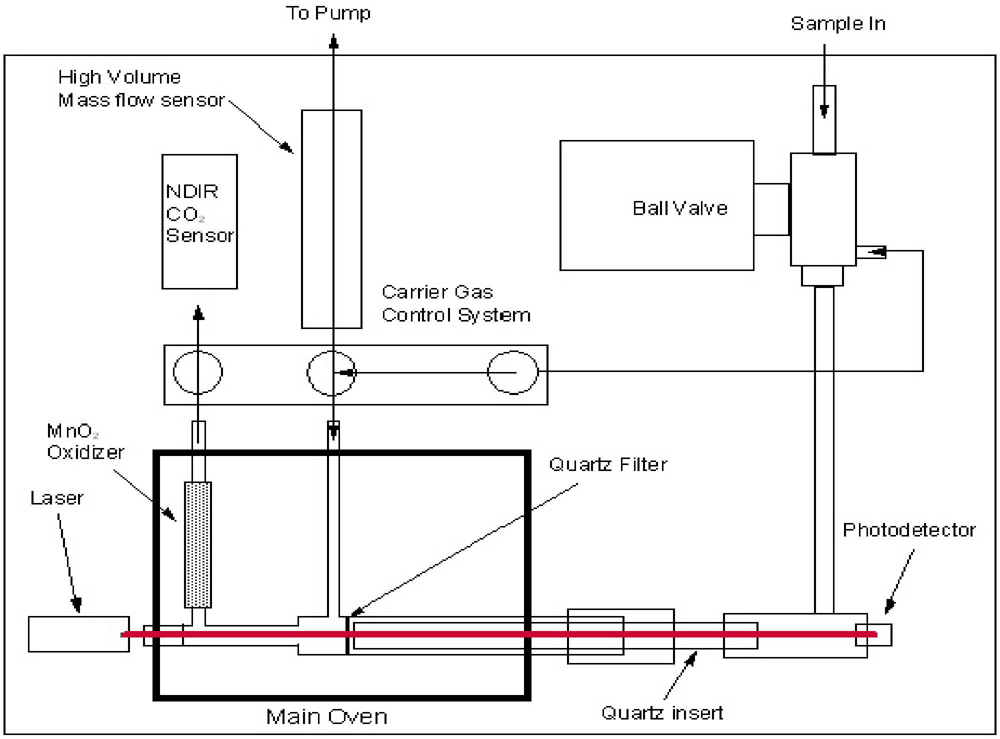

FIGURE 25. SUNSET LABORATORY SEMI-CONTINUOUS OC/EC

The OC/EC instrument works on the principle of oxidizing the organic carbon and elemental carbon collected by the quartz filter into CO_2 that is measured by a non-dispersive infra-red CO_2 sensor. The CO_2 signal is converted to total mass of OC and EC.

After PM is collected on the quartz filter for a specified period of time, the instrument triggers an OC/EC cycle, shown in Figure 26, by first flowing helium over the filter for OC desorption followed by a helium/oxygen blend for elemental carbon oxidation. The desorbed OC is converted to CO_2 over the MnO_2 catalyst before it reaches the CO_2 sensor. As a part of each analysis, a fixed volume of methane with known concentration is introduced to provide an internal standard to the response of the CO_2 sensor. At the end of the OC/EC cycle, the quartz filter is cleaned, and ready to be reused.

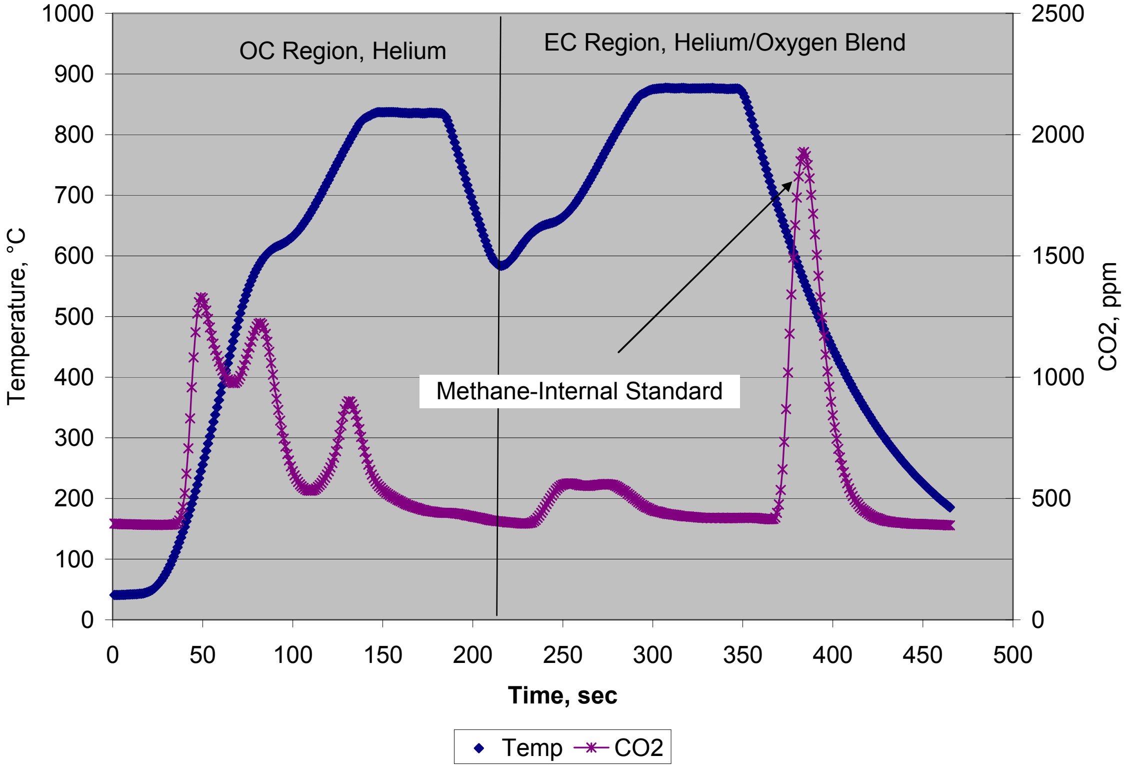

FIGURE 26. TYPICAL OC/EC ANALYSIS PROFILE

The split between OC and EC is determined by the laser transmittance through the filter during analysis. During the OC portion of the cycle, it is possible to form elemental carbon on the filter by pyrolysis. The transmitted laser signal strength decreases due to the formation of soot. During the EC portion of the cycle, the filter gets cleaner and the transmitted laser signal strength starts to increase again. The recovery of the signal back to the level when OC analysis started determines the OC/EC split.

3.6.2 Horiba MEXA 1370-PM

The Horiba MEXA 1370-PM [3], shown in Figure 27, provides information on PM organic carbon, elemental carbon, and sulfate. It was used for a limited time in Task 2. This instrument is different than the Sunset Laboratory semi-continuous OC/EC because it requires a different handling of the quartz filters used. In order to establish a clean filter baseline, the quartz filters are first baked in a muffle furnace at a high temperature of 1000 °C prior to PM collection. PM collection on a quartz filter takes place in the engine laboratory for a specified test. After PM collection, the filter is brought back for analysis by the MEXA 1370-PM.

Filter analysis is performed by first passing a nitrogen stream over the quartz filter, placed inside the first furnace that is maintained at a temperature of 980 °C, as shown in Figure 27. The OC portion of PM quickly desorb and oxidize with oxygen that is introduced upstream of a second furnace to produce CO_2. The sulfate portion of PM is decomposed at high temperature and reduced to SO_2. The CO_2 and SO_2 concentrations are detected via a CO_2 detector and a SO_2 detector, respectively. The elemental carbon portion of PM is analyzed by passing an oxygen stream over the filter to oxidize the elemental carbon into CO_2 that is detected by the CO_2 sensor.

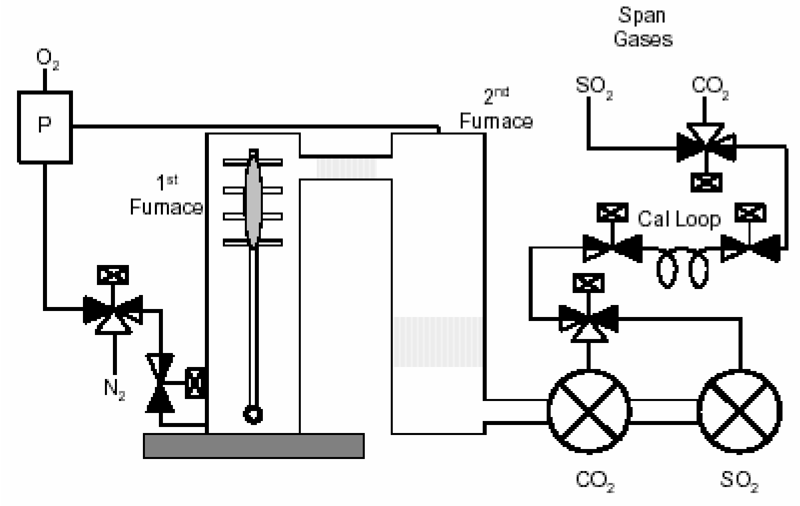

FIGURE 27. MEXA 1370-PM FLOW SCHEMATIC

3.6.3 Scanning Mobility Particle Sizer (SMPS)

The SMPS was used to measure particle concentrations and size distributions in the size range from 6 nm to 220 nm under steady-state engine operation. A diagram of the SMPS is shown in Figure 28. It consists of a neutralizer, a mobility section, a TSI Model 3025 condensation particle counter (CPC), and a computerized control and data acquisition system. Particles in the sample stream first pass through a Krypton 85 bipolar ion charger / neutralizer. The aerosol then enters the annular mobility section close to the inner surface of the outer cylinder. Clean sheath air flows close to the central rod. When a voltage scan is applied to the rod, charged particles move in the radial direction inward or outward, depending on their polarity. Particles with the right polarity and electrical mobility exit through holes at the bottom of the central rod. These particles are then detected by the CPC. During steady-state engine operation, a scanning time of 2 minutes gives accurate and repeatable size distributions. A scan time of 2 minutes was used throughout this work. The aerosol, sheath air, monodisperse, and excess flows were maintained at 1.5 lpm, 15 lpm, 1.5 lpm, and 15 lpm, respectively.

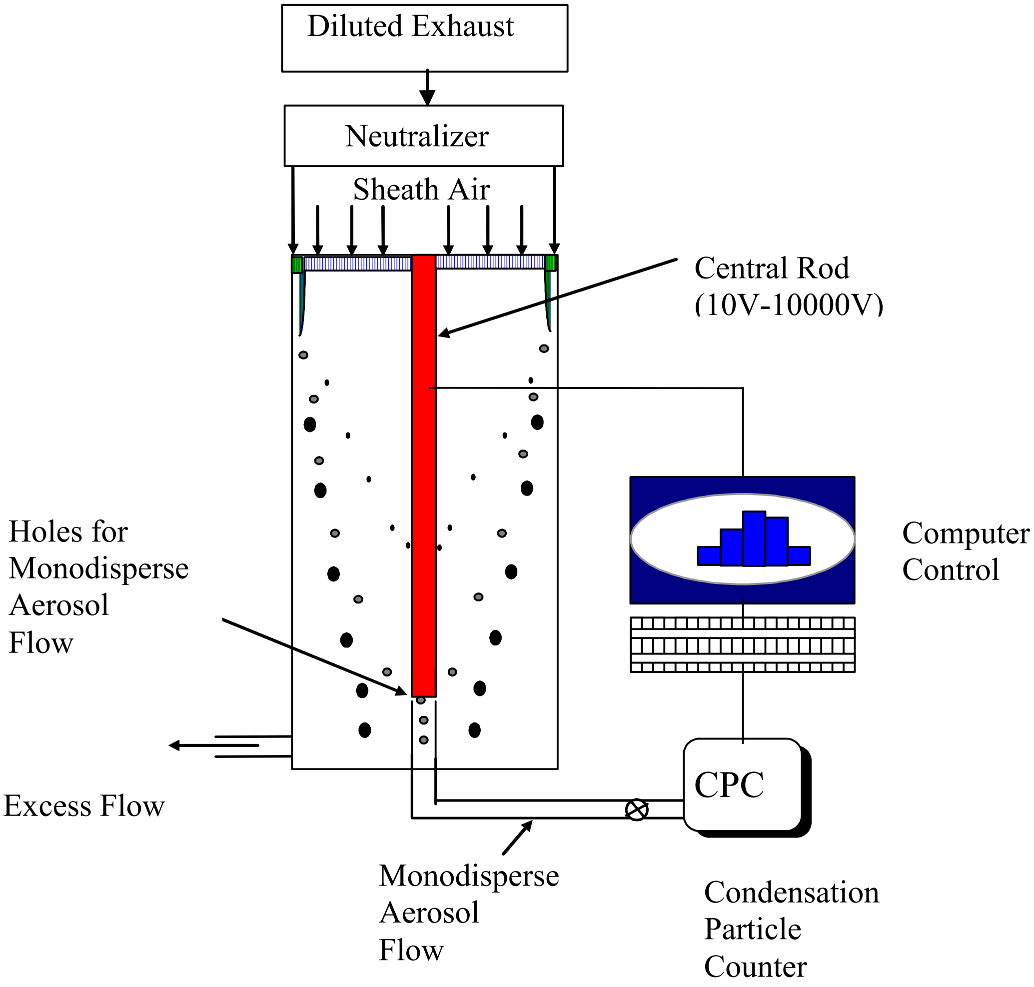

FIGURE 28. SCANNING MOBILITY PARTICLE SIZER (SMPS)

3.6.4 Engine Exhaust Particle Sizer (EEPS)

The EEPS [4], shown in Figure 29, is a state-of-the-art particle sizing instrument that measures the number-weighted size distribution of particles every 200 ms. The EEPS covers a size range from 5.6 nm to 560 nm with a resolution of 16 channels per decade. The EEPS is a mobility-based particle sizing instrument similar to the SMPS. An aerosol stream enters the instrument through a 1 µm cut cyclone at a nominal flow rate of 10 lpm and a pressure of 1 bar. The aerosol is then subjected to two unipolar diffusion chargers. First, the aerosol is exposed to a negative charger to reduce the number of highly positively charged particles and to prevent overcharging in the second charger. Second, the aerosol is exposed to a positive charger that puts a predictable net positive charge on the particles. The positively charged aerosol enters the mobility section that consists of 22 electrometers and a central rod that is divided to three insulated sections each maintained at a different voltage level. The upper section is set at 85 volt, the middle section is set at 470 volt, and the lower section is set at 1200 volt. Small particles are deposited first on the upper electrometers and large particles are deposited on the bottom electrometers.

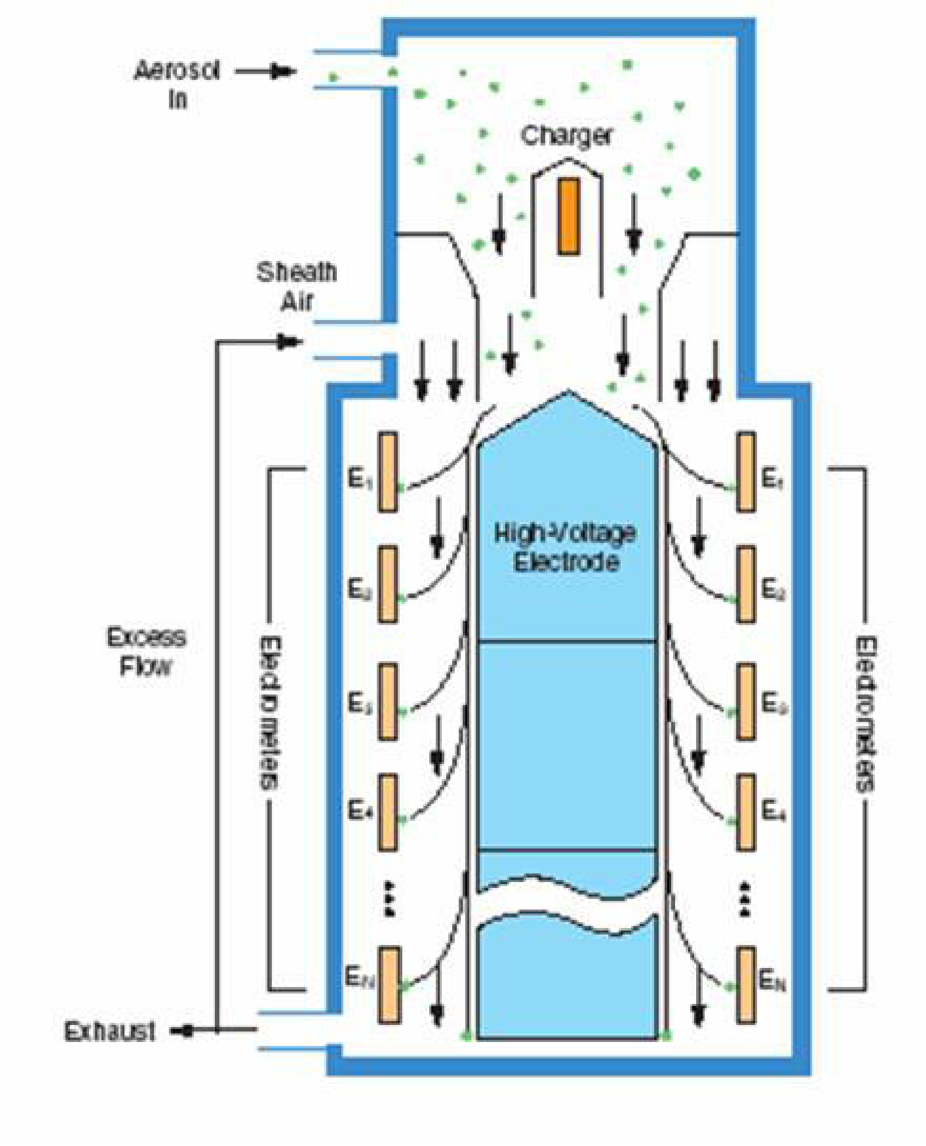

FIGURE 29. ENGINE EXHAUST PARTICLE SIZER (EEPS)

3.6.5 Dekati Mass Monitor (DMM-230)

The DMM-230 [5], shown in Figure 30, measures the mass concentration of particles on a second-by-second basis. The DMM-230 is based on the electrical low pressure impactor (ELPI) technology produced by Dekati. The DMM-230 basically measures the number-weighted aerodynamic particle size distribution using a combination of particle charging, series of impaction rods, and a series of electrometers that are connected to the impaction rods to provide information on number concentration from the current read by the electrometers.

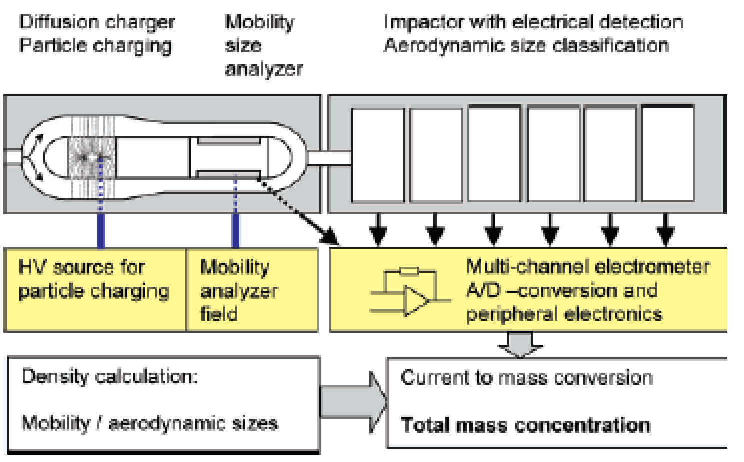

FIGURE 30. SCHEMATIC OF DMM-230 MASS MONITOR

In order to determine the mass-weighted distribution from the number-weighted distribution, the DMM-230 determines the average density of particles by matching the mean aerodynamic diameter with the mean mobility diameter. The DMM-230 determines the mean aerodynamic diameter from the measured aerodynamic size distribution, and it measures the mobility mean diameter from the current measured in the mobility section for sub-30 nm particles (I_{mob}) and the total current (I_{tot}), assuming a lognormal distribution, using the following equation [5]:

$$d_{\mathrm{p}} = 59\left(\frac{0.938}{\dfrac{I_{\mathrm{mob}}}{I_{\mathrm{tot}}} - 0.124} - 1\right)^{(1/2.13)}$$

Where dp is the mean mobility diameter, I_{mob} is the current measured by the mobility electrometer, and I_{tot} is the total current measured by the mobility electrometer and the impactor electrometers ($I_{mob} + I_{impactor}$). If the distribution is bimodal, the DMM-230 assumes an average density of 1 g/cm³. The aerosol flow rate through the DMM-230 is 10.5 lpm.

3.6.6 Quartz Crystal Microbalance (QCM)

The QCM, shown in Figure 31, measures the mass of particles deposited on an oscillating quartz crystal using the frequency shift in crystal oscillation. The mechanism of particle deposition on the oscillating quartz crystal is by first charging particles with positive ions then depositing the charged particles on the surface of the quartz crystal by electrostatic precipitation. The oscillating frequency of a clean piezoelectric crystal is on the order of 5000 HZ, about 1/1000 of its resonant frequency. The aerosol flow rate through the QCM is 1 lpm.

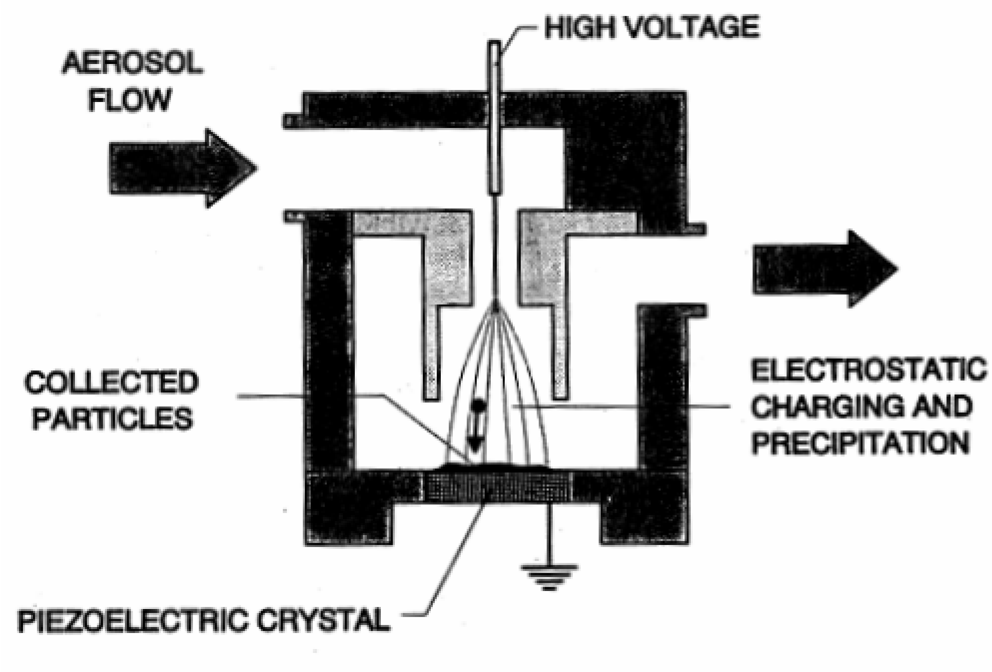

FIGURE 31. QUARTZ CRYSTAL MICROBALANCE (QCM)

4.0 EXPERIMENTAL PROCEDURES

4.1 Engine Operation

Six modes of steady-state engine operation, described in Table 4, were used in various experiments. The steady-state modes included high load, medium load, light load, and idle to cover a wide spectrum of PM composition.

TABLE 4. STEADY-STATE ENGINE OPERATION

Test Number	Speed Target, rpm	Speed Obs, rpm	Target Torque, lb.ft	Torque Obs, lb.ft
Mode A[1]	1800	1800	1225	1223
Mode B	1800	1802	612	612.7
Mode C	1800	1800	122	122.5
Mode D[2]	1200	1199	1625	1623.5
Mode E	1200	1201	812	815.2
Mode F[3]	600	600	0	12

[1] Rated Power.
[2] Peak Torque.
[3] Low Idle.

Two transient engine operations that included the hot-start portion of the FTP transient cycle, shown in Figure 32, and the European transient cycle (ETC), shown in Figure 33, were also used.

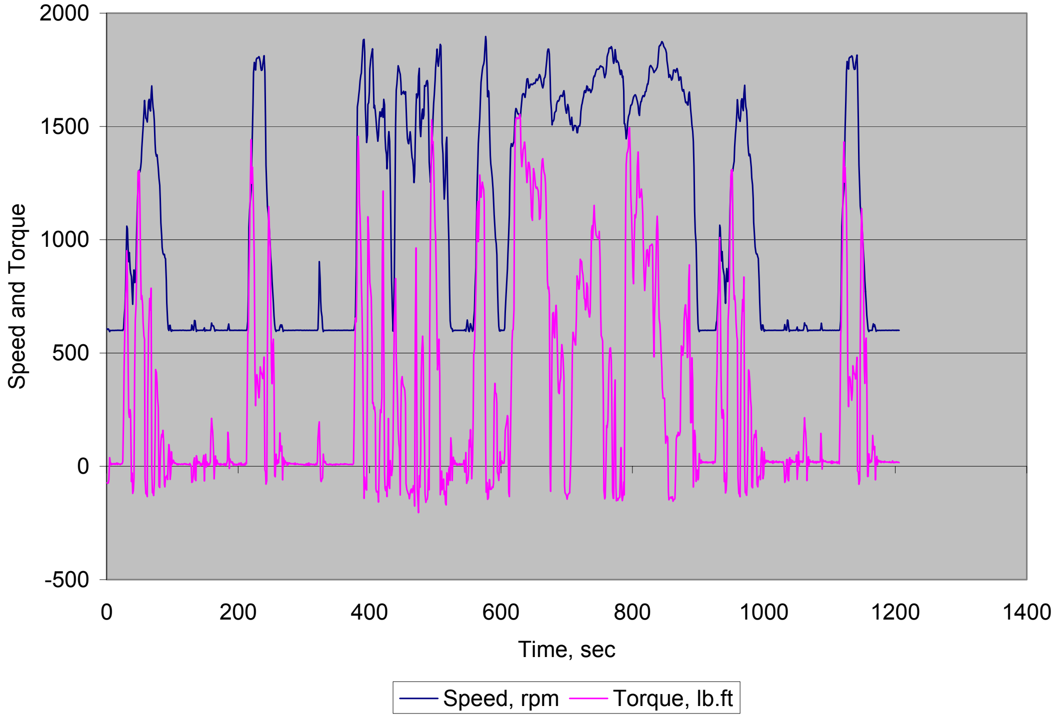

FIGURE 32. SPEED AND TORQUE PROFILE FOR THE FTP TRANSIENT CYCLE

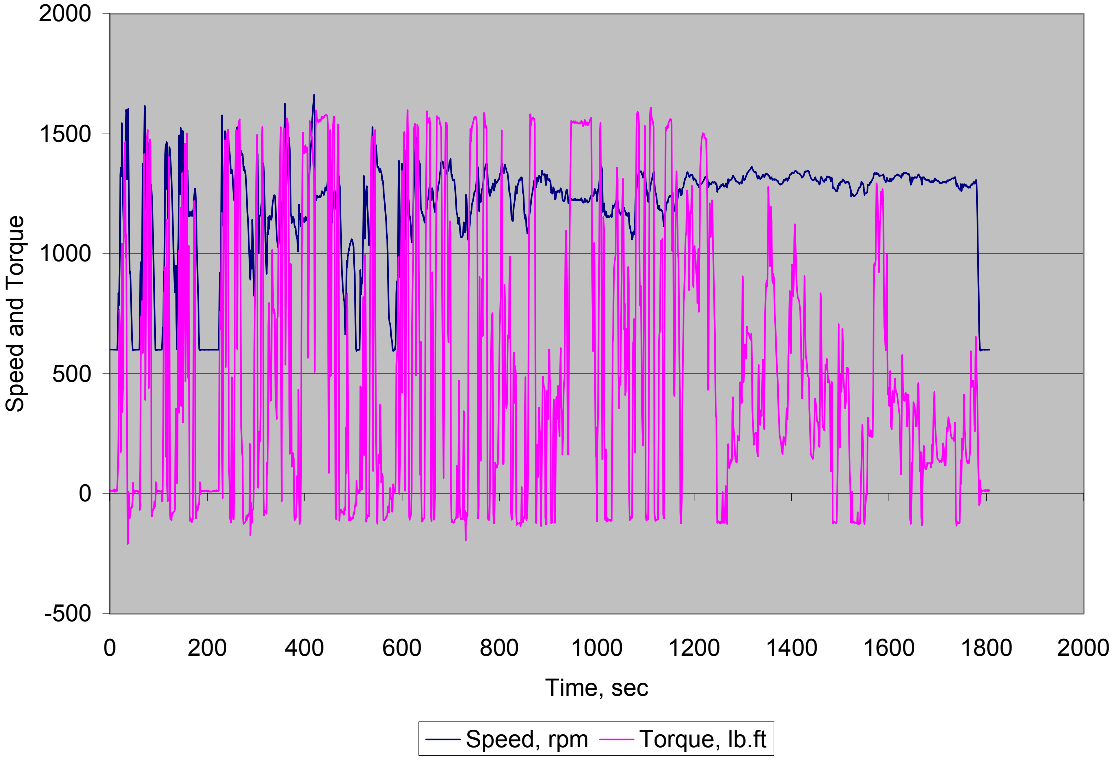

FIGURE 33. SPEED AND TORQUE PROFILE FOR THE ETC CYCLE

Prior to any steady-state or transient engine testing, conditioning of the engine exhaust, primary dilution system and secondary dilution system was performed at engine rated power for a period of 10 minutes. The purpose of the conditioning process was to provide a reference starting point prior to each run and to prevent mode-to-mode or cycle-to-cycle volatile PM interferences, which is the subject of the next phase of Project E-66.

4.2 Filter Media

4.2.1 Filter Media Characteristics

Seven different filter media, shown in Figure 34, were used during this work. Some of the characteristics of each filter media are described in Table 5.

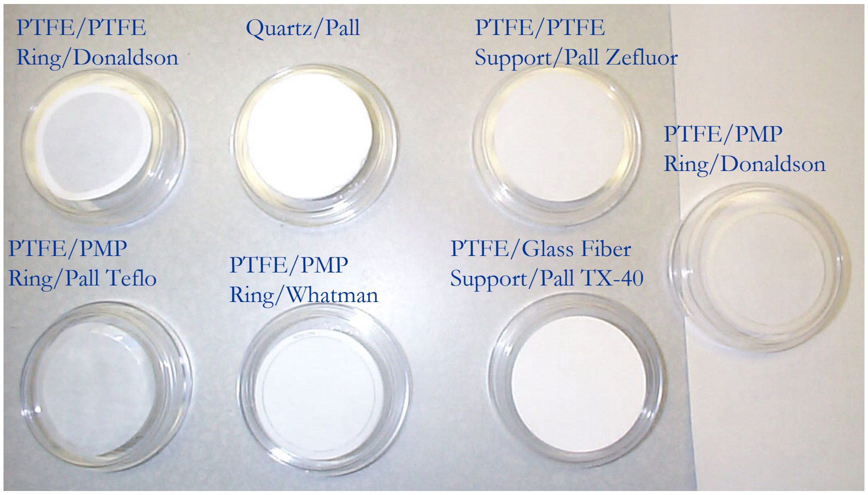

FIGURE 34. ILLUSTRATION OF DIFFERENT FILTER MEDIA

TABLE 5. CHARACTERISTICS OF DIFFERENT FILTER MEDIA

Filter Media	Manufacturer	Initial Weight, mg	Material	Efficiency,[d] %	Thickness, µm	Pressure Drop,[g] inH_2O
Teflo	Pall	180	PTFE[a] Memberane with PMP[b] ring	99.99	46/508[e]	30
Teflon	Whatman	143	PTFE Membrane with PP[c] ring	99.70	40/ 380[e]	90
PTFE-PP	Donaldson	157	PTFE Membrane with PP[c] ring	99.99[f]	40/508[e]	78
PTFE-PE	Donaldson	119	PTFE Membrane with PTFE ring	99.99[f]	40/254[e]	78
Zefluor	Pall	242	PTFE Membrane with PTFE support	99.99	152	60
TX-40	Pall	91	PTFE Coated Borosilicate Glass Fiber	99.90	178	30
Quartz	Pall	103	Pure Quartz/No Binder	99.90	432	44

[a] Polytetrafluoroethylene (Teflon®)
[b] Polymethylpentene
[c] Polypropylene
[d] Following ASTM D 2986-95A 0.3 µm (DOP) at 32 L/min/100 cm^2 filter media.
[e] Total Ring Thickness
[g] Approximate pressure drop at 75 cm/sec

4.2.2 Filter Handling

All filter media used were initially stored in a clean weighing chamber for at least 24 hours. The filters were then baked in a vacuum oven for 24 hours at a temperature of 52 °C. The pre-baked filters were brought back to the weighing chamber and were conditioned for at least 24 hours prior to initial weighing. Each filter was initially weighed at least three times, and the average buoyancy corrected weight value was used as the official filter initial weight.

After initial weighing, each filter was put in a clean filter cassette. The cassette was placed in a covered Petri dish and was stored in a clean weighing chamber, ready to be used for testing.

Routinely, a Petri dish containing a weighed filter in a cassette was picked up and checked out of the weighing chamber as needed for testing. After testing was completed, the cassette was placed in its Petri dish and was checked back in to the clean weighing chamber.

After at least 30 minutes of conditioning time, the filter was weighed again three consecutive times and an average buoyancy-corrected weight was recorded.

The filter weight gain was determined from the difference between the initial average weight and the final average weight.

4.3 Test Matrices

4.3.1 Task 1- Carbon Denuder Experiments

Table 6 shows the test matrix for the denuder experiments. Five to seven repeats with all indicated measurements were performed at each engine operation. Figure 24 shows the experimental setup that compliments the testing with the denuder.

4.3.2 Task 2- Filter Media Experiments

The test matrix for the filter media experiments is shown in Table 7. Two similar secondary dilution systems (B and F) were run in parallel during each test. Teflo filters were always used in System B and the other filter media including Teflo were all used in System F up to eight or seven repeats as designated in Table 7. In order to eliminate bias in the PM emission results due to engine performance, the time between two repeats using a particular filter media in System F was separated by the time needed to run all other filter media one time.

The test matrix shown in Table 7 was conducted twice for the FTP transient cycle with and without a bypass around the CRT-DPF in the exhaust. The bypass around the CRT-DPF was installed in the engine exhaust system to increase PM emissions to near the 2007 PM limit.

TABLE 6. TEST MATRIX FOR DENUDER PERFORMANCE EVALUATION

Test Number	Engine Speed	Engine Load, %	HC UP	HC Down	CPC Down	SMPS Up	SMPS Down	EC/OC Down	Filter Up	Filter Down, Top	Filter Down, Bottom
Denuder-M4	Rated	25	Yes	Yes	Yes	NO	NO	Yes	Yes	Yes	NO
Denuder-M2	Rated	75	Yes	Yes	NO	Yes	Yes	Yes	NO	Yes	Yes
Denuder-M5	Rated	10	Yes	Yes	NO	Yes	Yes	Yes	NO	Yes	Yes
No Denuder-M5	Rated	10	N/A	N/A	NO	NO	N/A	Yes	N/A	Yes	Yes

M2,4,5: Modes 2, 4, and 5 of the ISO 11-mode test
HC UP: Hydrocarbon Measurement Taken Upstream of Denuder
HC Down: Hydrocarbon Measurement Taken Downstream of Denuder (location common to the path with or without Denuder)
CPC Down: Particle Number Measurement Taken Downstream of Denuder (location common to the path with or without Denuder)
SMPS UP: Particle Size Distribution Measurement Taken Upstream of Denuder using a scanning mobility particle sizer
SMPS Down: Particle Size Distribution Measurement Taken Downstream of Denuder (location common to the path with or without denuder)
Filter UP: Filter Collection Taken Upstream of Denuder
Filter Down, Top: Filter Collection Taken Downstream of Denuder Using Top location in two-Stage filter holder (location common to the path with or without denuder)
Filter Down, Bottom: Filter Collection Taken Downstream of Denuder Using Bottom location in two-Stage filter holder (location common to the path with or without denuder)

TABLE 7. TEST MATRIX BY SYSTEM, FILTER MEDIA, AND REPEATS

Filter Media		Teflo	Teflo	Zefluor	Teflon	TX-40	PTFE-PE	PTFE-PP	Quartz	Quartz
Secondary System		B	F	F	F	F	F	F	FT[a]	FB[b]
Number of Test Repeats										
Transient	Transient	40	8	8	8	8	8	None	None	None
1800 rpm	100% Load	49	7	7	7	7	7	7	7	7

[a] FT: Secondary Dilution System F-Top Position in Filter Holder.
[b] FB: Secondary Dilution System F-Bottom Position in Filter Holder.

4.3.3 Task 3- Filter Face Velocity and PM Loading Experiments

The filter face velocity and PM loading experiments, shown in Tables 8 and 9, were conducted at four different nominal filter face velocities of 24, 60, 90, and 120 cm/sec. The engine exhaust configuration included the ceramic substrate bypass in addition to the CRT-DPF. The bypass flow was set to give 70 percent of the 2007 PM standard at a filter face velocity of 75 cm/sec.

The first series of experiments was conducted using the hot-start FTP transient cycle. The second series of experiments was conducted using Mode C at rated speed and 10 percent load.

Additional experiments were conducted using the FTP transient cycle and the exhaust bypass configuration that gave a PM level close to 30 percent of 2007 PM standard. These tests were conducted using a filter face velocity of 60 cm/sec and 120 cm/sec.

TABLE 8. TEST MATRIX USING SEVEN SINGLE OR DUPLICATE RUNS OF THE HOT-START FTP TRANSIENT CYCLE

		Filter Face Velocity, cm/sec			
Loading Time, minutes	**Filter Face Temperature, °C**	**120**	**90**	**60**	**24**
Secondary Dilution System A					
20	47 °C	7	7	7	7
40	47 °C	7	7	7	7
Secondary Dilution System B					
20	25 °C	7	7	7	7
40	25 °C	7	7	7	7

TABLE 9. TEST MATRIX USING SEVEN SINGLE OR DUPLICATE RUNS OF MODE C (RATED SPEED, 10 PERCENT LOAD)

		Filter Face Velocity, cm/sec			
Loading Time, minutes	**Filter Face Temperature, °C**	**120**	**90**	**60**	**24**
Secondary Dilution System A					
30	47 °C	7	7	7	7
60	47 °C	7	7	7	7
Secondary Dilution System B					
30	25 °C	7	7	7	7
60	25 °C	7	7	7	7

4.3.4 Task 4- Particle Instrument Experiments

Four particle instruments that included the SMPS, EEPS, QCM, and DMM-230 were used in parallel to the filter-based method. A sample was taken from upstream of the filter holder in the sampling train and distributed to all four instruments. The total nominal flow for all instruments was 22 lpm.

Table 10 shows the test matrix of the experiments. At each engine operation, seven repeats performed. A 10 minute conditioning time at rated power was performed in between test repeats.

TABLE 10. TEST MATRIX USING SEVEN REPEATS AT EACH ENGINE OPERATION SEPARATED BY 10 MINUTES OF CONDITIONING TIME

	Sampling Time, min	Filter	SMPS	EEPS	QCM	DMM-230
Mode A	20	7	7	7	7	7
Mode B	25	7	7	7	7	7
Mode C	30	7	7	7	7	7
Mode D	20	7	7	7	7	7
Mode E	25	7	7	7	7	7
Mode F	30	7	7	7	7	7
FTP	20	7	7	7	7	7
ETC	30	7	7	7	7	7

5.0 RESULTS

5.1 Carbon Denuder Performance

5.1.1 Particle Size and Number

Tables 11 and 12 show information on particle statistics from data collected upstream and downstream of the carbon denuder, using the scanning mobility particle sizer (SMPS). The test matrix was described in Table 6. The data reported are based on an average of 20 scans at each measuring point either upstream or downstream of the denuder using dilute engine exhaust in the secondary dilution tunnel coupled to the CVS tunnel. Table 13 shows a summary of the ratios of the statistical parameters obtained for the downstream position over that of the upstream position. The ratios suggest that all particle statistical parameters were similar.

As for the total concentration, the losses in the denuder based on particle number were within 7 percent, and the losses based on particle mass or volume were within 12 percent.

Note also that the dilute mass concentration based on SMPS was 0.9 μg/m^3, a very low concentration. The overall dilution ratio was about 8.5, achieved in a two-stage dilution process. The CVS dilution ratio was estimated to be 5 and the secondary dilution ratio was 1.7. This suggests that the mass concentration in the exhaust based on the SMPS was about 8 μg/m^3.

TABLE 11. SUMMARY OF SMPS STATISTICAL PARAMETERS FOR SAMPLING POSITION UPSTREAM OF DENUDER

	Denuder-M2-Upstream- Average Values				
	Number	**Diameter**	**Surface**	**Volume**	**Mass**
Median (nm)	48.4	82.1	112.6	139.3	139.3
Mean (nm)	58.8	90.2	117.4	139.1	139.1
Geo. Mean (nm)	44.3	75.4	104.9	129.2	129.2
Mode (nm)	48.2	107.0	158.7	186.8	186.8
Geo. St. Dev.	2.2	1.9	1.7	1.5	1.5
Total Conc.	2329.4 (#/cm³)	0.1 (mm/cm³)	3.8E+07 (nm²/cm³)	7.5E+08 (nm³/cm³)	0.9 (µg/m³)
	Denuder-M2-Upstream- Standard Deviation				
	Number	**Diameter**	**Surface**	**Volume**	**Mass**
Median (nm)	8.5	1.7	4.3	6.5	6.5
Mean (nm)	5.9	1.1	3.4	5.2	5.2
Geo. Mean (nm)	6.9	3.5	1.9	4.5	4.5
Mode (nm)	24.3	18.1	6.3	15.6	15.6
Geo. St. Dev.	0.1	0.1	0.1	0.0	0.0
Total Conc.	696.0 (#/cm³)	0.0 (mm/cm³)	9.4E+06 (nm²/cm³)	1.9E+08 (nm³/cm³)	0.2 (µg/m³)

TABLE 12. SUMMARY OF SMPS STATISTICAL PARAMETERS FOR SAMPLING POSITION DOWNSTREAM OF DENUDER

	Denuder-M2-Downstream- Average Values				
	Number	**Diameter**	**Surface**	**Volume**	**Mass**
Median (nm)	50.9	79.4	105.9	132.6	132.6
Mean (nm)	59.5	87.5	112.6	134.9	134.9
Geo. Mean (nm)	46.3	74.2	100.9	124.6	124.6
Mode (nm)	53.7	97.1	166.9	195.1	195.1
Geo. St. Dev.	2.1	1.9	1.7	1.5	1.5
Total Conc.	2160.0 (#/cm³)	0.1 (mm/cm³)	3.5E+07 (nm²/cm³)	6.6E+08 (nm³/cm³)	0.8 (µg/m³)
	Denuder-M2-Downstream- Standard Deviation				
	Number	**Diameter**	**Surface**	**Volume**	**Mass**
Median (nm)	4.3	3.5	4.1	3.8	3.8
Mean (nm)	4.1	3.0	3.2	4.0	4.0
Geo. Mean (nm)	4.5	3.5	2.9	3.6	3.6
Mode (nm)	10.8	6.0	27.0	4.1	4.1
Geo. St. Dev.	0.1	0.1	0.0	0.0	0.0
Total Conc.	419.1 (#/cm³)	0.0 (mm/cm³)	8.9E+06 (nm²/cm³)	1.6E+08 (nm³/cm³)	0.2 (µg/m³)

TABLE 13. SMPS STATISTICAL RATIOS OF DOWNSTREAM OF DENUDER OVER UPSTREAM POSITION

	Ratios of Downstream to Upstream				
	Number	Diameter	Surface	Volume	Mass
Median (nm)	1.05	0.97	0.94	0.95	0.95
Mean (nm)	1.01	0.97	0.96	0.97	0.97
Geo. Mean (nm)	1.04	0.98	0.96	0.96	0.96
Mode (nm)	1.12	0.91	1.05	1.04	1.04
Geo. St. Dev.	0.95	0.97	0.99	1.01	1.01
Total Conc.	0.93	0.95	0.92	0.88	0.88

5.1.2 Denuder Performance –Total Hydrocarbon

Total hydrocarbon was measured upstream and downstream of the denuder using two flame ionization detector instruments. Figure 35 shows the hydrocarbon removal efficiency for a total of seven repeats of engine steady-state operation, 30 minutes each, at rated speed and 25 percent load. The denuder initially showed a high HC removal efficiency; however, the efficiency deteriorated after conditioning the denuder overnight with a stream of clean air at 300 °C, as shown in Figure 36. The deterioration in denuder efficiency was puzzling, with the efficiency remaining at approximately 30 percent. Even after regenerating the denuder in a stream of helium at 375 °C, the performance relative to HC removal did not improve, as shown in Figure 37.

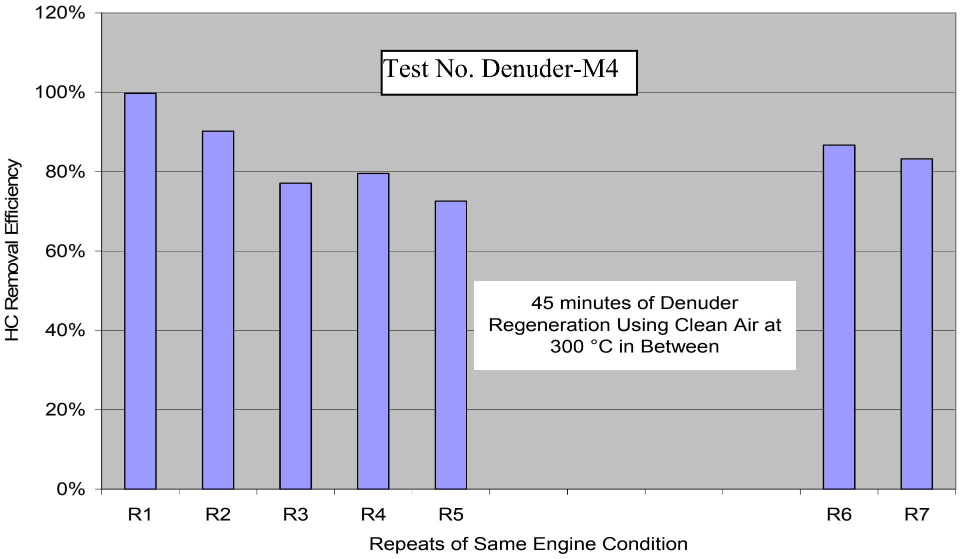

FIGURE 35. INITIAL DENUDER PERFORMANCE RELATIVE TO TOTAL HYDROCARBON REMOVAL

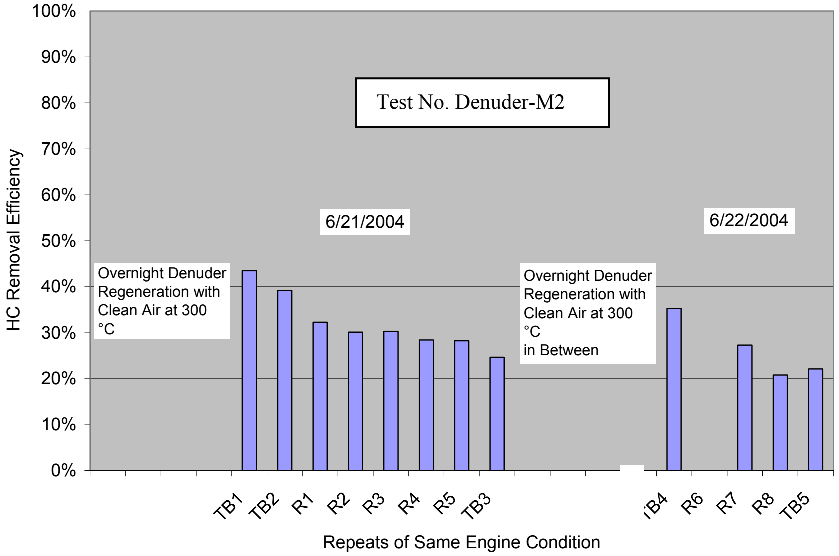

FIGURE 36. DENUDER PERFORMANCE AFTER OVERNIGHT REGENERATION WITH CLEAN AIR AT 300 °C

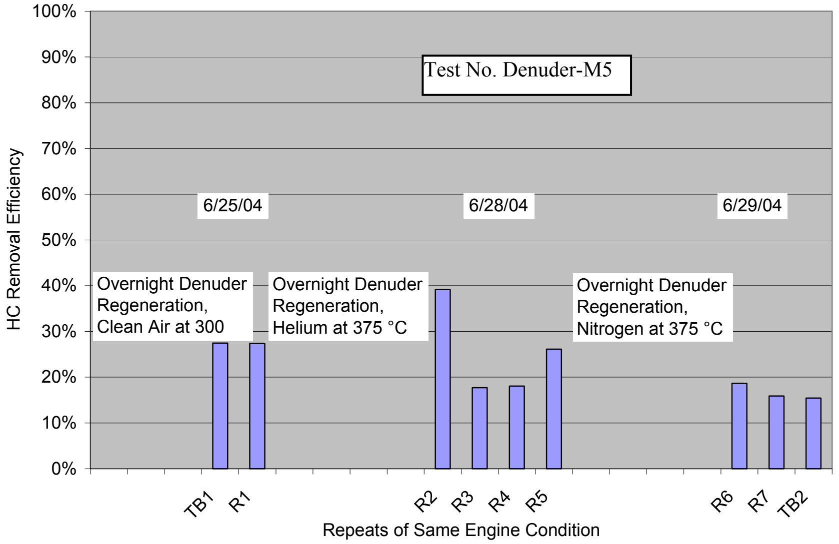

FIGURE 37. DENUDER PERFORMANCE AFTER OVERNIGHT REGENERATION WITH HELIUM AND NITROGEN AT 375 °C

5.1.3 Tygon Tubing

Before proceeding with any experiments involving the EC/OC instrument, it was discovered that the use of Tygon tubing at the sampling inlet of the EC/OC introduces a positive artifact during particle collection on a carbon impregnated filter. Figure 38 shows an example when sampling ambient air with and without a Tygon tube. The length of the Tygon tube was about 1 meter and the flow rate through the EC/OC instrument was about 2.5 lpm. The use of a Tygon tube had no influence on particle size and number as was observed with the SMPS.

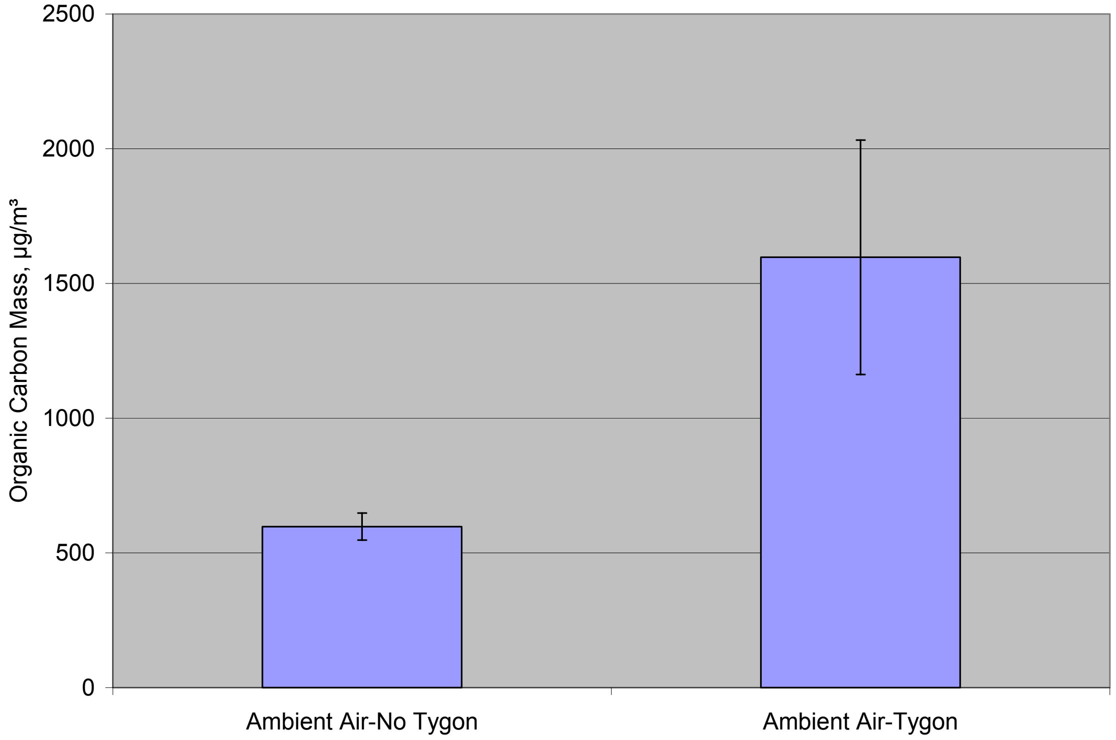

FIGURE 38. POSITIVE ARTIFACT IN PM COLLECTION USING A CARBON IMPREGNATED FILTER DUE TO TYGON TUBING IN SAMPLING LINE

5.1.4 Carbon Impregnated Versus Teflo Filters

The Sunset laboratory EC/OC instrument was used to collect data downstream of the denuder in parallel to PM mass collected on a Teflo filter. Typically, a pair of quartz filters are loaded inside the instrument for PM collection using a stream of dilute exhaust. After the collection is complete, the flow through the filter is cycled from a helium stream at 850 °C followed by oxygen in helium stream at 850 °C to determine the organic carbon (OC) and elemental carbon (EC) of PM collected on the filters, respectively, via a CO_2 detector.

For the experiments performed with the carbon impregnated filters using the EC/OC instrument, a Whatman fiber glass carbon impregnated filter was loaded into the EC/OC instrument with a backup quartz filter. Only OC analysis was performed after PM collection by exposing the filter to a stream of helium at 300 °C, as shown in Figure 39. This low temperature was chosen to prevent the possibility of forming soot at the filter surface at a higher temperature.

Figure 40 shows the PM concentration from data collected downstream of the carbon denuder using a Pall Teflo filter following the EPA 2007 PM sampling protocol in parallel to a carbon impregnated glass fiber filter using the EC/OC instrument. Note in Figure 40 that there was a significant difference in the reported dilute particle mass concentration between using the carbon impregnated filter and the Teflo filter. Another example of the difference between data reported using a carbon impregnated filter and a Teflo filter is shown in Figure 41 for a different engine operating condition and for a tunnel blank (TB) taken without the engine running.

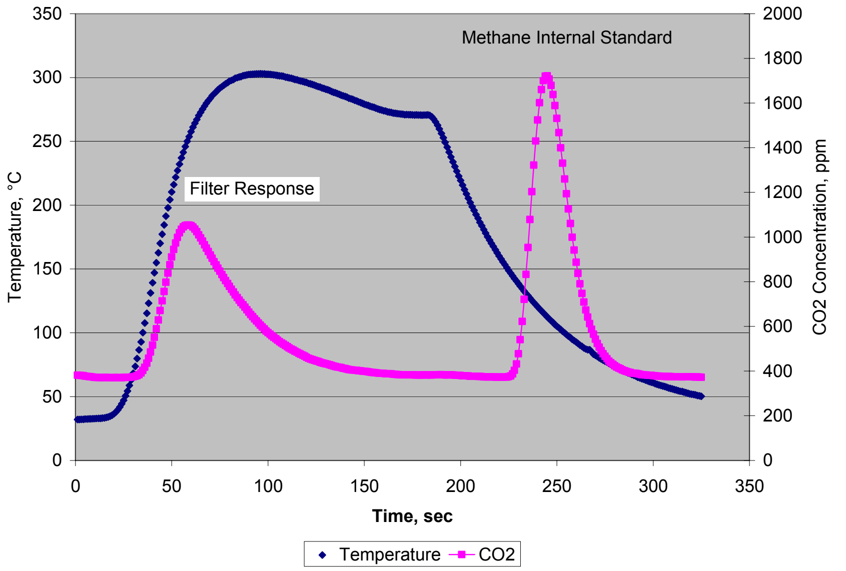

FIGURE 39. TEMPERATURE AND CO2 PROFILE DURING ANALYSIS OF A CARBON IMPREGNATED FILTER USING EC/OC INSTRUMENT

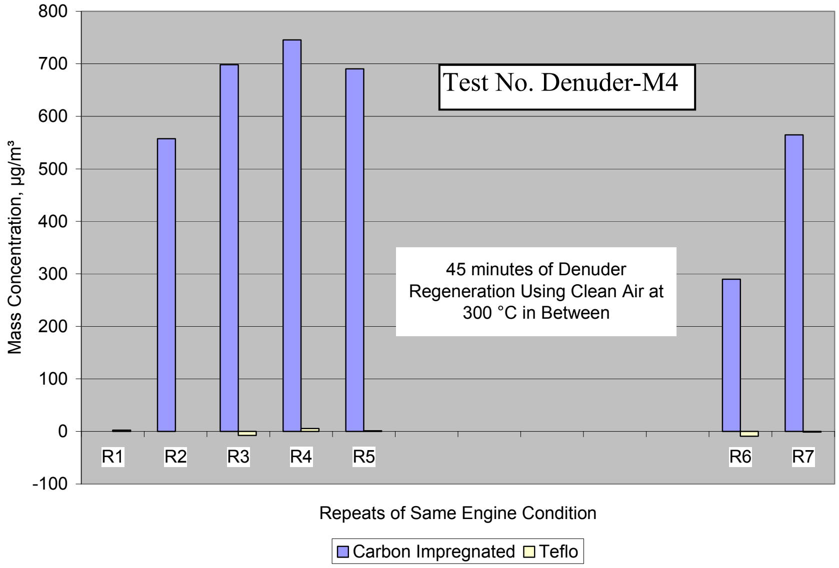

FIGURE 40. COMPARISON IN DILUTE MASS CONCENTRATION AFTER THE TEFLO FILTER AND DENUDER USED IN SERIES

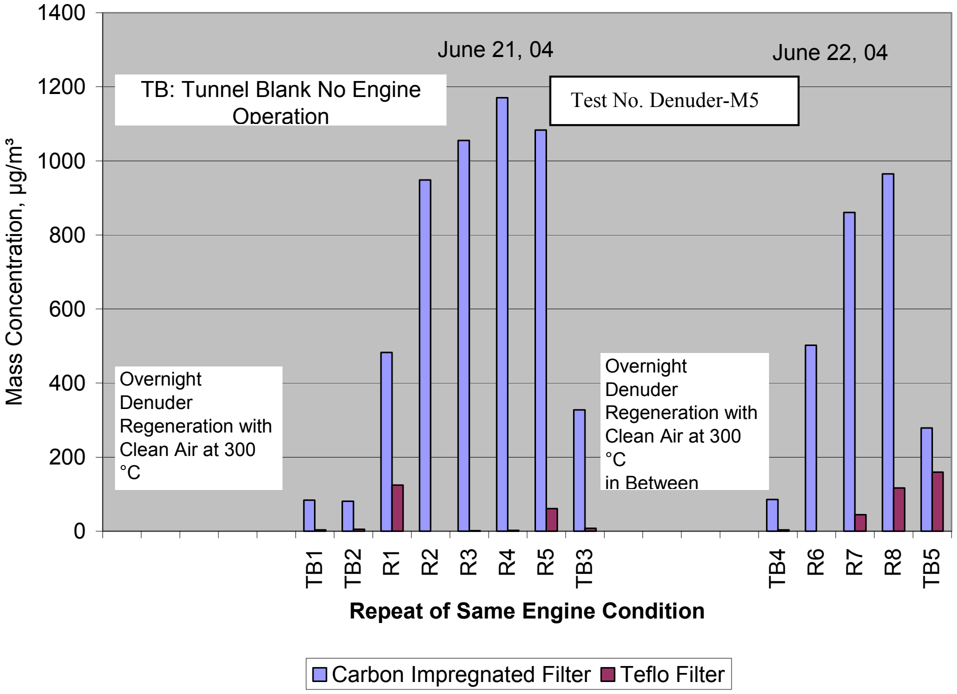

FIGURE 41. COMPARISON OF DILUTE MASS CONCENTRATION AFTER THE DENUDER USING CARBON IMPREGNATED AND TEFLO FILTERS

The data suggest that a carbon impregnated filter collects a significant level of positive artifact. Thus a carbon impregnated filter cannot be used as a back up filter to study particle loss downstream of a Teflo filter.

The Teflo collects a very small quantity of mass (< 5 µg) during 30 minutes of sampling downstream of the denuder thereby resulting in poor reproducibility due to weighing errors. The low level of PM mass collection with the Teflo filter is more realistic and more inline with the SMPS data than the carbon impregnated filter.

While the denuder is not capable of fully removing the organic carbon collected on a carbon impregnated filter, its efficiency of removing OC was around 70 percent, as shown in Figure 42. This efficiency was calculated based on TB data taken with and without the denuder.

The denuder did not seem to be very efficient in removing the organic carbon when using a carbon impregnated filter. It also seemed to cause an increase in PM emissions due to out-gassing of material with continuous use as shown in Figure 40 between R2, R3, and R4, and in Figure 41, between R1, R2, R3, and R4. Thus, the denuder seemed to cause an unnecessary complication to the measuring process due to out-gassing.

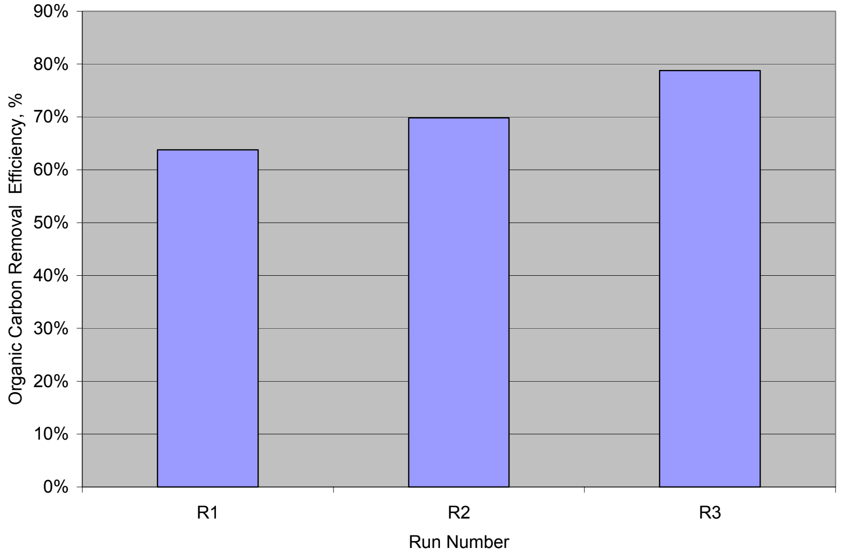

FIGURE 42. DENUDER ORGANIC CARBON REMOVAL EFFICIENCY USING A CARBON IMPREGNATED FILTER WITH AND WITHOUT A DENUDER

5.1.5 Denuder Performance-Quartz Filter

The carbon impregnated filter was removed from the EC/OC instrument and was replaced with a pair of Pall quartz filters. It was learned during the course of this part of the work that the initial conditioning required to clean a quartz filter in the EC/OC instrument is crucially important.

Figure 43 shows the temperature and the laser response when a new quartz filter is first exposed to helium followed by an oxygen/helium flow at high temperature. During helium exposure, the laser transmittance signal decreased suggesting soot formation in/on the filter, possibly due to pyrolysis of hydrocarbon compounds originally present in/on the filter. During the follow-up oxygen/helium exposure, the laser transmittance signal increased but not back to the original level suggesting that soot oxidation was not complete. This is important information relative to all EC/OC measurements taken in the past using quartz filters and the way the conditioning process is performed. If the new quartz filter is not first cleaned by exposing it to oxygen at high temperature, as shown in Figure 43, it may be contaminated with organic carbon or soot if it is first treated with helium.

Figure 44 shows the CO_2 response when exposing a new quartz filter to a high temperature. It also shows the good repeatability of the internal standard used for each run using methane. The amount of mass desorbed from a new filter was on the order of 38 to 40 µg of organic carbon.

Figure 45 shows organic carbon concentration in the secondary tunnel using a quartz filter in an EC/OC analyzer. The ND-30 minutes and ND-10 minutes were based on collecting data for a period of 30 minutes and 10 minutes, respectively, without the denuder. The D-10 minutes were based on a collection time of 10 minutes with the denuder. The concentration based on 30 minutes of collection time is less than half the concentration based on 10 minutes of collection time.

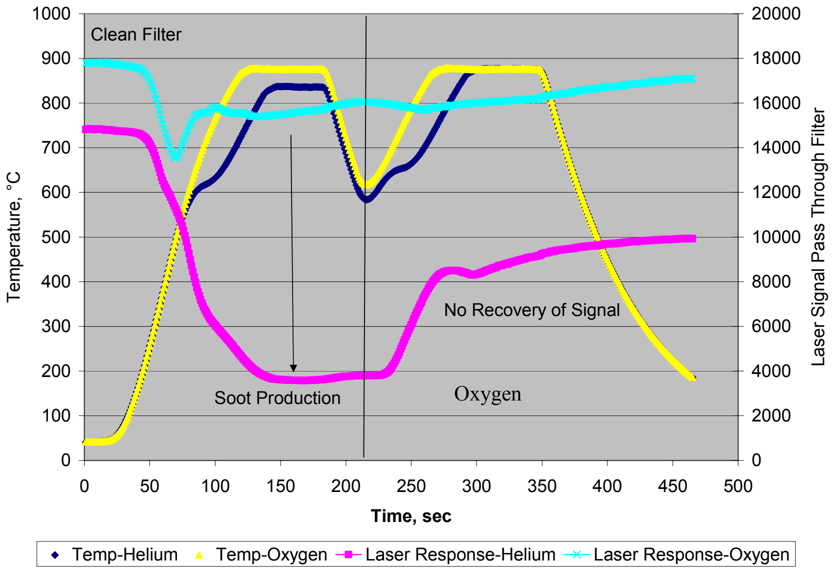

FIGURE 43. NEW QUARTZ FILTER CONDITIONING IN EC/OC INSTRUMENT

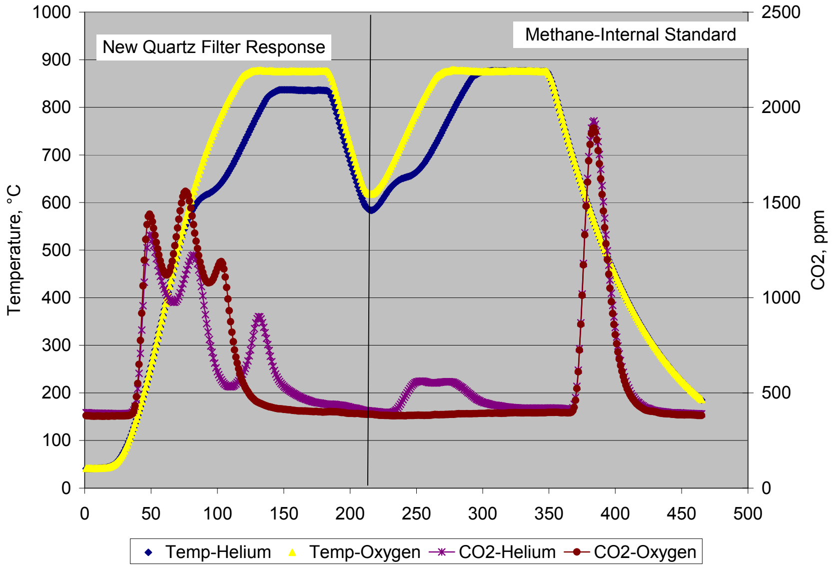

FIGURE 44. RESPONSE OF NEW QUARTZ FILTER DURING CONDITIONING

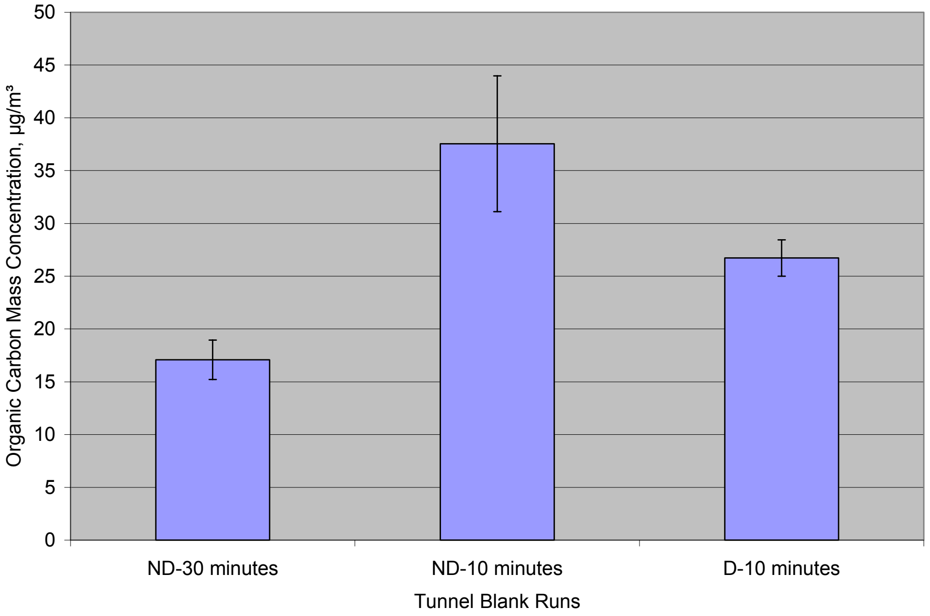

FIGURE 45. EFFECT OF SAMPLING TIME ON PM CONCENTRATION

Figure 46 shows a comparison between the concentration in the secondary dilution tunnel obtained with a pair of quartz filters used in the EC/OC analyzer and a single Teflo filter used in the main secondary tunnel. The sampling time with EC/OC was 15 minutes and the sampling time for Teflo was 30 minutes. The quartz collected about 3 µg of material at 4.5 lpm and the Teflo collected an average of 3 µg of material at a flow rate of about 50 lpm. Again, there was a significant difference in the concentration level obtained using the two methods.

Figure 47 shows the denuder efficiency relative to a pair of quartz filters. The efficiency of organic carbon removal ranged from 50 percent to less than 10 percent. Note also the deterioration in denuder performance with time.

5.1.6 Nature of Collected Particles

Figure 48 shows the nature of particles collected on a pair of quartz filters when collecting a sample from the dilution system without engine operation (Tunnel Blank). All material collected on the filter was organic carbon with no presence of soot. There seemed to be a peak around 300 °C and another small peak at higher temperature.

Figure 49, shows a similar graph to that of Figure 48, but with engine operation at rated speed with 10 percent load. Again all particles collected were mainly organic carbon similar to tunnel blank.

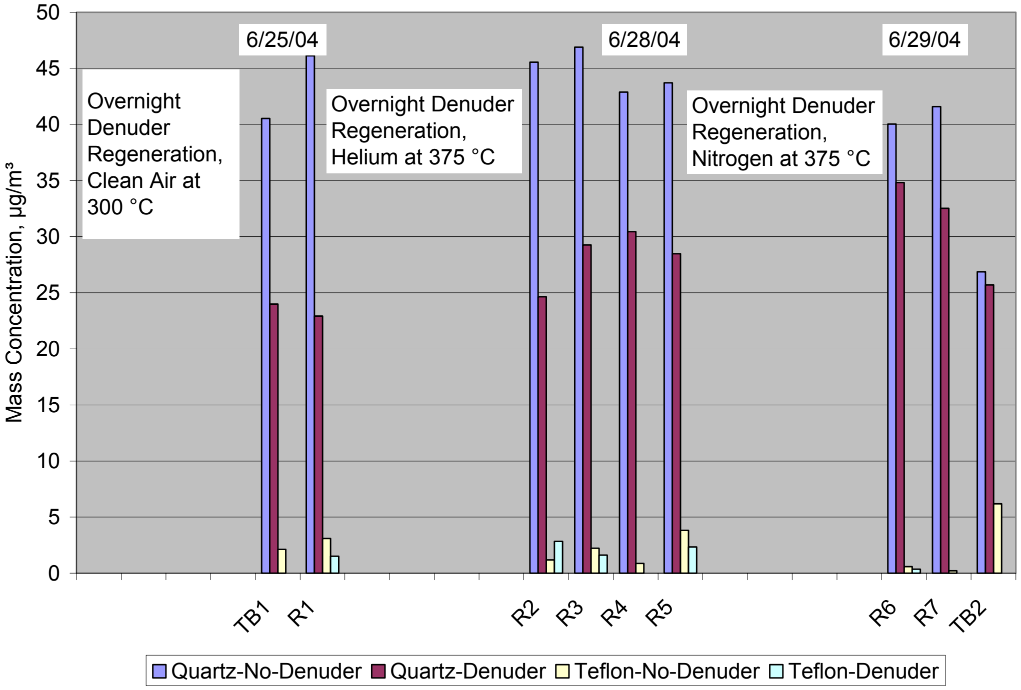

FIGURE 46. PERFORMANCE OF QUARTZ AND TEFLON FILTERS WITH AND WITHOUT THE DENUDER

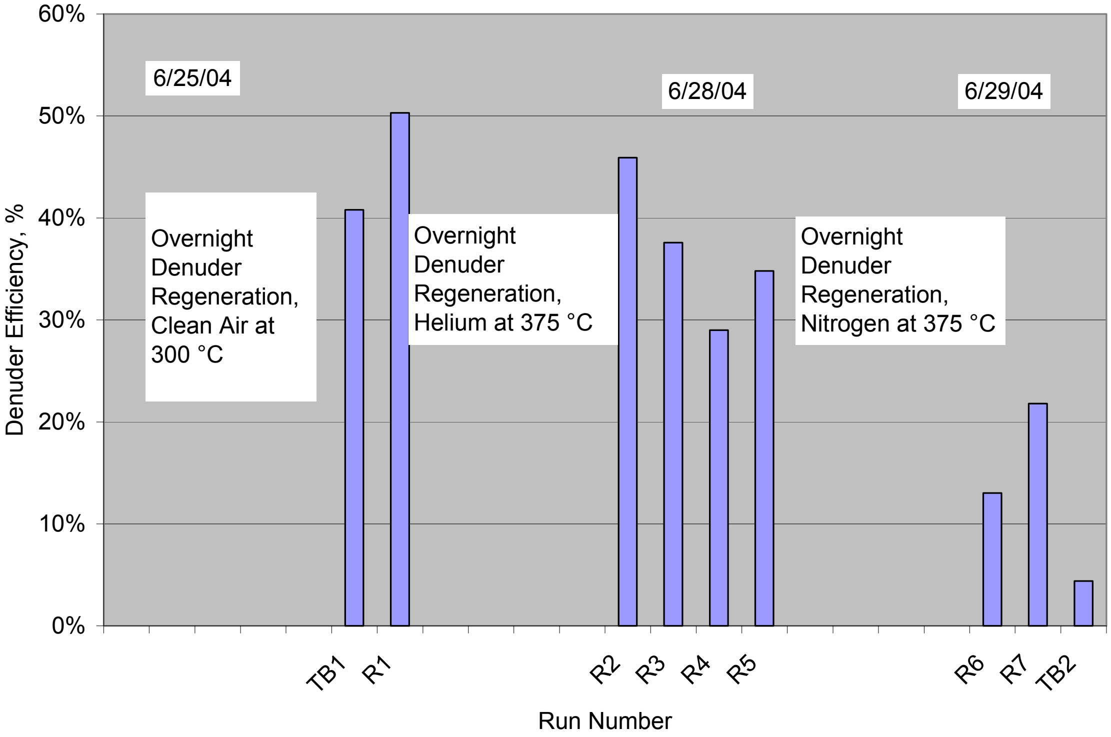

FIGURE 47. DENUDER EFFICIENCY USING AN EC/OC QUARTZ FILTER WITH AND WITHOUT DENUDER

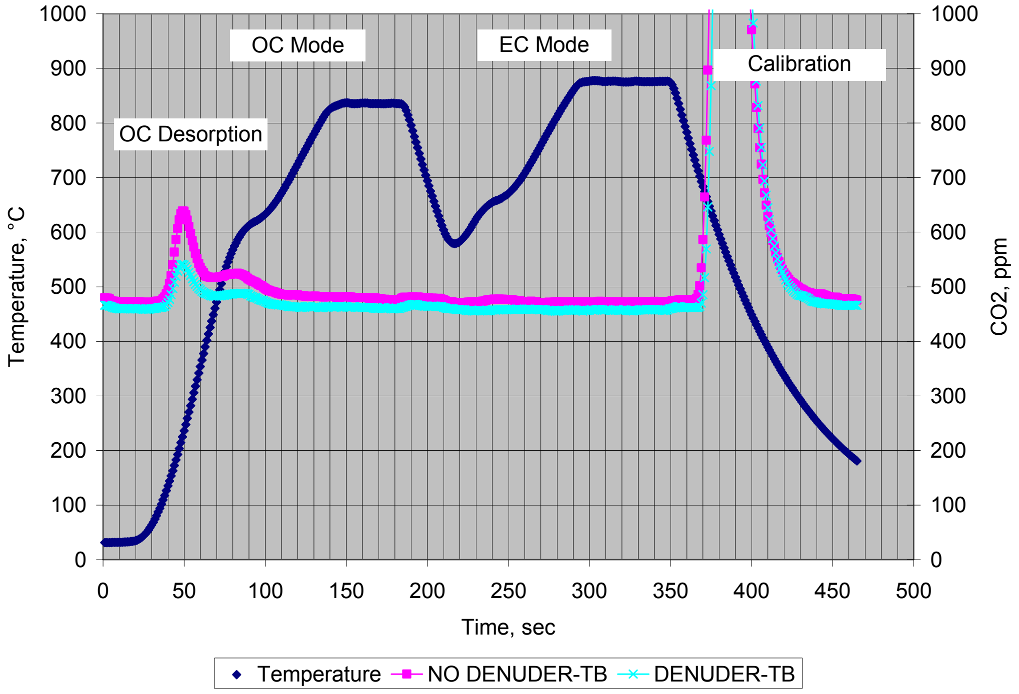

FIGURE 48. OC/EC PROFILE OF PM COLLECTED FOR TUNNEL BLANK

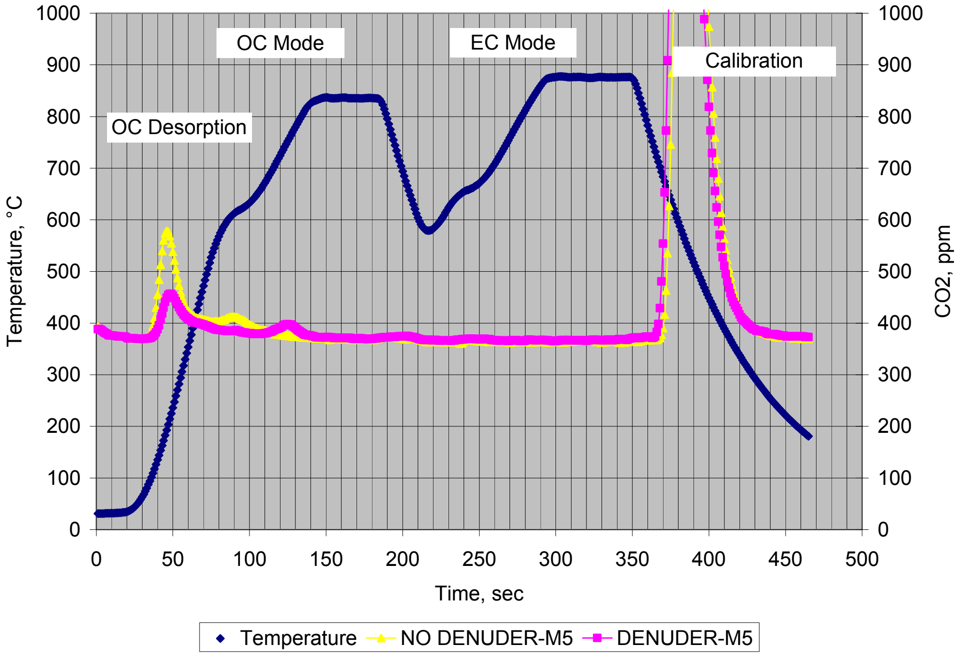

FIGURE 49. OC/EC PROFILE OF PM COLLECTED AT RATED SPEED, LIGHT LOAD

5.2 Filter Media

This section of the results will cover the effect of filter media pre-baking and conditioning on clean filter weight. It will also cover the effect of filter media on PM emissions for the FTP transient cycle and Mode A (Rated Power) steady-state operation with an engine exhaust configuration with and without a bypass around the CRT-DPF.

5.2.1 Clean Filter Media Pre-Baking and Conditioning

In order to minimize negative artifacts (filter weight loss) during PM collection on a filter at a temperature of 47 °C ± 5 °C, it was decided to pre-bake all filter media in a vacuum oven for 24 hours at a temperature of 52 °C, the maximum allowed filter face temperature for PM sampling. After filter pre-baking, a series of tests were conducted to study the effect of different conditioning times in the weighing chamber at a temperature of 22 °C ± 1 °C and a dew point of 9.5 °C ± 1 °C, as required by EPA 2007 PM sampling protocol. Two filters were chosen from each filter media and two filter weighings were performed per filter, per day, with the first weight taken after 30 minutes of conditioning time after pre-baking. Figures 50 through 54 show the average filter weight at different times and dates over a period of four days. Each filter weight was an average of five multiple repeat weighings. Generally, the difference between the maximum and the minimum average filter weight after 24 hours of conditioning was 50 µg, 4.5 µg, 1.5 µg, 2.5 µg, and 0.4 µg, for Quartz, Teflon, TX-40, Zefluor, and Teflo filters, respectively. Figure 55 shows that the average standard deviation in repeat multiple weighing was within 0.5 µg.

Figure 56 shows the effect of pre-baking on Teflo filter absolute weight. The limited set of data indicates that the Teflo filter looses about 5 µg after pre-baking.

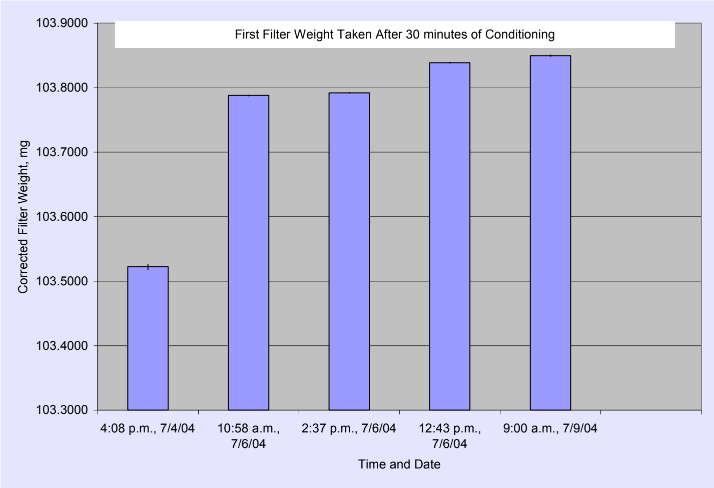

FIGURE 50. QUARTZ FILTER WEIGHT AT DIFFERENT CONDITIONING TIME

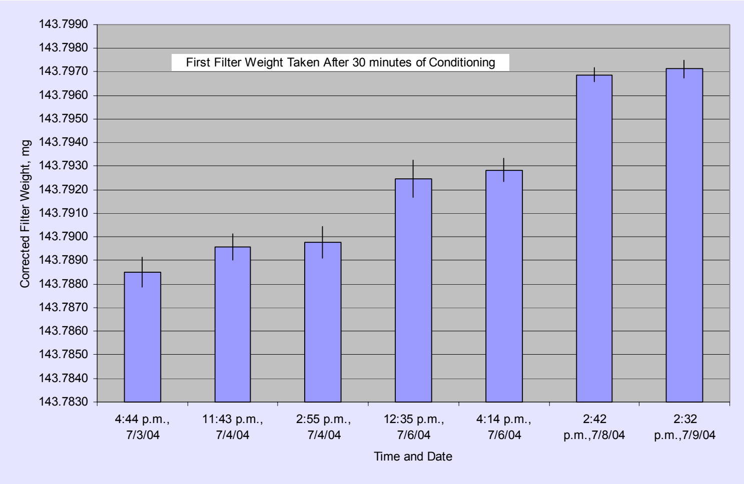

FIGURE 51. TEFLON FILTER WEIGHT AT DIFFERENT CONDITIONING TIME

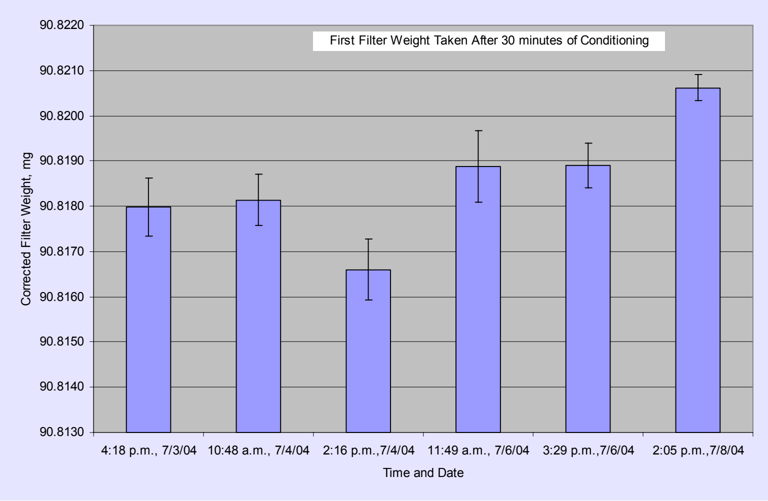

FIGURE 52. TX-40 FILTER WEIGHT AT DIFFERENT CONDITIONING TIME

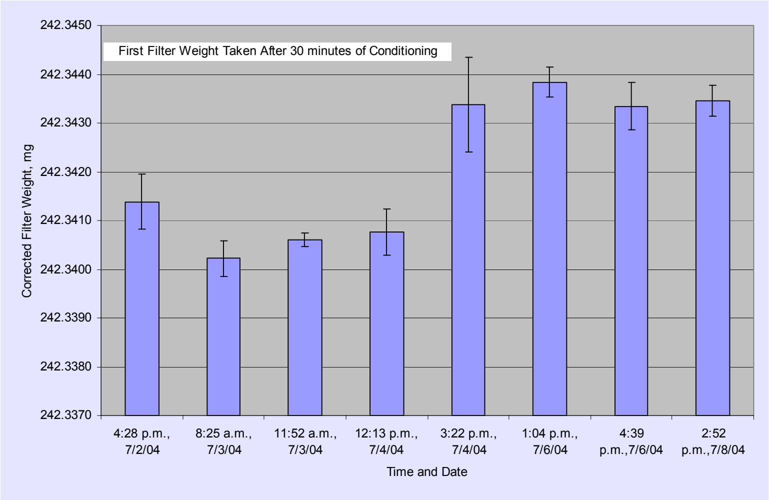

FIGURE 53. ZEFLUOR FILTER WEIGHT AT DIFFERENT CONDITIONING TIME

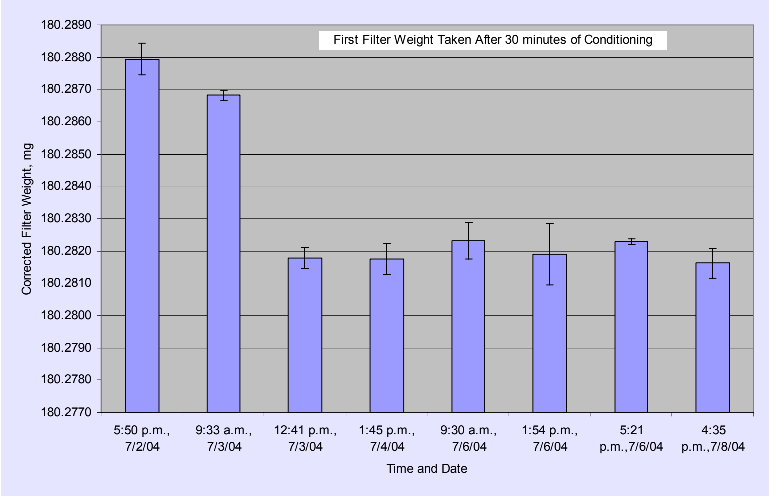

FIGURE 54. TEFLO FILTER WEIGHT AT DIFFERENT CONDITIONING TIME

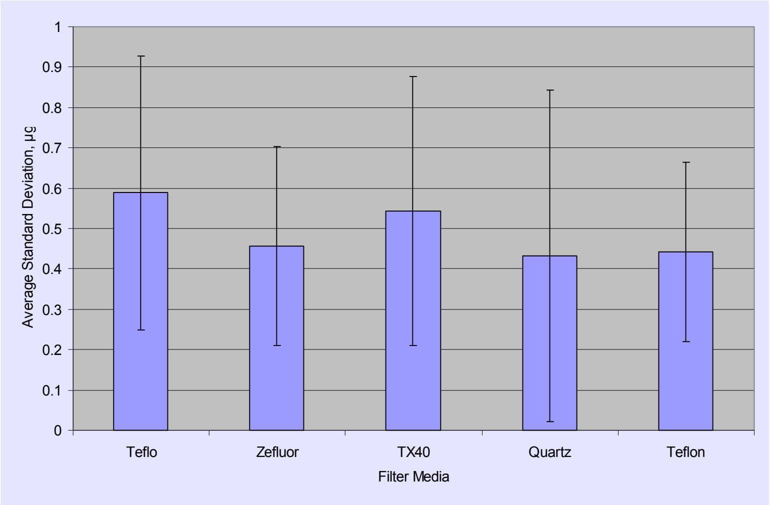

FIGURE 55. AVERAGE VARIABILITY IN WEIGHING DIFFERENT FILTER MEDIA MULTIPLE CONSECUTIVE TIMES

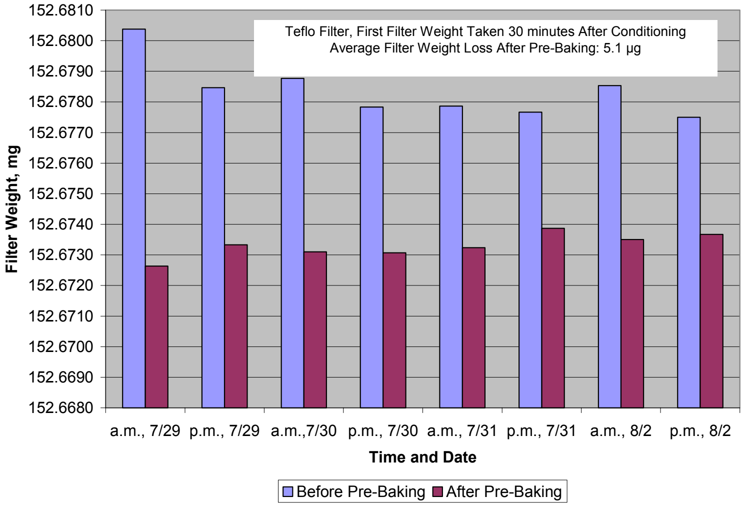

FIGURE 56. FILTER WEIGHT LOSS DUE TO PRE-BAKING AT 52 °C

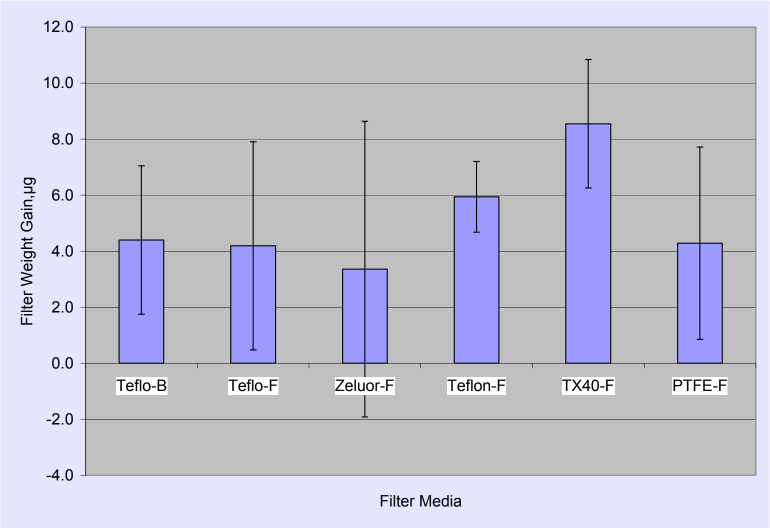

FIGURE 57. AVERAGE VARIABILITY IN FILTER WEIGHT GAIN FOR DIFFERENT FILTER MEDIA

5.2.2 Teflo Filter Pre-Baking

For this project, filters were pre-baked for 24 hours in a vacuum oven at 52 °C, the maximum allowable filter face temperature by EPA, to desorb materials from the filter media that may otherwise be desorbed during testing, contributing to a filter negative artifact. Filter pre-baking in earlier E-66 work improved data quality, particularly with filter media such as Zefluor. While filter pre-baking seemed to be a good practice, it was important to validate whether or not filter pre-baking is necessary.

To investigate the effect of filter pre-baking on PM measurement using Teflo filters, seven pairs of each pre-baked and unbaked Teflo filters were used. Each pre-baked or unbaked filter pair, primary and a backup filter, was used alternately for one hot-start FTP transient run for a total of fourteen runs. The backup filter was used to quantify the positive artifact on the primary filter.

Figure 58 shows the performance of the pre-baked and unbaked filters using a CRT-DPF with a bypass. Table 14 presents the average, standard deviation, and coefficient of variation in PM emissions for each set of seven filters. The data showed no significant difference in performance between the pre-baked and unbaked filters. The average PM emission based on pre-baked or unbaked primary filter was 0.0073 g/hp-hr with a coefficient of variation of 4 percent. The primary filter weight gain over a transient test was on the order of 60 µg.

The data also indicated that the PM emission rate associated with the backup filter was relatively small compared to the primary filter. The filter weight gain on a backup filter during a transient cycle ranged between ± 3 µg, a value that is close to the range of clean filter weight variability of about ± 2.5 µg. Thus, the backup filter weight gain for a transient cycle (positive artifact) appears to be negligible and within the uncertainty of the filter weighing measurement.

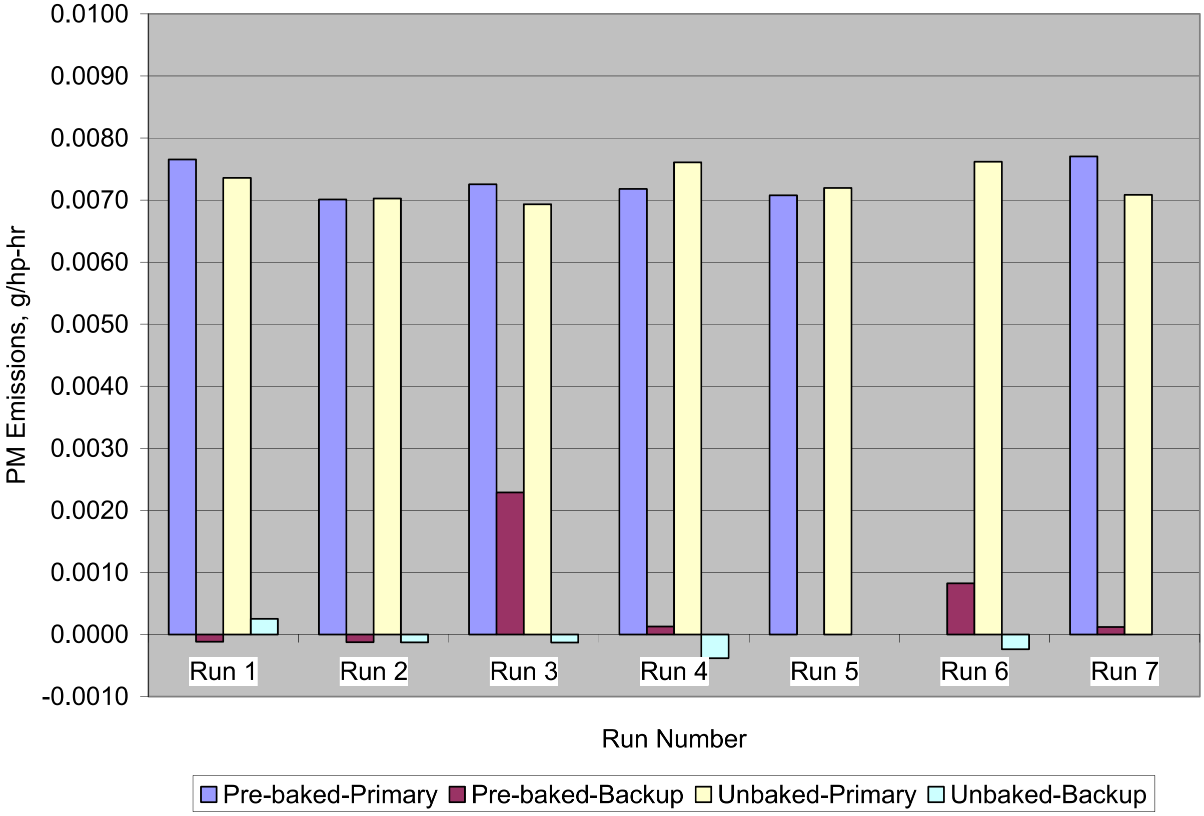

FIGURE 58. COMPARISON IN PARTICULATE MATTER EMISSION PERFORMANCE BETWEEN PRE-BAKED AND UNBAKED TEFLO FILTERS USING THE HOT-START FTP TRANSIENT CYCLE

TABLE 14. SUMMARY OF PM EMISSION PERFORMANCE USING SEVEN REPEATS OF PRE-BAKED AND UNBAKED TEFLO FILTERS USING THE HOT-START FTP TRANSIENT CYCLE

Teflon Filter Condition	Baked		Unbaked	
	Primary Baked g/hp-hr	Backup Baked g/hp-hr	Primary Unbaked g/hp-hr	Backup Unbaked g/hp-hr
Average	0.00730	0.00052	0.00730	-0.00009
Std. dev.	0.00030	0.00093	0.00028	0.00020
COV, %	4.0	180	3.8	220

In conclusion, there seemed to be no difference in PM emission performance between a pre-baked and unbaked Teflo filter. Furthermore, the filter weight gain of a backup filter was negligible and within the uncertainty of the filter weighing method, suggesting that the positive artifact collected by the primary filter was also negligible. As a result, a backup Teflo filter was inadequate for quantifying a correction for any positive artifact on the primary filter.

5.2.3 Filter Media-CRT-DPF

The data discussed in this section includes FTP transient testing and steady-state testing at rated engine power. The exhaust configuration included the CRT-DPF without any exhaust bypass around it.

5.2.3.1 FTP Transient Testing

Figure 59 shows the variability in filter weight gain for different repeats of the FTP transient cycle using Teflo filters. The filter weight gain for all filter media was very small, below 10 µg. The low filter weight gain and the variability in the measurement made it very difficult to compare the performance of different filter media, although the average filter weight gain of the TX-40 was the highest.

The low filter weight gain indicated that the engine emission level was much lower than the required 2007 PM emission level. Figure 60 shows that the average PM emissions with all filter media was below 10 percent of the 2007 PM emission standard of 0.01 g/hp-hr, except the data with the Quartz filter which were at about 20 percent of the standard. It is important to note, however, that the data reported with the Quartz was based on two-filters used in series. Using a single filter should nearly cut the measured emission value by half.

Figures 61 and 62 indicate that the total particle number emissions, particularly nanoparticles below 18 nm in diameter, increase sharply at high engine power conditions with high exhaust temperature, especially during the third 5-minute segment of the transient cycle. While engine power is not expected to have any influence on particle formation downstream of a trap, it is known that high exhaust temperature promotes the conversion of SO_2 to SO_3 on a platinum loaded oxidation catalyst like that found in a CRT ahead of the bare wall flow trap. The presence of SO_3 in the exhaust leads to sulfuric acid formation, and nucleation and growth of nanoparticles during dilution and cooling of the hot exhaust. This phenomenon was observed many times in the past with the use of diesel fuel with about 350 ppm sulfur. It is interesting that this phenomenon continues to occur with the combination of ultra-low sulfur fuel and low sulfur lube oil. This phenomenon is very important and warrants further investigation.

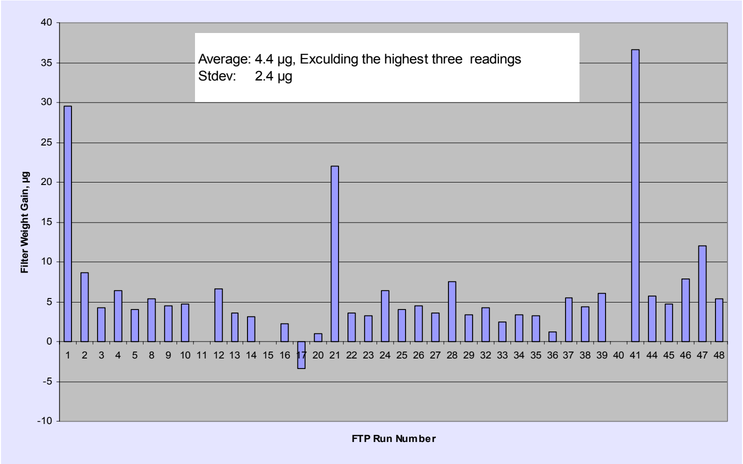

FIGURE 59. VARIABILITY IN FILTER WEIGHT GAIN AT A PM EMISSION LEVEL EQUIVALENT TO 5 PERCENT OF 2007 STANDARD

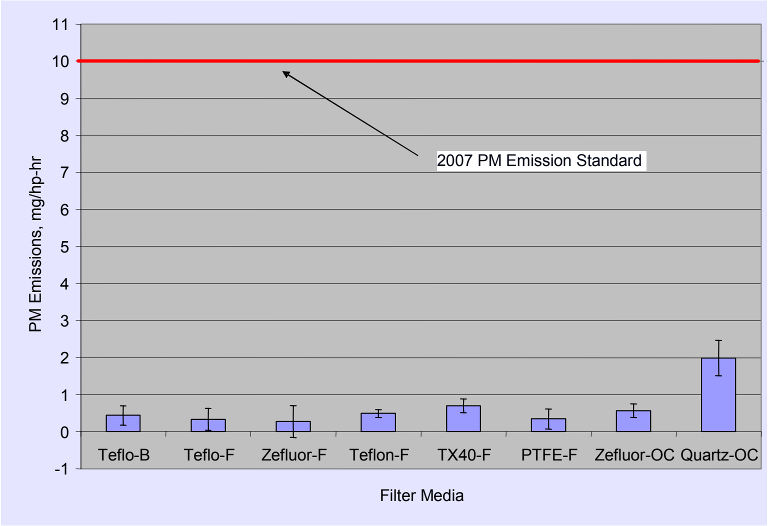

FIGURE 60. PM EMISSIONS DURING FTP TRANSIENT CYCLE USING DIFFERENT FILTER MEDIA

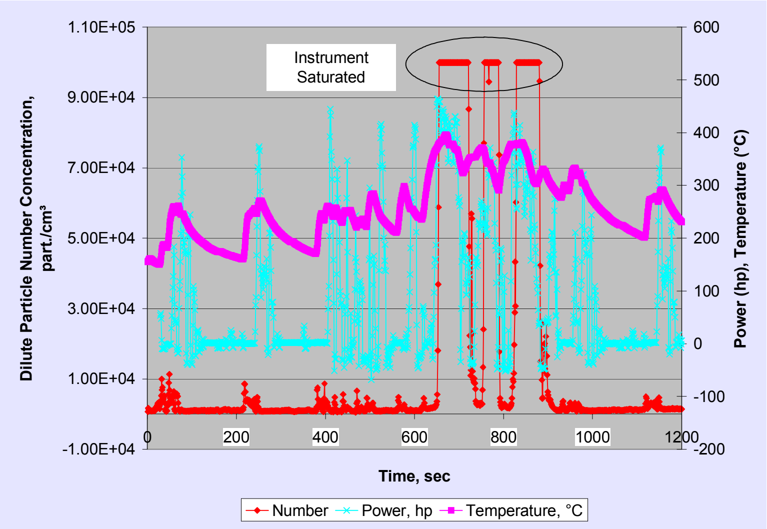

FIGURE 61. PARTICLE NUMBER EMISSION PROFILE DURING THE FTP TRANSIENT CYCLE

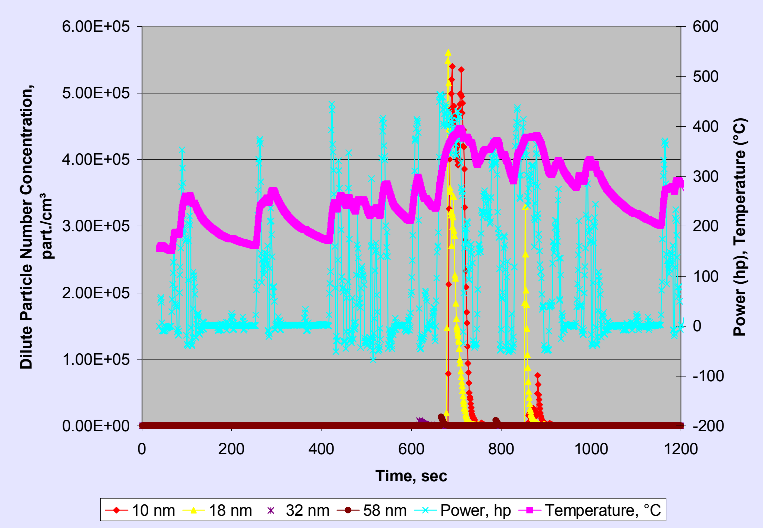

FIGURE 62. NANOPARTICLE NUMBER EMISSION PROFILE DURING THE FTP TRANSIENT CYCLE

5.2.3.2 Steady-State Testing at Rated Engine Power

The filter weight gain during a 20-minute steady-state test at engine rated power was higher than that collected during the FTP, but still very low, on the order of 10 µg. Figure 63 shows the filter weight gain using a Teflo filter for a total of 48 repeats. The average filter weight gain was 9.99 µg and the standard deviation was 3.57 µg.

Figure 64 shows the average filter weight gain with each of the filter media based on a total of seven repeats. While no formal statistical comparison was made, it is clear that the TX-40 and the Quartz using the Horiba MEXA 1370 gave at least twice the filter weight gain reported using other filter media. The Quartz backup filter gave nearly the same, or slightly higher, weight gain than the Teflon and the PTFE-PP. By subtracting the weight gain of the backup filter from that of the primary Quartz filter, the weight gain based on the difference became similar to that of Teflon and the PTFE-PP. Based on the Horiba MEXA 1370, the sulfate level was about 20 percent of the total weight gain. This was true for both the primary and the backup filter. The presence of sulfate on the backup filter suggests that gas phase sulfuric acid may adsorb onto a filter media and contribute to a positive artifact just like organic carbon. This issue warrants further investigation.

5.2.4 Filter Media-Exhaust Bypass Around CRT-DPF

Figure 65 shows Teflo filter weight again during many repeats of the hot-start FTP transient cycle. Good repeatability was obtained with an average filter weight gain of 63 µg, a standard deviation of 5.6 µg, and a coefficient of variation of 9 percent. Similarly, Figure 66 shows the brake specific PM emissions. The average emission level was 0.007 g/hp-hr with a standard deviation of 0.0006 g/hp-hr and a coefficient of variation of 8.5 percent. These data showed a significant improvement over the data reported for an emission level at below ten percent of the 2007 PM emission standard that had a coefficient of variation of more than 50 percent, as shown in Figure 59.

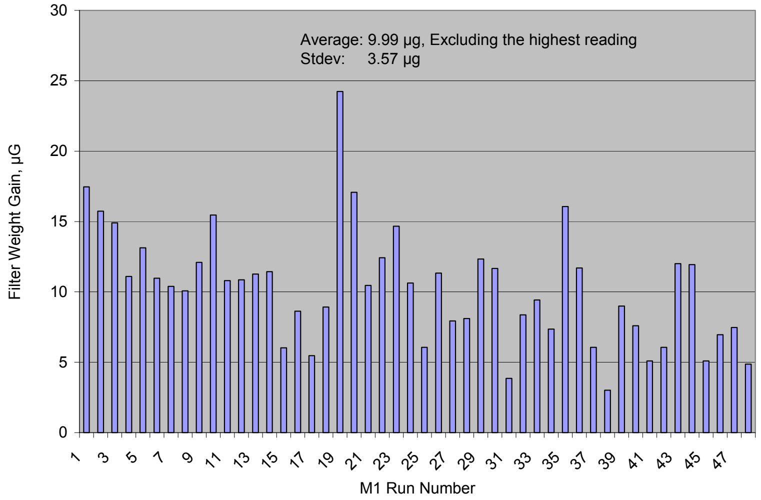

FIGURE 63. VARIABILITY IN FILTER WEIGHT GAIN USING A TEFLO FILTER FOR THE ENGINE RATED POWER CONDITION

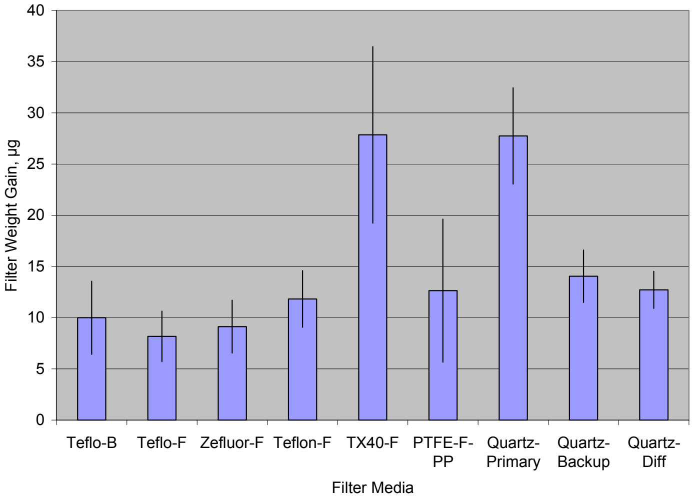

FIGURE 64. AVERAGE FILTER WEIGHT GAIN USING DIFFERENT FILTER MEDIA FOR ENGINE RATED POWER CONDITION

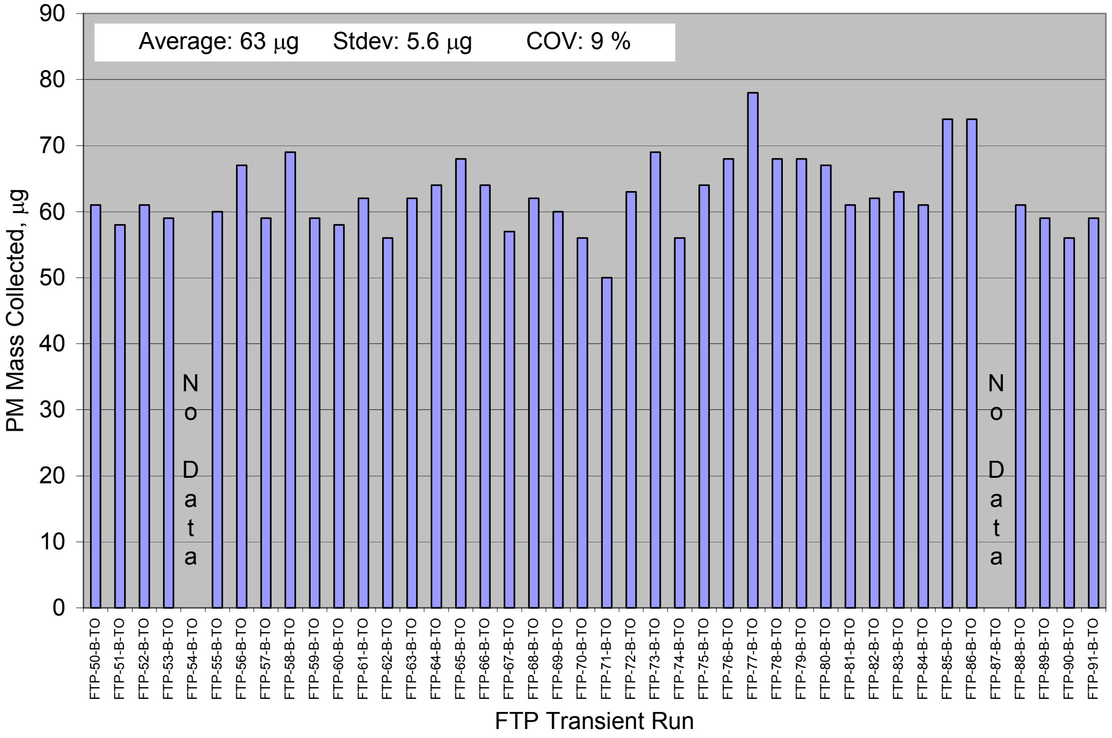

FIGURE 65. PM MASS COLLECTED ON A TEFLO FILTER FOR MULTIPLE REPEATS OF THE HOT-START FTP TRANSIENT CYCLE

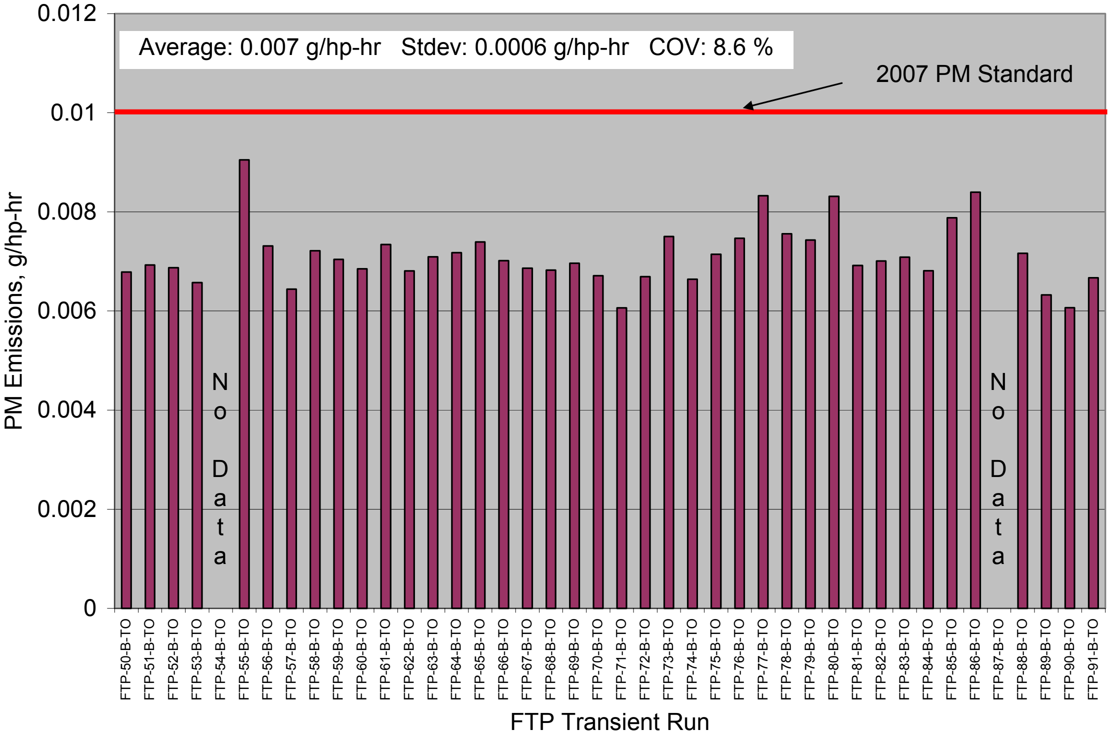

FIGURE 66. BRAKE-SPECIFIC PM EMISSIONS FOR MULTIPLE REPEATS OF THE HOT-START FTP TRANSIENT CYCLE USING A TEFLO FILTER

Figure 67 shows the average PM mass collected during a hot-start FTP transient cycle using different filter media. The different filter media showed a similar performance, except for the TX-40 where a slight increase in PM mass was observed. Figure 68 is similar to Figure 67 but it shows the brake specific emission level obtained using different filter media. It is worth noting that the Teflo filter seemed to give a low coefficient of variation of less than 5 percent for a total of seven repeats of the transient cycle. The coefficient of variation with the rest of the filters ranged from 10 percent to 18 percent, with the highest COV for the TX-40 filter media.

Figure 69 shows the PM composition using the Sunset Laboratory elemental carbon/ organic carbon (EC/OC) instrument. With the new exhaust configuration, 54 percent of the PM collected on the filter was elemental carbon and 46 percent was organic carbon. It is worth noting that when the CRT was used without a bypass, the PM composition was mainly organic carbon and no elemental carbon was detected. It is also worth noting that two quartz filters were used and the amount of organic carbon may be dominated by positive artifact. Thus, the organic fraction in other filter media may be much lower.

Due to the high presence of elemental carbon in the exhaust, the positive artifact fraction associated with organic carbon adsorption onto the non-quartz filters may become a small fraction of the overall PM emissions. In addition, if elemental carbon is present in the dilute exhaust, the surface area of those particles may act as an adsorption site while suspended in air as well as after depositing on a filter during PM collection, regardless of the nature of the filter media. Thus, with the new exhaust configuration, the PM collected on a TX-40 filter was only about 12 percent higher than the total PM mass collected on a Teflo filter. The rest of the filters showed a similar performance, but the Teflo filter showed the least coefficient of variation among the different filter media. Thus, it is recommended that the Teflo filter be used for the remainder of the E-66 program.

Figures 70 through 74 show the average particle number concentration profile for different size particles of 10 nm, 18 nm, 32 nm, 58 nm, and 100 nm. The average is based on four different random repeats of the hot-start FTP transient cycle. The data were very repeatable. The number concentration of 10 and 18 nm particles, using CRT-DPF with bypass, was more than a factor of ten lower than the concentration observed using the CRT-DPF without bypass, as shown in Figure 62. This suggests that the presence of soot downstream of the CRT-DPF with bypass may act as an adsorption site for volatile and semi-volatile species during dilution and cooling of the exhaust, and limit the nucleation of volatile nanoparticles.

Figure 75 shows the average volume concentration for the different particle sizes measured under transient operation. The point of Figure 75 is to show that the volume or mass of PM emission was dominated by 58 nm and 100 nm particles that are highly likely to be mainly soot particles, further supporting that the mass emissions were dominated by elemental carbon.

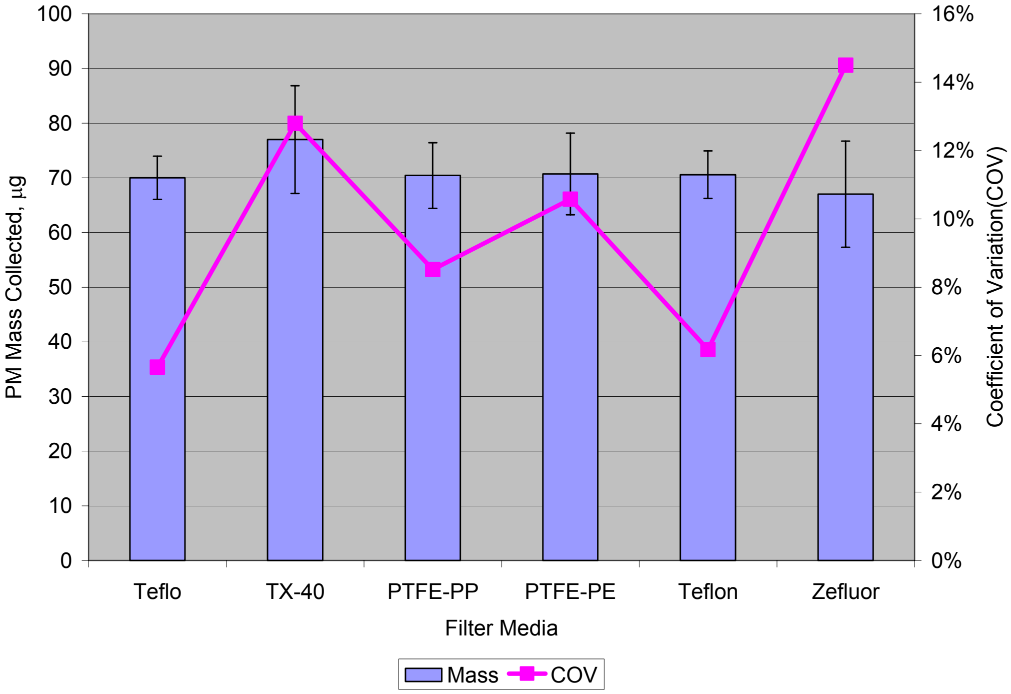

FIGURE 67. AVERAGE PM MASS COLLECTION USING DIFFERENT FILTER MEDIA

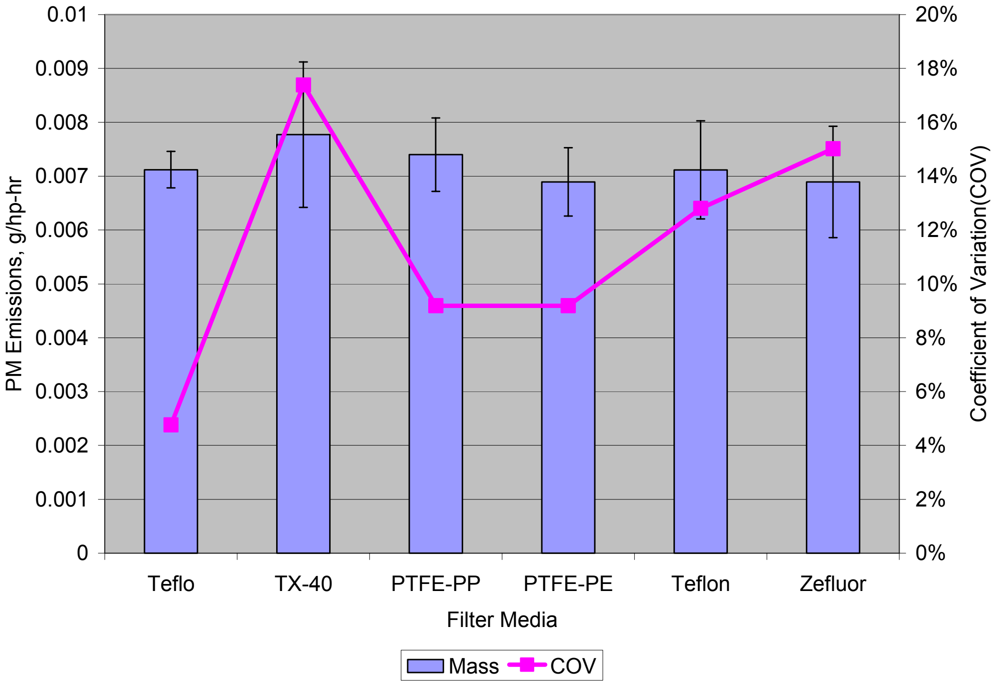

FIGURE 68. AVERAGE BRAKE-SPECIFIC PM EMISSIONS USING DIFFERENT FILTER MEDIA

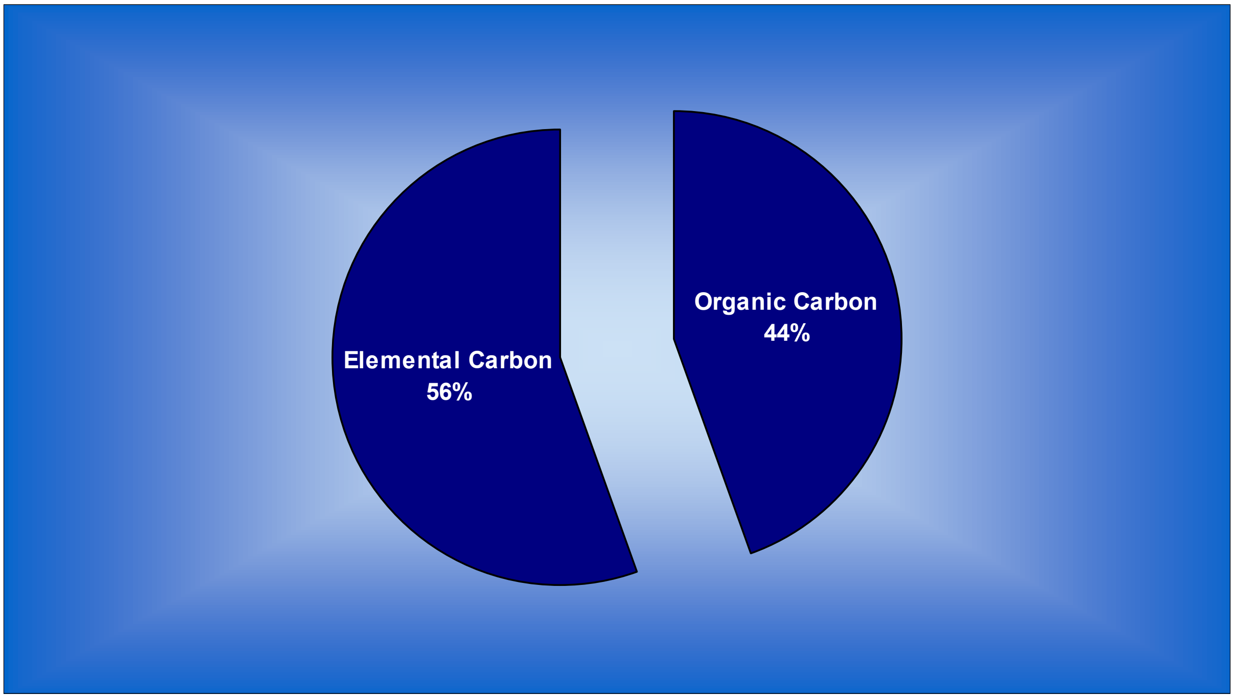

FIGURE 69. PM COMPOSITION FOR THE HOT-START FTP TRANSIENT CYCLE USING TWO QUARTZ FILTERS

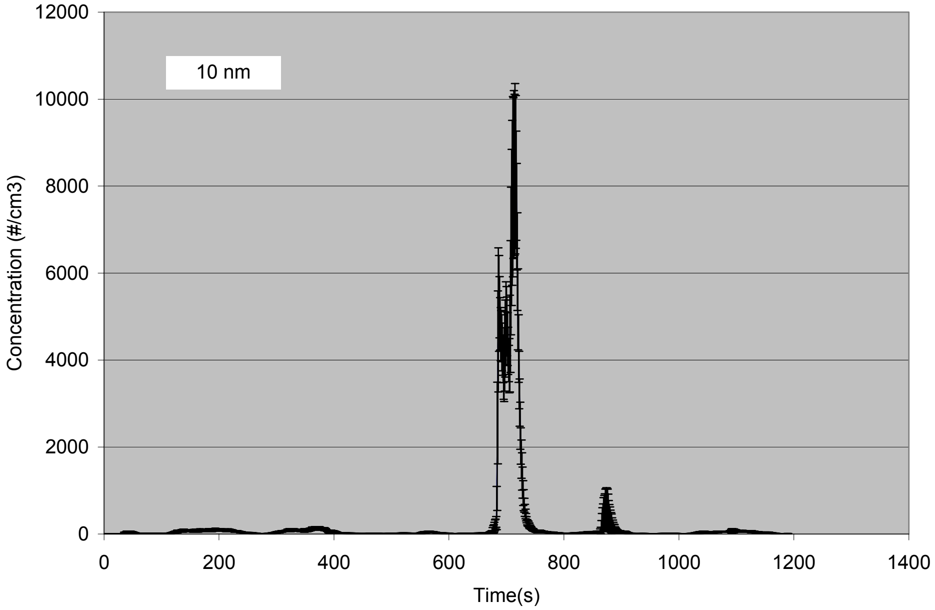

FIGURE 70. AVERAGE PARTICLE NUMBER CONCENTRATION FOR 10 NM PARTICLES

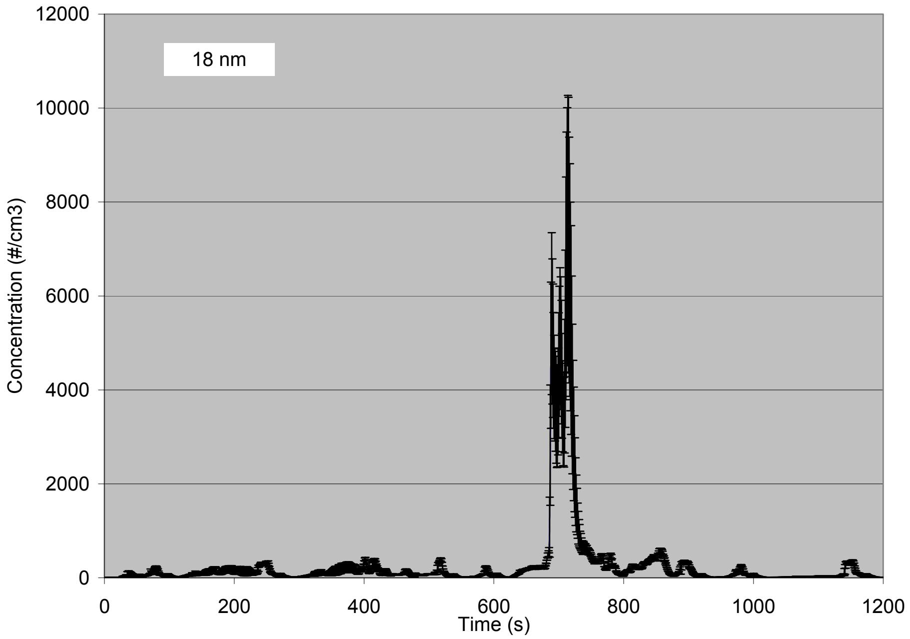

FIGURE 71. AVERAGE PARTICLE NUMBER CONCENTRATION FOR 18 NM PARTICLES

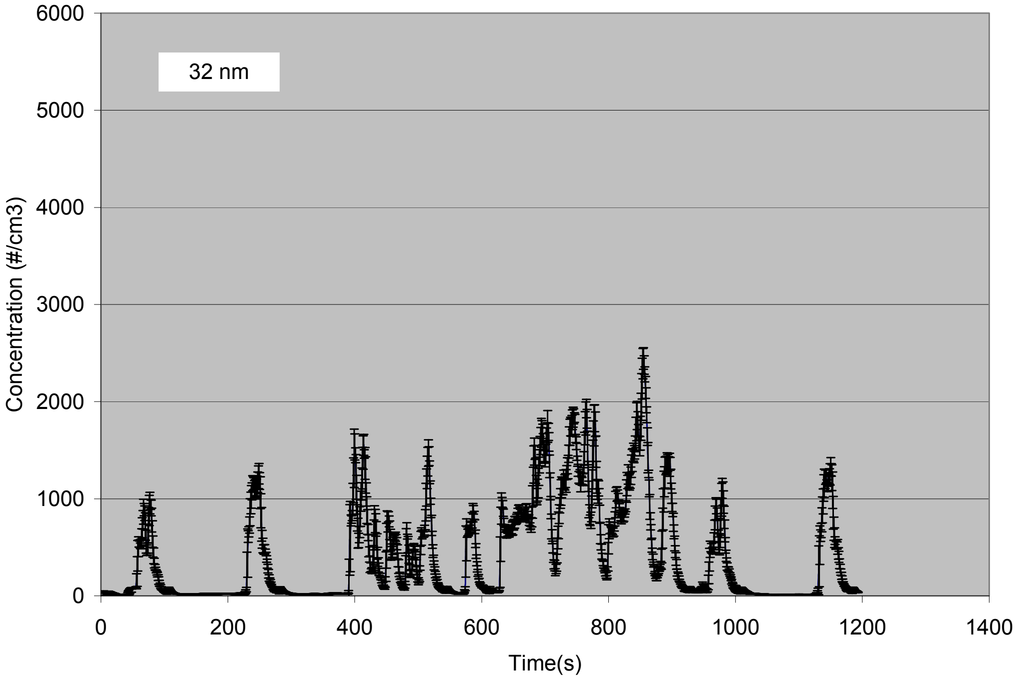

FIGURE 72. AVERAGE PARTICLE NUMBER CONCENTRATION FOR 32 NM PARTICLES

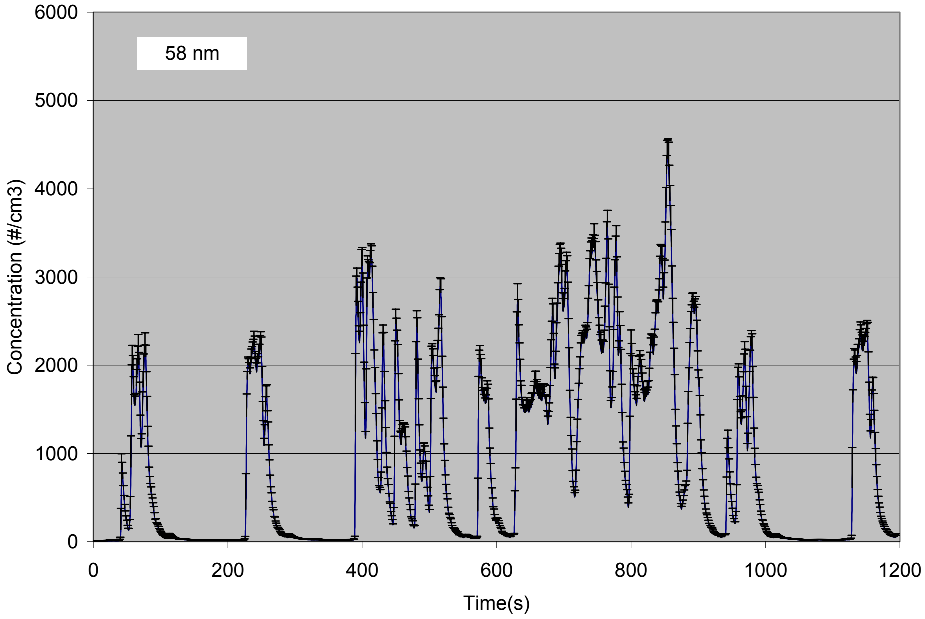

FIGURE 73. AVERAGE PARTICLE NUMBER CONCENTRATION FOR 58 NM PARTICLES

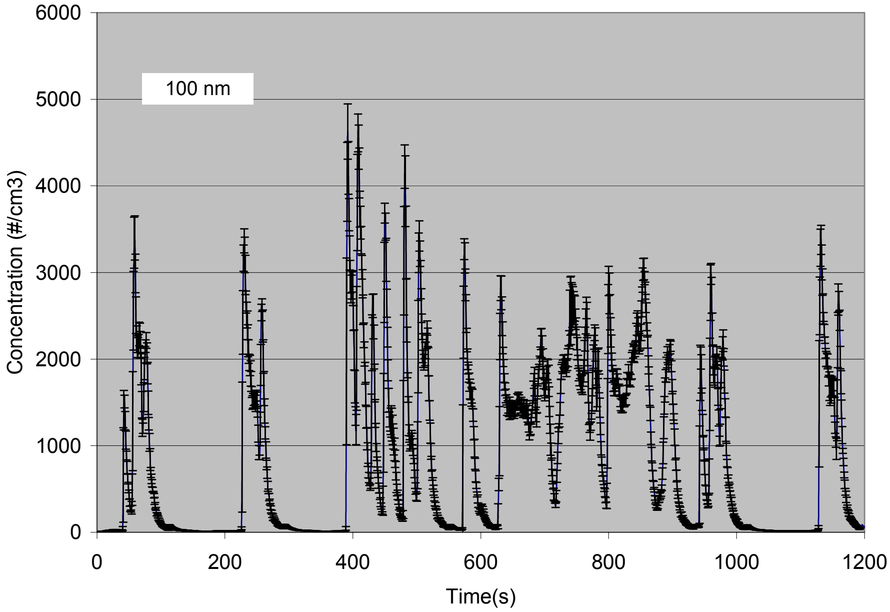

FIGURE 74. AVERAGE PARTICLE NUMBER CONCENTRATION FOR 100 NM PARTICLES

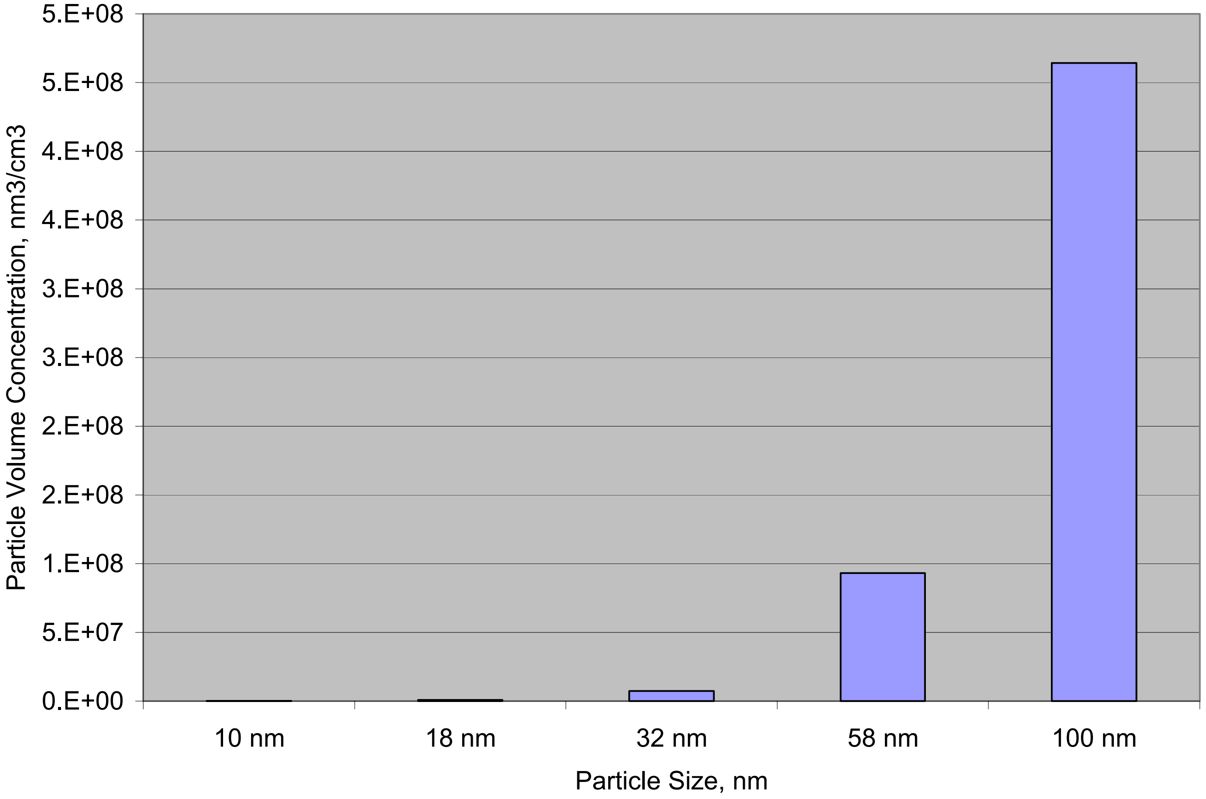

FIGURE 75. DILUTE AVERAGE PARTICLE VOLUME CONCENTRATION FOR THE HOT-START FTP TRANSIENT CYCLE

5.3 Filter Face Velocity

5.3.1 FTP Transient

The filter face velocity experiments were performed using two identical secondary sampling systems, A and B, designated for a fixed filter face temperature of 47 °C ±5 °C and 25 °C ± 5 °C throughout all experiments, respectively. Two filter loading times, 20 minutes and 40 minutes, using a single or duplicate hot-start FTP transient runs, respectively, were used to investigate the effect of filter loading time on PM emission measurement. The four nominal filter face velocities targeted during this work included 24 cm/sec, 60 cm/sec, 90 cm/sec, and 120 cm/sec. Figure 76 shows the actual filter face velocity for each condition plotted against the targeted filter face velocity. There was a deviation of 10 to 15 percent from the targeted velocities but the overall desired range of filter face velocities of 24 cm/sec to 120 cm/sec was examined.

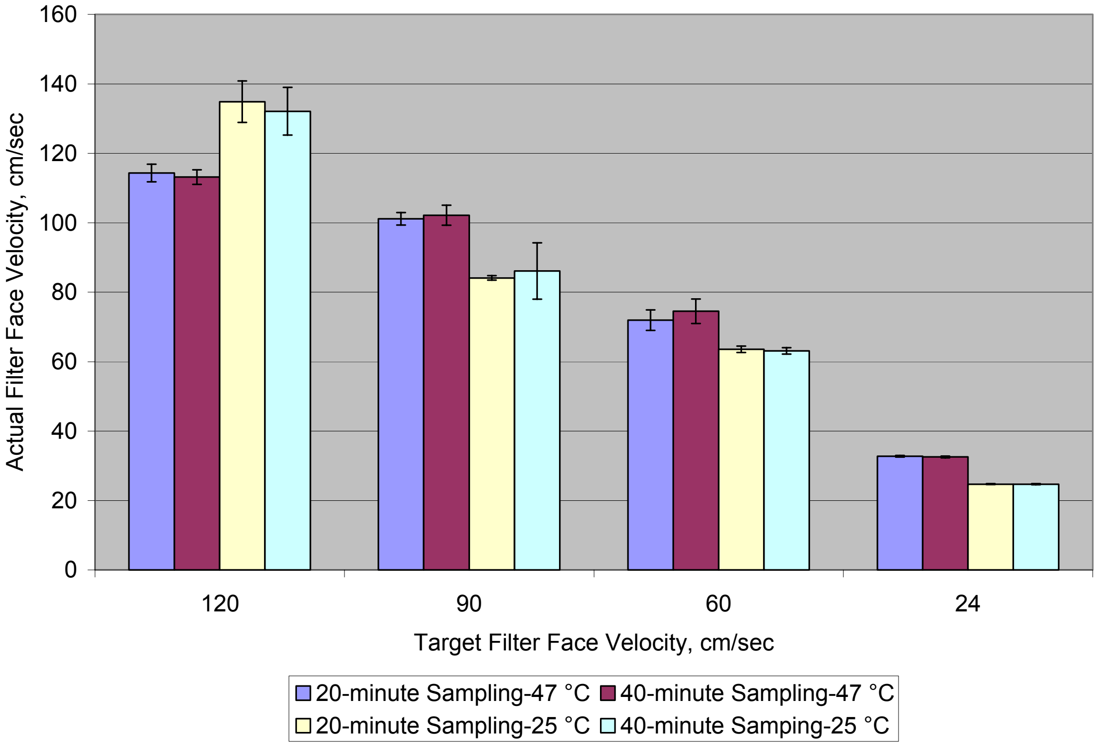

FIGURE 76. ACTUAL FILTER FACE VELOCITY USED DURING EXPERIMENTS PLOTTED AGAINST THE TARGET FILTER FACE VELOCITY

Figure 77 shows PM emissions for different filter face velocities, filter face temperature of 47 °C, and 20-minute and 40-minute loading times. Lower filter face velocity appears to lead to higher PM emissions for both the 20-minute and 40-minute loading times.

The longer loading time of 40 minutes seems to produce a lower PM emission level compared with a shorter loading time of 20 minutes, except at the lowest filter face velocity of 33 cm /sec, where the PM emission level was similar.

Figure 78 is similar to Figure 3, but the filter face temperature is 25 °C instead of 47 °C. The results at 25 °C were similar to those at 47 °C, except at a filter face velocity of 24 cm/sec at 25 °C, where the 40-minute loading time led to a noticeably lower PM emission level compared to the 20-minute loading time.

Figure 79 shows a comparison in PM emissions between a filter face temperature of 47 °C and 25 °C for a filter loading time of 20 minutes. At both temperatures, PM generally increased as filter face velocity decreased. In addition, the PM emission level is similar at the different filter temperatures over a small range of face velocities.

Figure 80 is similar to Figure 79, but it is for a filter loading time of 40 minutes. The data are relatively similar, except at the lowest filter face velocity, where the emission at a filter face temperature of 47 °C was higher than at 25 °C.

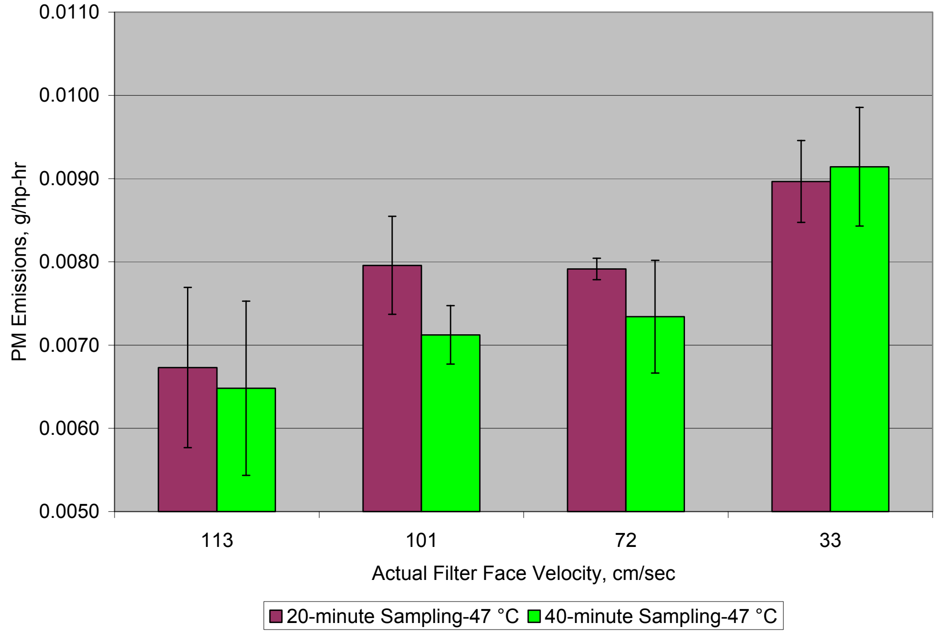

FIGURE 77. PM EMISSIONS AT DIFFERENT FILTER FACE VELOCITY AND LOADING TIME FOR A FILTER FACE TEMPERATURE OF 47 °C

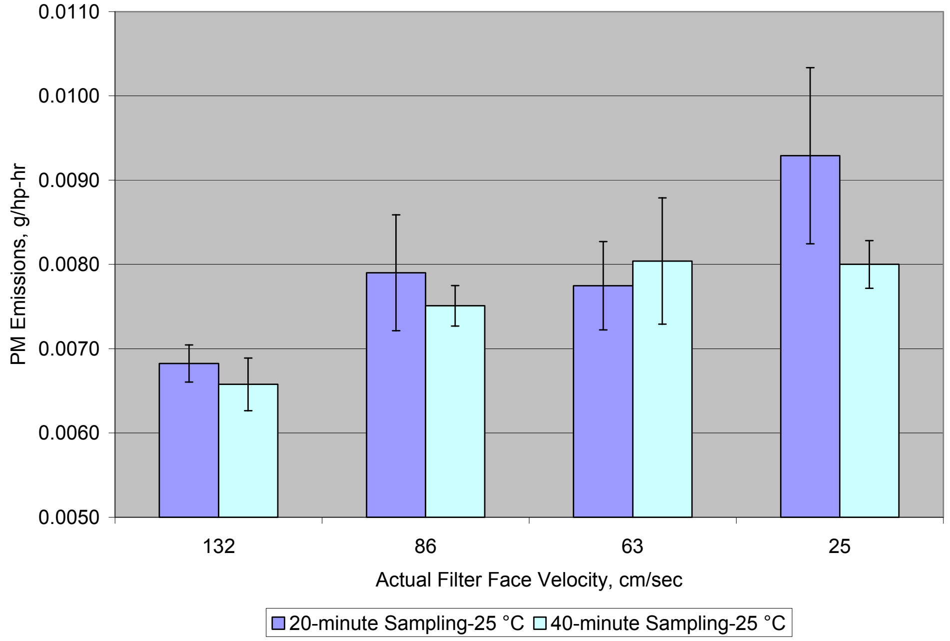

FIGURE 78. PM EMISSIONS AT DIFFERENT FILTER FACE VELOCITY AND LOADING TIME FOR A FILTER FACE TEMPERATURE OF 25 °C

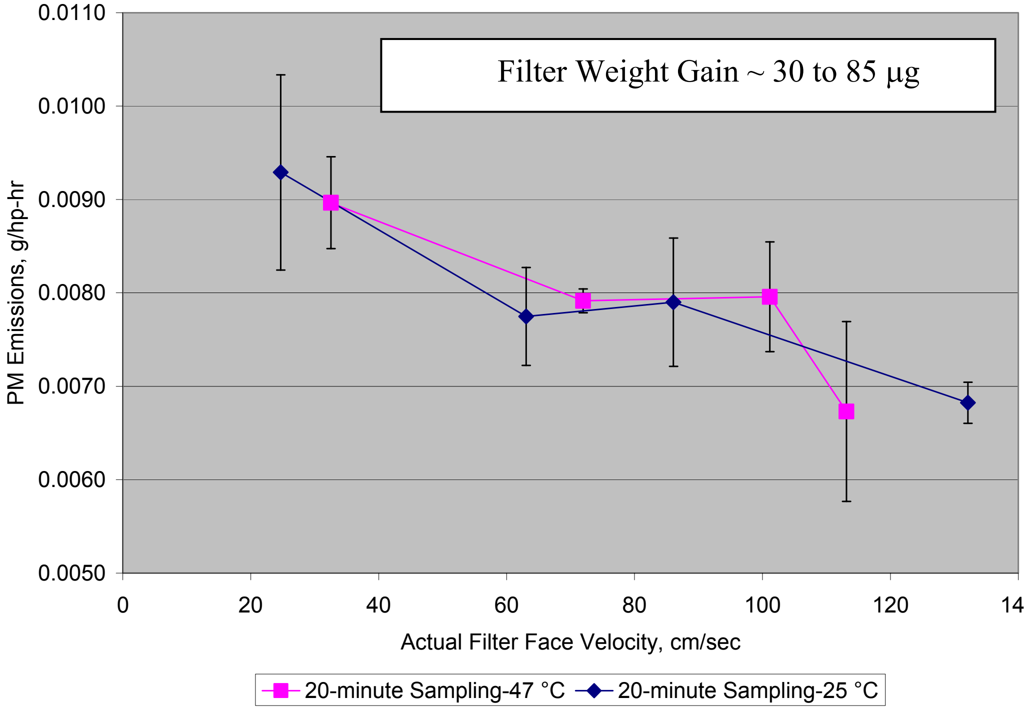

FIGURE 79. PM EMISSIONS AT DIFFERENT FILTER FACE VELOCITY AND TEMPERATURE WITH 20-MINUTE LOADING TIME

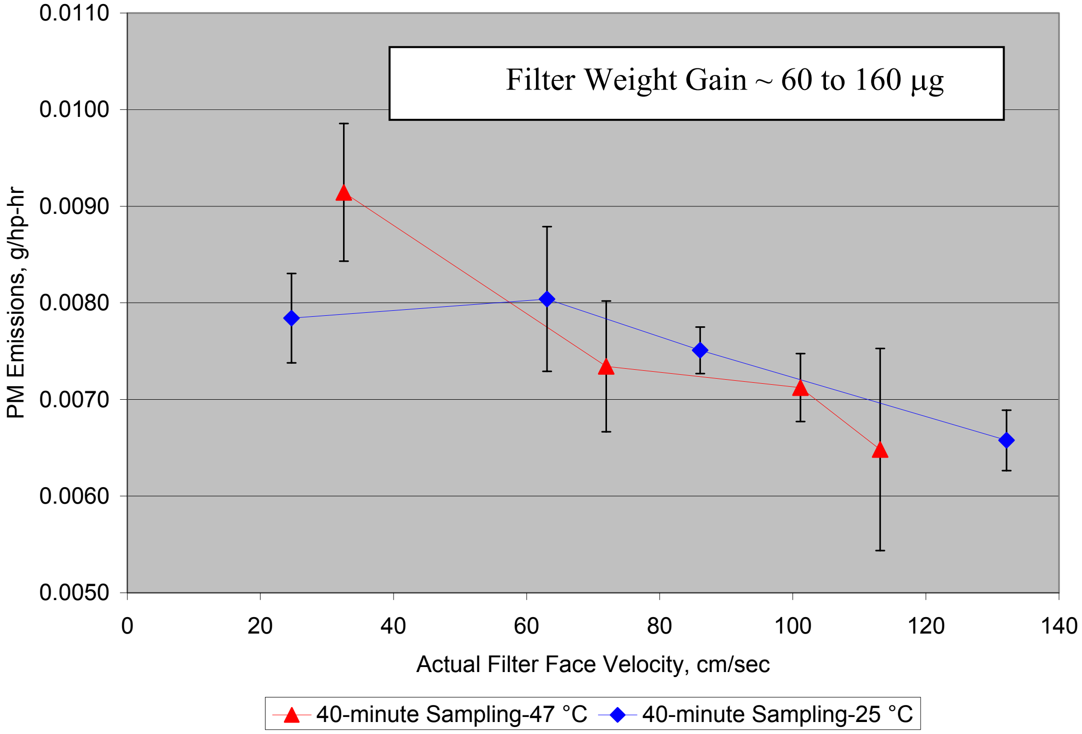

FIGURE 80. PM EMISSIONS AT DIFFERENT FILTER FACE VELOCITY AND TEMPERATURE WITH 40-MINUTE LOADING TIME

Figure 81 shows the normalized emissions relative to the lowest filter face velocity. The data indicate that the PM emission at a filter face velocity between 60 cm/sec and 100 cm/sec is about 15 to 10 percent lower than measured using a filter face velocity of 24 to 33 cm/sec. The PM emission using a filter face velocity between 110 cm/sec and 140 cm/sec is about 25 percent lower than measured using 24 to 33 cm/sec.

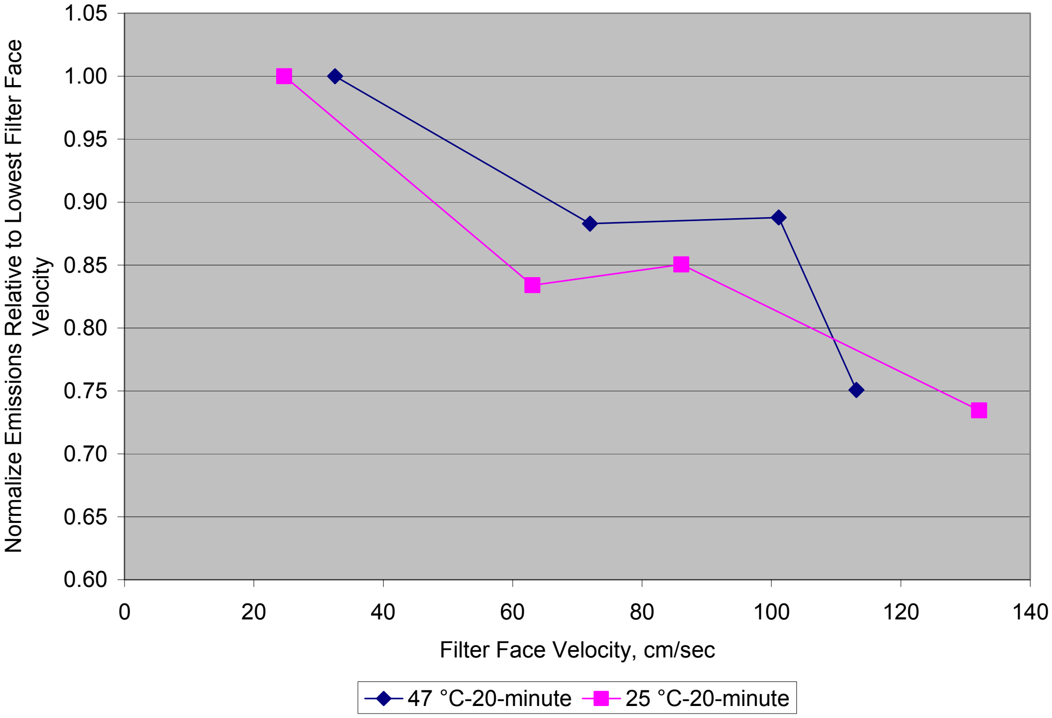

FIGURE 81. NORMALIZED EMISSIONS RELATIVE TO THE LOWEST FILTER FACE VELOCITY

5.3.2 Light-Load Steady-State Condition (Rated Speed, 10 Percent Load)

Figure 82 shows the brake-specific PM emissions at different filter face velocities for light-load engine operation, Mode C. The PM emissions increased at lower filter face velocity similar to the trend observed with the FTP transient cycle. However, the relative change in PM emissions as a function of filter face velocity was much higher for Mode C in comparison to the FTP. For the FTP, the reduction in PM emission as a result of changing filter face velocity from 60 cm/sec to 90 cm/sec was about 15 percent, compared to more than 60 percent for Mode C, as shown in Figure 83.

It is known from previous work that Mode C has more than 90 percent SOF. With high volatile PM composition, it is likely that the filter face velocity will have a greater influence on PM emissions.

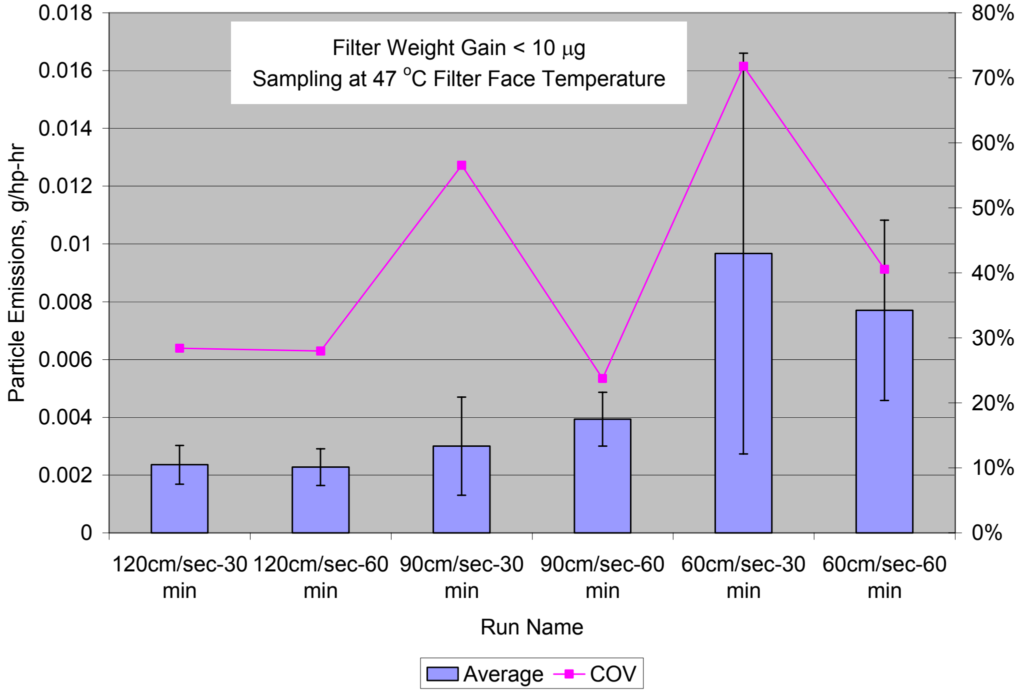

FIGURE 82. EFFECT OF FILTER FACE VELOCITY ON PM EMISSIONS AT LIGHT-LOAD ENGINE OPERATION

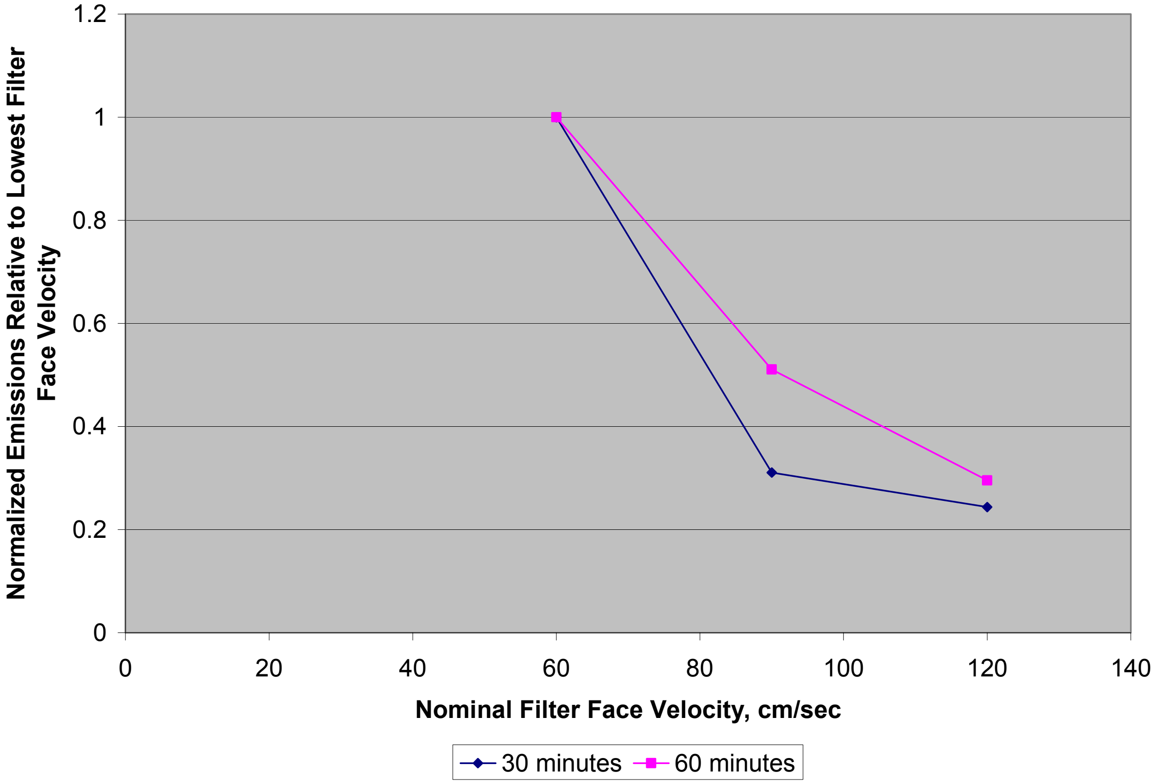

FIGURE 83. NORMALIZED EMISSIONS RELATIVE TO LOWEST FILTER FACE VELOCITY

In this work, the filter face velocity experiments were performed at the same dilution ratio. Thus, gas and particle concentrations upstream of the filter used for PM collection were similar, independent of the filter face velocity. At high filter face velocity, equilibrium between the gas phase and the filter adsorption sites may be reached in shorter time than at a low filter face velocity. If equilibrium is reached early during filter sampling, additional sampling time will contribute to lower PM emissions because the additional volume going through the filter is not contributing to any PM loading. This may be the case here in explaining why at higher filter face velocity, the PM emission is lower.

The loading of soot on the filter may also change the state of equilibrium between the gas phase and filter phase due to differences between the adsorbtivity of the filter material and the soot.

Real time instruments like the DMM-230 and the EEPS should not be sensitive to changes in filter face velocity or flow at a fixed dilution ratio. During the filter face velocity experiments at Mode C, data were also collected with the DMM-230 upstream of the filter used for PM collection. Figure 84 shows the concentration observed using the DMM-230, compared to that observed using the filter-based technique. The DMM-230 was insensitive to changes in filter face velocity and also was much more effective in measuring the emission level; even at an equivalent filter face velocity of 24 cm/sec, because the concentration upstream of the filter was the same, regardless of the filter face velocity.

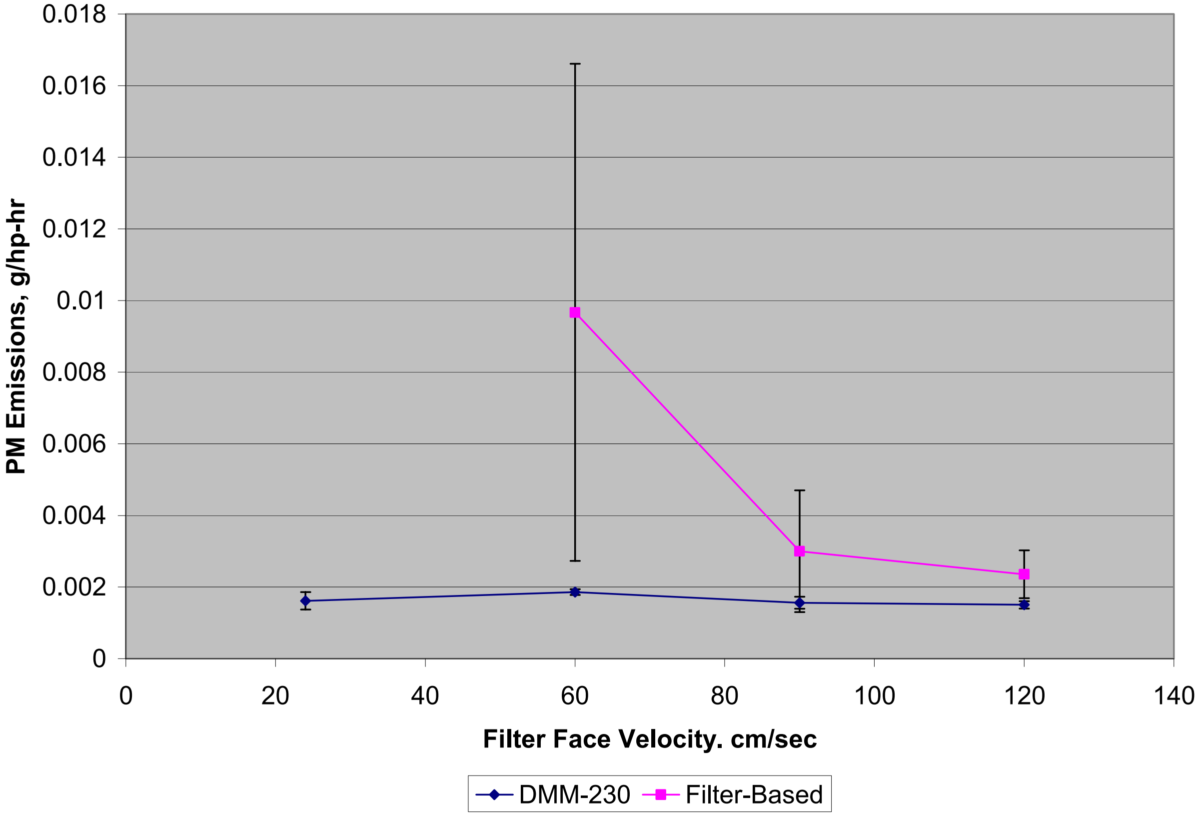

FIGURE 84. COMPARISON BETWEEN FILTER-BASED AND DMM-230-BASED PM EMISSIONS AT DIFFERENT FILTER FACE VELOCITIES

5.4 Filter-Based and Instrument-Based PM Measurement

The SMPS, EEPS, DMM-230, and QCM were all used to sample from a location immediately upstream of the filter used for PM collection. This section discusses the results obtained in comparing the filter-based technique with the different real time instruments at very different steady-state and transient engine operating conditions that included six steady-state modes and two transients including the FTP and the ETC. The filter face velocity was about 90 cm/sec and the secondary dilution ratio was about 2.5.

The QCM results are not included because of some technical issues that will be discussed separately in 5.4.3.

5.4.1 Comparison with Filter-Based Method

Figure 85 shows a comparison between the filter-based method, SMPS, EEPS, and DMM-230. For the SMPS and the EEPS, a density of 1 g/cm3 was used to convert from number to mass, assuming spherical particles. Good correlation was obtained between the DMM-230, EEPS, SMPS, and the filter-based method.

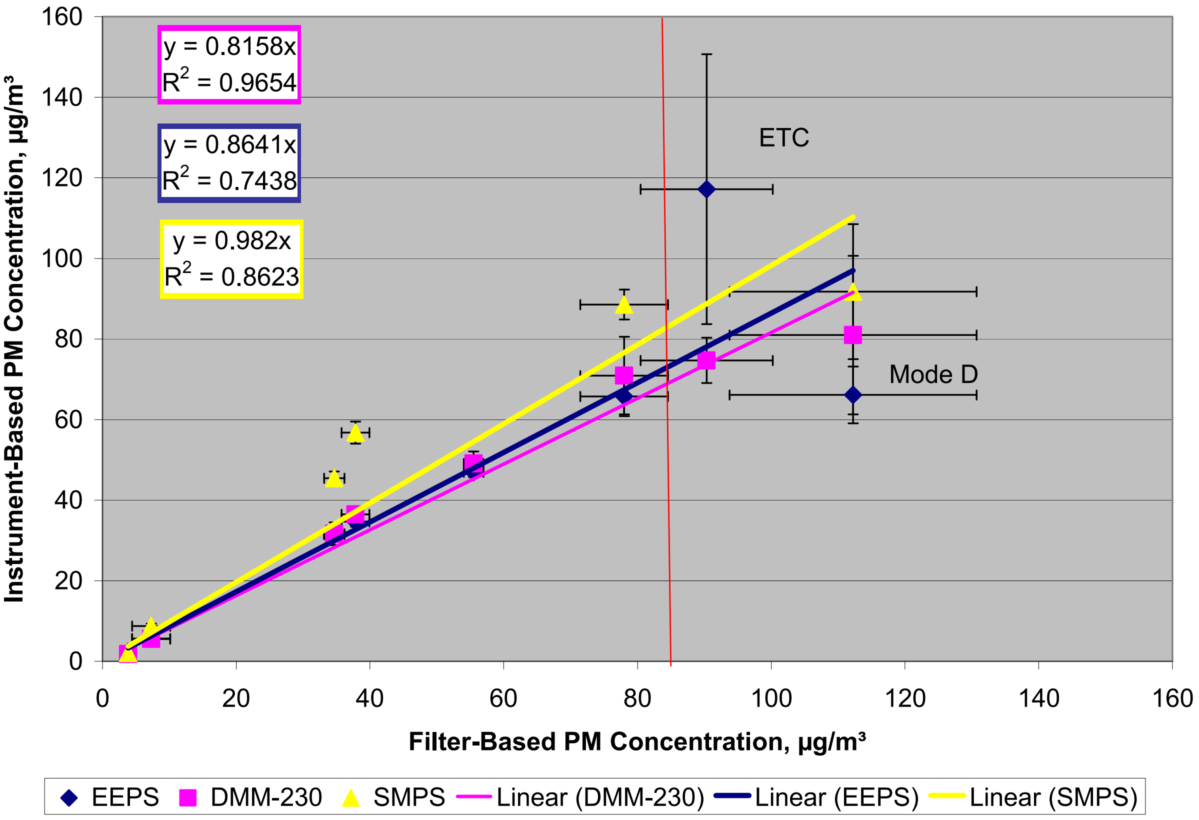

FIGURE 85. CORRELATION BETWEEN INSTRUMENT-BASED AND FILTER-BASED PM MEASUREMENT. (AVERAGE DATA BASED ON SEVEN REPEATS)

For the DMM-230, good correlation was obtained with the filter-based method, but the concentration was about 20 percent lower.

The EEPS correlation was good, except for high load operations like Mode D (Peak Torque) and the ETC. The concentration reached a very high level during these engine operations and that may have contributed to the shift in the mass correlation due to the lack of good calibration with the EEPS at such a high concentration level. In some instances at two engine conditions, the instrument registered out of range.

The SMPS correlation was only applicable to steady-state operation. Like the EEPS, Mode D skewed the correlation. Mode D was the only mode where the concentration recorded by the CPC was over 10,000 part./cm3 and for some sizes it was out of the instrument range, above 100,000 part./cm3. Particle concentration below 5,000 part./cm3 is desired for accurate particle counts with the CPC in order to avoid correction for the probability of having two or more particles in the focused volume that may be counted as one particle. For a particle concentration above 10,000 part./cm3, the scattered light is correlated with particle concentration and that may not give accurate results as well.

For the purpose of demonstrating the improvement of correlation using the EEPS and the SMPS, Mode D and the ETC were both removed. For the DMM-230, Mode D and the ETC were also removed for representative comparison.

Figure 86 showed the improved correlation between the filter-based method and all three instruments, after removing the high load engine operation modes. All three instruments showed a better correlation with the filter-based method when Mode D and the ETC were removed.

It is important to note that the SMPS-based mass was derived from fitting a lognormal distribution to the calculated mass distribution from the measured data. All mass distributions for all engine operations were very well represented by a lognormal distribution. The reason a lognormal fit was needed is because the SMPS covered only a size range from 7 nm to 220 nm, while the EEPS covered a size range from 7 nm to 520 nm.

5.4.2 EEPS and SMPS

Data were accumulated with the EEPS and SMPS at steady-state over a wide range of engine operation. A difference between the number-weighted and the mass-weighted size distributions was observed. Figures 87 and 88 show the difference in the response of the two instruments at Mode A (Rated Power). Generally, the EEPS gave a higher particle number concentration in the ultrafine particle size range below 100 nm in diameter and a lower number concentration in the size range above 100 nm, as shown in Figure 87. Figure 88 indicates that on a mass weighting basis, the SMPS gave a higher mass in the range above 100 nm. A similar observation can be made for Mode D (Peak Torque) and Mode F (Idle), as shown Figures 89 and 90, respectively. However, the relative changes in particle mass between the two instruments seem to depend on engine operation.

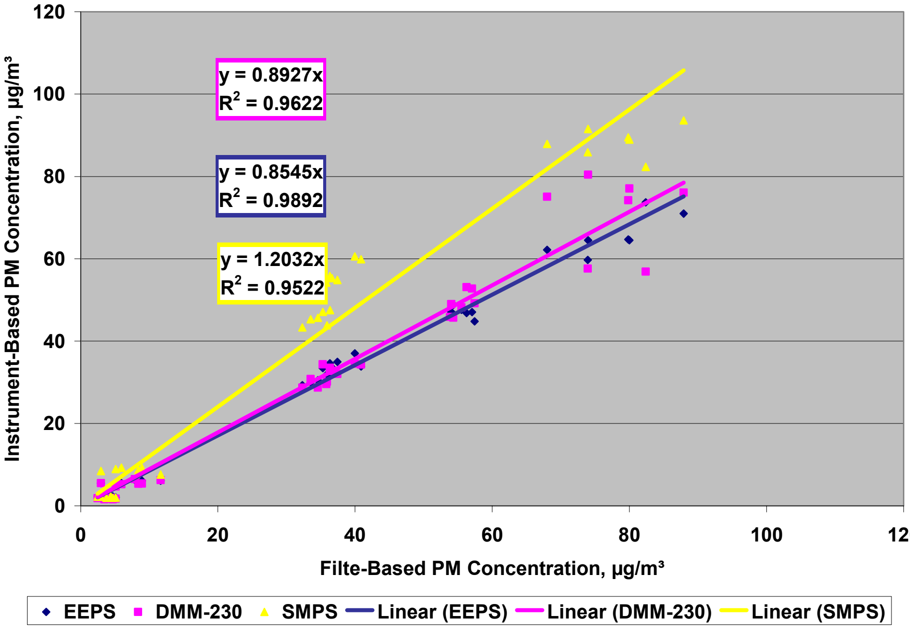

FIGURE 86. CORRELATION BETWEEN INSTRUMENT-BASED AND FILTER-BASED MEASUREMENT EXCLUDING MODE D AND THE ETC

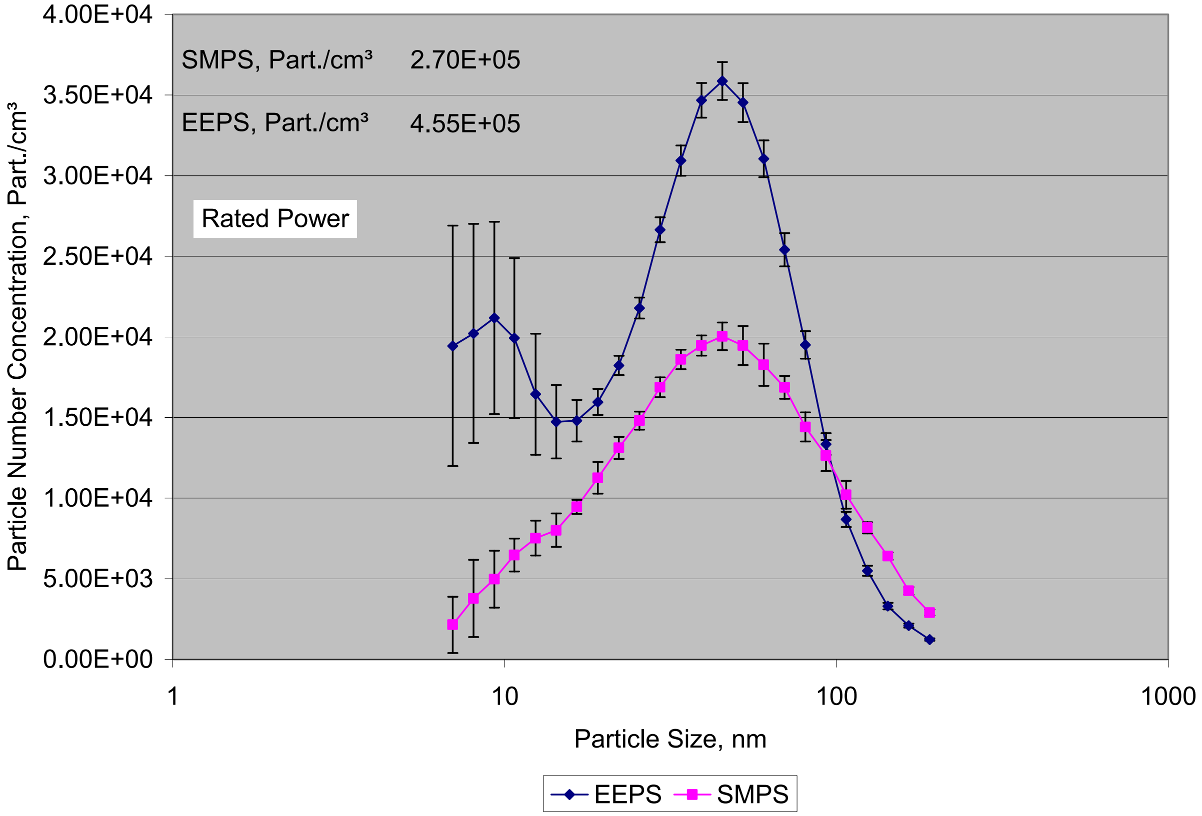

FIGURE 87. DIFFERENCE IN THE NUMBER-WEIGHTED SIZE DISTRIBUTION BETWEEN SMPS AND EEPS AT MODE A OF ENGINE OPERATION

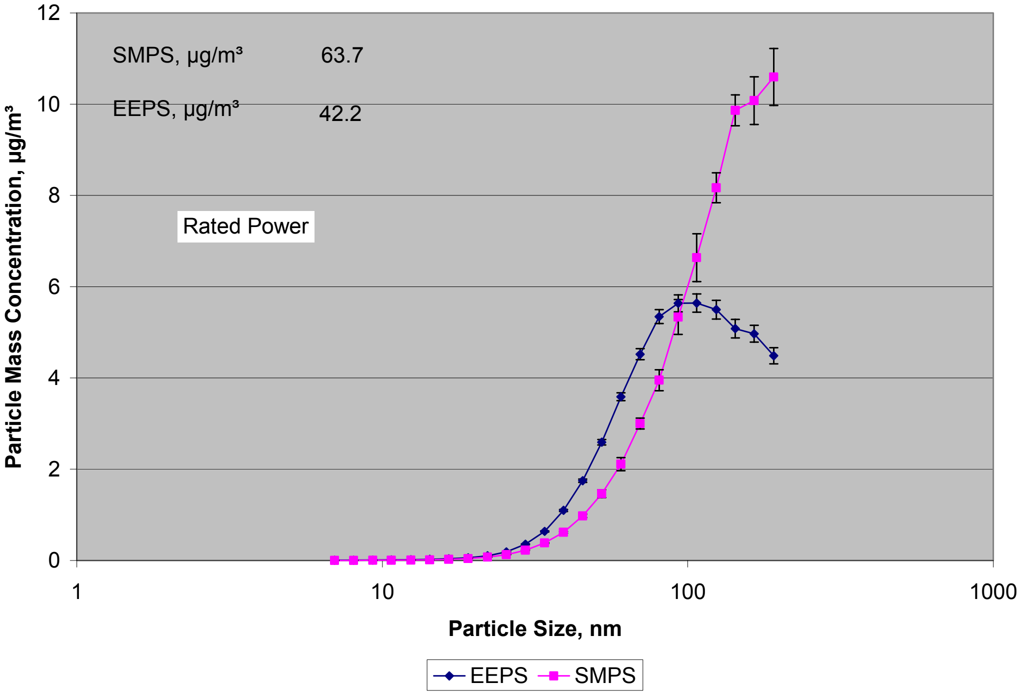

FIGURE 88. DIFFERENCE IN THE MASS-WEIGHTED SIZE DISTRIBUTION BETWEEN SMPS AND EEPS AT MODE A OF ENGINE OPERATION

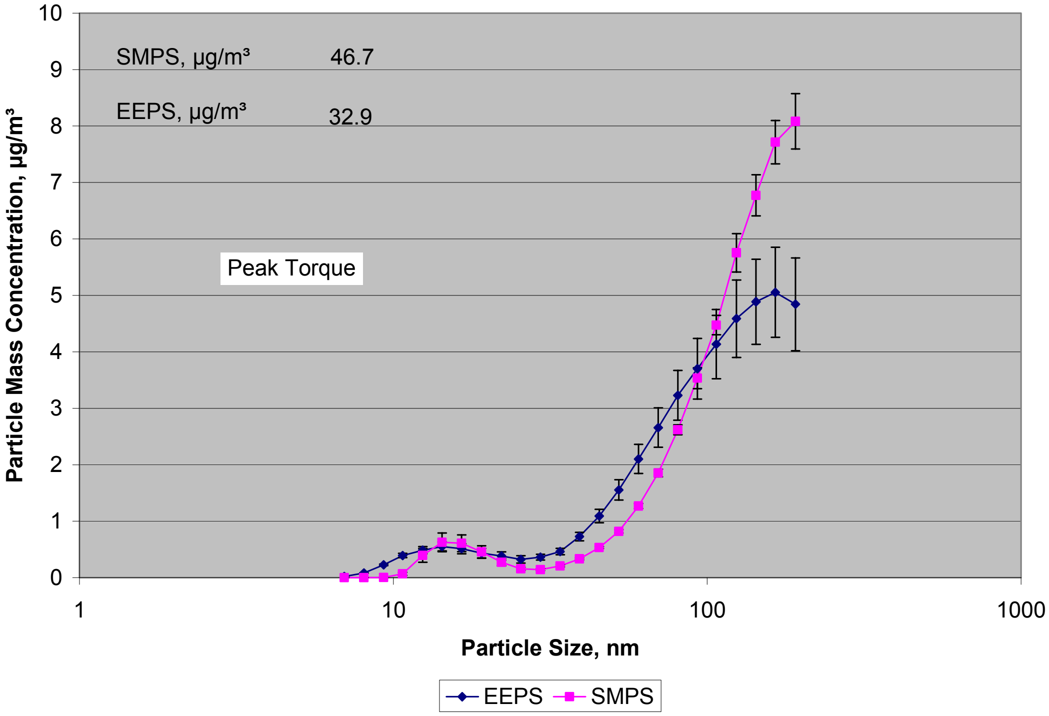

FIGURE 89. DIFFERENCE IN THE MASS-WEIGHTED SIZE DISTRIBUTION BETWEEN SMPS AND EEPS AT MODE D OF ENGINE OPERATION

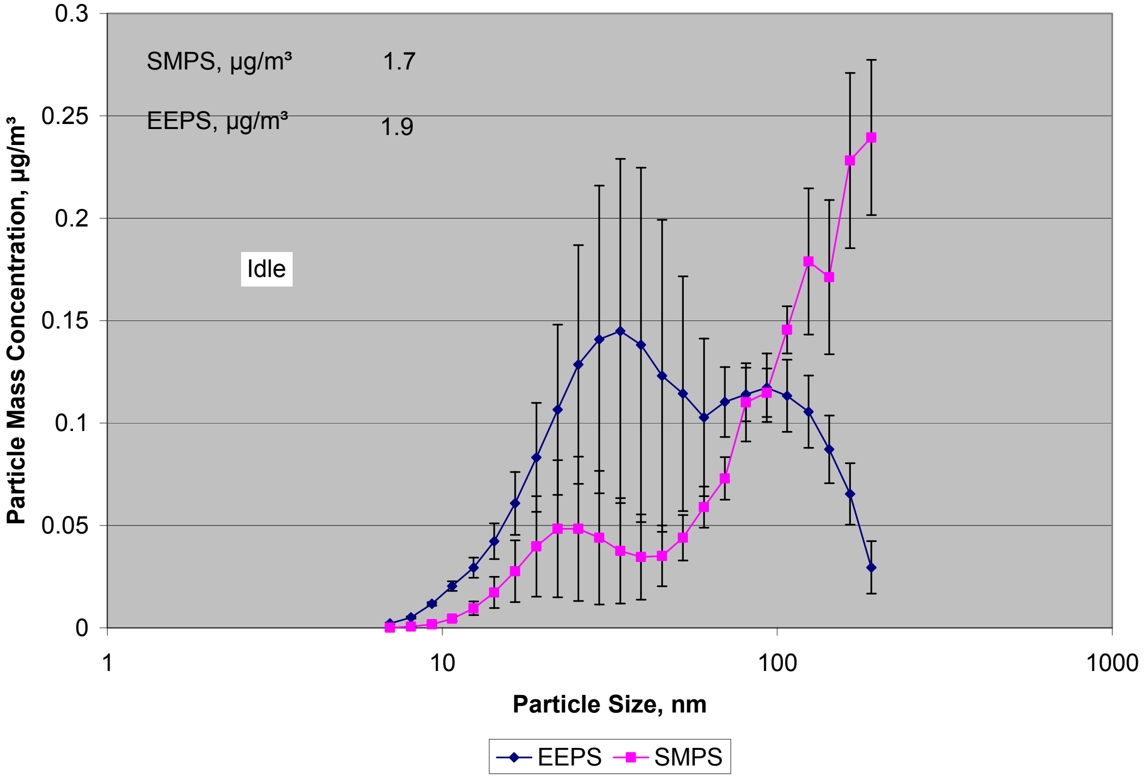

FIGURE 90. DIFFERENCE IN THE MASS-WEIGHTED SIZE DISTRIBUTION BETWEEN SMPS AND EEPS AT MODE F OF ENGINE OPERATION

The EEPS response time of 200 ms is much faster than the response time of the SMPS, which can be on the order of 2 seconds from inlet to detection for a single particle, and about 2 minutes for an entire size distribution. In addition, the EEPS is subject to very low particle losses and diffusion broadening of the size distribution because of the high polydisperse inlet flow, which is about 6 times higher than the SMPS, assuming an SMPS inlet flow of 1.5 lpm, and the very short residence time in the mobility section of the instrument (< 200 ms). This suggests that the EEPS should perform much better than the SMPS particularly in accurately capturing the nanoparticle particle concentration below 50 nm in diameter.

The difference between the two instruments can also be related to the way particle charging is implemented and predicted. In the SMPS, the minimum Boltzmann distribution of charge is achieved via a bipolar radioactive source. In the EEPS, the particles are exposed to positive ions to increase the charge level on them so the electrometer reads a higher signal. Such differences in particle charge conditioning between the two instruments may lead to the changes observed. Earlier limited work conducted by Johnson et al. [4] revealed similar information on the difference between the SMPS and the EEPS, but the differences were not clearly observed graphically because they were plotted on a log scale rather than a linear scale, as presented here.

More work is needed to settle the difference between the two instruments, but the EEPS advantage in providing real time size distribution of particles is a great advancement to understanding particle size dynamics under transient operation. Figure 91 shows the performance of EEPS and SMPS using a single size bin of 18 nm in diameter for the ETC transient cycle in the time window between 400 and 600 seconds. Certainly, the EEPS is capturing more changing events in the real time concentration profile compared to the SMPS.

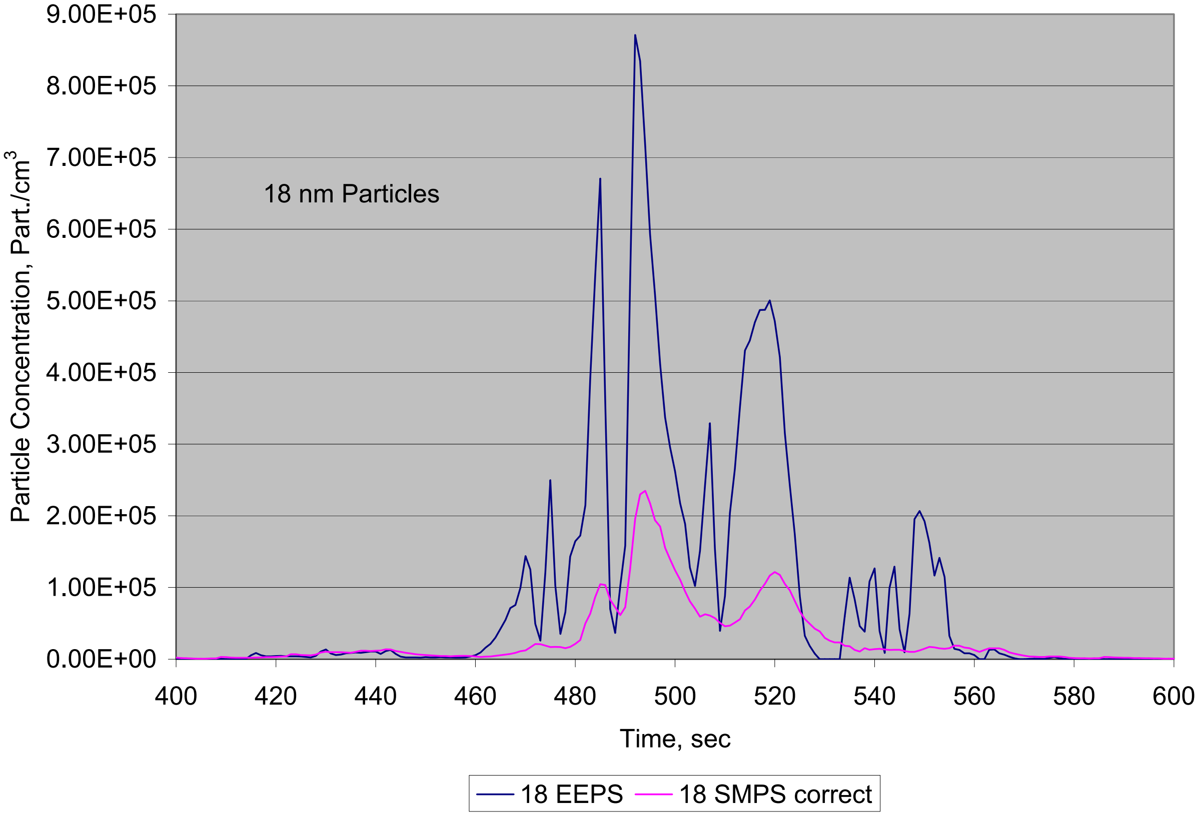

FIGURE 91. THE PERFORMANCE OF EEPS AND SMPS USING A TIME WINDOW DURING THE ETC

5.4.3 QCM Issues

The QCM was used during this study, but the data were not reported in more detail due to several factors. The QCM is very sensitive to changes in the sample flow temperature, pressure, relative humidity, and PM composition. The QCM response also depends on whether the crystal is coated or uncoated with vacuum grease. However, the main reason the data were not reported in more detail is because the instrument was reaching a saturation level under most engine operating conditions, particularly the high load engine operation and the transient cycles, due to the presence of solid particles. The presence of solid particles seemed to limit the amount of material that can be collected on the quartz crystal. Additional dilution to the QCM was required to lower the PM concentration and limit instrument saturation. This was not done in order avoid changes to the existing experimental setup, and continue to compare instrument performance at the same dilution ratio used for the filter-based method and other instruments.

Figure 92 shows the effect of inlet pressure and flow changes on the accumulated PM mass. A change in flow or pressure will affect the instrument, particularly if it is severe like the example shown in Figure 92.

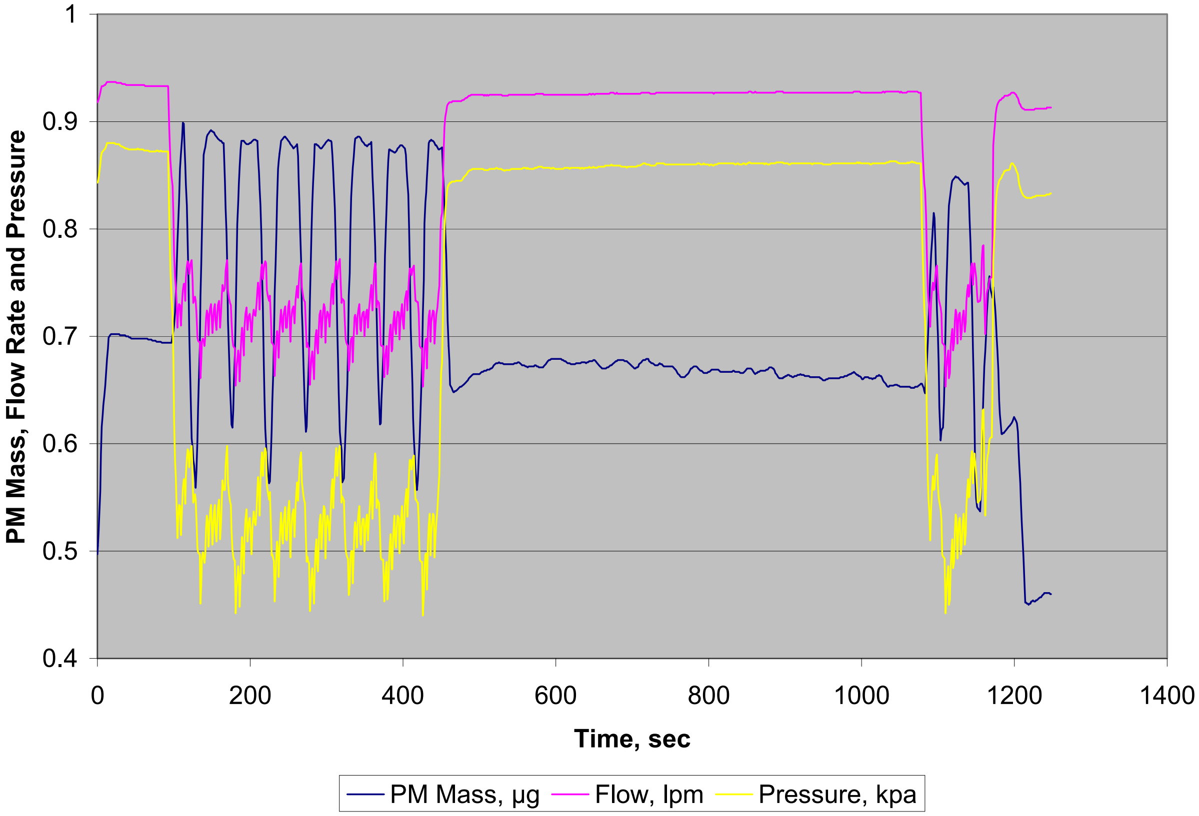

FIGURE 92. EFFECT OF FLOW AND INLET PRESSURE ON PM MASS MEASUREMENT BY THE QCM

Figure 93 shows an example of instrument saturation at different operating conditions. The presence of soot (in the sample line) seemed to limit the amount of mass that can be accumulated on the quartz crystal. At light load engine operation, where the concentration was lower and the nature of PM was different, the QCM seemed to respond properly in its mass accumulation against loading time. However, the mass concentration from Mode C and F measured by the QCM was at least twice as much as the filter-based and DMM-230-based mass concentration.

The quartz crystal is subject to gas phase adsorption just like the filter. The adsorption capacity and the surface area of quartz crystal are not known. However, it is very well known, based on previous experience and this work, that it is very sensitive to dew point changes.

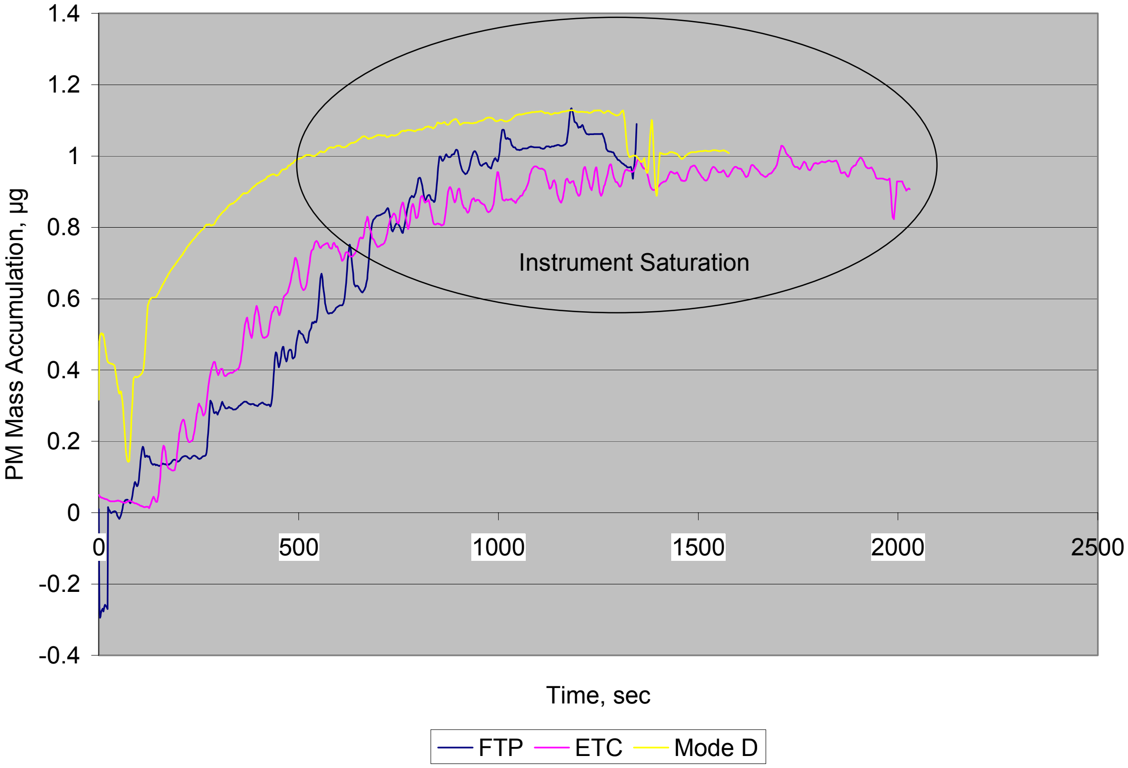

FIGURE 93. QCM SATURATION DUE TO THE PRESENCE OF SOOT PARTICLES AT HIGH LOAD

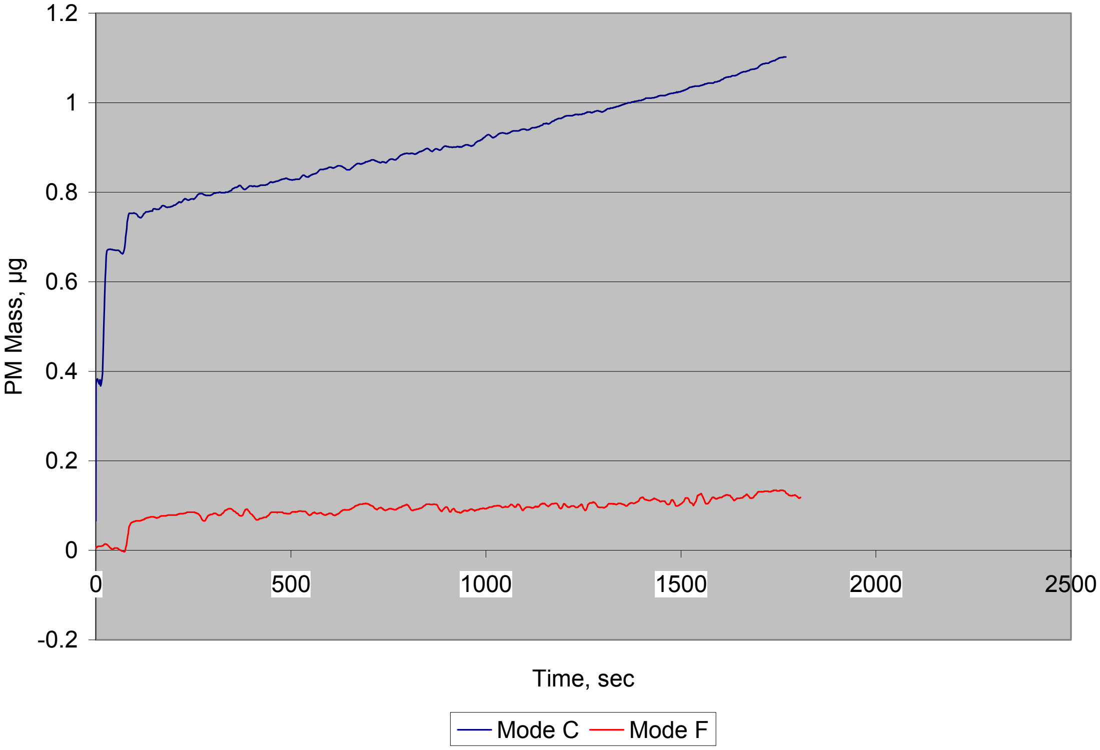

FIGURE 94. QCM PERFORMANCE AT LIGHT LOAD OF ENGINE OPERATION

6.0 CONCLUSIONS

Below are some of the important conclusions based on this work.

6.1 Carbon Denuder

- The use of the carbon denuder upstream of the filter used for PM collection was helpful in minimizing gas phase volatile compounds from depositing on the filter during sampling, but its performance was not consistent and repeatable, and it deteriorated with short running time.

- Attempts were made to regenerate the carbon denuder by supplying an inert gas stream at a temperature of about 400 °C, but the performance did not improve relative to its ability to remove volatile material from the gas phase with high efficiency.

- The use of the carbon denuder was abandoned early during this phase of the work. More research effort is needed to develop, test, and regenerate a carbon denuder. The carbon selectivity and carbon coating process need to be re-examined.

6.2 Filter Media

- This program was successful in demonstrating the ability to measure a clean filter weight with repeatability of better than ± 2.5 μg.

- No major difference in clean filter weight was observed over a range of different conditioning times in the weighing chamber. A 24-hour conditioning time prior to initial weighing seemed to be a safe practice to stabilize the filter weight using Teflo filters.

- The Teflo membrane filter media with a polymethylpentene (PMP) ring gave the least positive artifacts and the lowest coefficient of variation compared to TX-40 and other filter media tested.

- The Donaldson Teflon membrane filter with a Teflon ring gave a similar performance to the Pall Teflo and may be more suited for chemical analysis because of its inert ring. However, a detailed chemical analysis assessment to check the inertness of this filter will be needed.

- Teflo filter pre-baking in a vacuum oven for 24 hours at 52 °C resulted in a filter weight loss of about 7 μg. However, there was no difference in the performance between an unbaked and pre-baked Teflo filter for FTP transient PM measurements, using CRT-DPF with bypass.

6.3 Filter Face Velocity

- Higher filter face velocity resulted in lower PM emissions. For the FTP transient runs with a small exhaust bypass around the CRT-DPF, the PM was 25 percent lower at about 120 cm/sec, compared to 24 cm/sec. However, for Mode C (rated speed, very light load) of engine operation, more than a 60 percent reduction in measured PM was observed as a result of increasing the filter face velocity from about 24 cm/sec to 120 cm/sec.

- No notable additional difference in measured PM was observed between filter face temperatures of 47 °C and 25 °C when the filter face velocity changed.

  It is important to note, however, that all filter face velocity and temperature experiments were conducted with an exhaust configuration that included the CRT-DPF with the bypass. It is expected that the changes in filter face temperature may affect PM emissions at lower levels when a CRT-DPF is used without a bypass. This is mainly due to the expected changes in PM composition, changing from mainly elemental carbon with the bypass to being all volatile without the bypass.

- Gas phase adsorption and saturation of the filter may be responsible for the changes in PM mass collected at different filter face velocities. At a higher filter face velocity, but with the same dilution ratio, the filter may saturate in a shorter period of time during PM collection and reach equilibrium. When equilibrium is reached between the filter adsorption sites and the gas phase, additional sampling will contribute to the total volume sampled but not to additional PM adsorption of volatile material, thus lowering the measured PM concentration relative to the upstream PM concentration at the filter surface.

  The equilibrium phase may also be affected by soot accumulation on the filter. Soot accumulation may effectively change the filter media composition from being a Teflon membrane to a Teflon-Soot membrane which presents a unique properties and different adosorption capacity than a pure Teflon membrane.

- The effect of filter face velocity on PM emission measurement added further complication to the process of filter-based PM measurement. The effect of filter face velocity may be filter dependent, such that different filter media may result in different responses to filter face velocity, changing measured PM emissions.

6.4 Particle Instruments

- Good correlation was observed between the filter-based method and the DMM-230, EEPS, and SMPS. The correlation coefficient was better than 0.95. The DMM-230 gives information on real time particle mass and the EEPS gives information on real time particle number, size, and mass. The SMPS is limited to steady-state engine operation.

It is important to note, however, that this conclusion only applies to engine running with an exhaust bypass around the DPF, where solid particles are still contributing to PM emissions. It is not clear whether or not the same conclusion will hold when using DPF without bypass, where the PM emission is mainly volatile material.

- The real time instruments such as the DMM-230 and EEPS gave more robust information on PM emissions compared to the filter-based method, particularly at light-load engine operation. This was due to the variability associated in handling and weighing a very low PM mass (< 10 µg) collected by the filter.

- Inconsistency was found between the SMPS and the EEPS concentration and size distribution. While the trends were similar, the EEPS indicated a higher concentration in the ultrafine particle size range (< 100 nm) compared to the SMPS. Particle charge and response time differences between the two instruments may have led to such a discrepancy. The EEPS, however, has an advantage in its ability to provide size distributions every 200 ms. The EEPS provides new information and a better understanding of the dynamics of particle size and number emissions under steady-state and transient engine operation.

- The QCM did not perform in a consistent manner. The QCM reached saturation at medium and high engine loading due to the presence of solid particles. More work is needed to improve the instrument and make it more robust in measuring PM, particularly when both solid and volatile PM is present.

6.5 Engine Emissions

Using a Teflo filter media, engine and dilution system conditioning at rated engine power, and HEPA filters for the secondary dilution air, contributed to the measurement of very low PM emissions from a 1998 HDD engine equipped with a CRT-DPF. The emission level was below 0.001 g/hp-hr or 10 percent of the 2007 PM standard. Such impressive reduction in PM suggests that a high efficiency DPF like the one used in this program may not be needed to meet the 2007 PM standard. A DPF with lower efficiency may be acceptable. A lower efficiency DPF may have several benefits such as requiring fewer regeneration events, better durability, and lower backpressure that might provide fuel saving benefits.

It is important to note, however, that the engine used in this program meets only the 2007 PM standard and not the 2007 NO_x and PM standard. If this engine is to meet the 2007 NO_x and PM standard, a massive exhaust gas recirculation (EGR) level may be required. While it is known that EGR increases soot, it may also increase the emission of soluble organic compounds because of the low combustion temperature caused by EGR. Thus, the PM emission from an engine that meets the 2007 NO_x and PM standard may be different from the PM emission obtained in this work.

7.0 RECOMMENDATIONS

Several recommendations are made based on the work completed so far.

- It is recommended that Teflo membrane filters be used for PM emission measurement. In case chemical analysis is required, it is recommended that we explore the feasibility of using the Donaldson-based Teflon membrane filter with the Teflon ring.

- As a general practice, it is recommended that filters be weighed at least three consecutive times before and after testing in order to determine an average weight gain. This practice was very beneficial in getting a robust filter weight before and after testing.

- This work did not show a difference in performance between a pre-baked and unbaked filter Teflo filter media, using the CRT-DPF with exhaust bypass. Thus, it is recommended that filter pre-baking in a vacuum oven for 24 hours at 52 °C becomes optional for CRT-DPF with bypass or similar configurations like engine-out. It is still recommended that filters be baked when using a DPF without exhaust bypass.

- For this work it is also recommended that clean filters be conditioned for at least 24 hours in the weighing chamber before first weighing.

- Rubber, Tygon, Silicon, or any other non-inert tubing should not be used in any part of the exhaust and sampling system for filter-based PM measurement. Degassing of material from tube internal surface may lead to positive artifact and may introduce some foreign species to chemical analysis that may not be related to engine emissions.

- Engine and sampling system conditioning at rated engine power for a period of 10 minutes in between engine tests seems to provide more repeatable measurement of the PM emission. Phase 2 of Project E-66 will allow for a better quantification of the effect of conditioning on PM emission measurement.

- The allowable range for filter face velocity should be narrowed. In CFR Part 1065, the filter face velocity is specified to be below 100 cm/sec. A narrower definition such as 90 cm/sec ± 10 cm/sec will reduce lab-to-lab measurement variability for the FTP transient cycle.

  More work, however, is needed for a more complete understanding of the relationship between filter face velocity and filter loading, and their effect on volatile and solid PM collection on a filter.

- The DMM-230 compared well with the filter-based method. It is recommended that the DMM-230 be used on the remainder of Project E-66 to provide information on real time PM mass emission.

- The EEPS also compared well with the filter-based method. It is recommended that the EEPS be used on the remainder of Project E-66 to provide information on real time particle size, number, and mass emissions.

- Both the DMM-230 and the EEPS do not depend on PM accumulation history to provide real time PM emission information like the QCM and TEOM. The concentration reported by the DMM-230 and EEPS at time t_o is independent of the concentration at time t_o+ 1. Such measurement strategies will have a better chance in meeting real time on-vehicle measurement requirements because they are not sensitive to measurement artifact associated with adsorption and desorption of volatile material.

8.0 CLOSURE

Phase 1 of Project E-66 is completed. Future tasks will include investigating the influence of primary and secondary dilution ratio and residence time, and engine and dilution tunnel conditioning on PM measurement. It will also include investigating the performance of partial flow sampling systems relative to the CVS method. It may further include natural gas engine emission measurements and possibly gasoline engine work, even though gasoline PM measurement is not officially part of the E-66 current scope.

This work and the planned work should lead to better PM emission measurement and characterization from different engine sources.

9.0 REFERENCES

1- Code of Federal Regulations (CFR) 40, Part 86, 86.1310.2007.
2- Spears, Matt, "EPA's Heavy-Duty Diesel PM Changes and Other Mass Measurement Research," CRC Workshop on Vehicle Exhaust Particulate Emission Measurement Methodology, San Diego, CA, Oct. 2002.
3- Akard, M, K. Oestergaard, R. Chase, J. Richert, H. Fukushima, and M. Adachi,"Comparison of an Alternative Particulate Mass Measurement with Advanced Microbalance Analysis," SAE Paper 2004-01-0589, 2004.
4- Johnson, T., R. Caldow, A. Pocher, A. Mirme, and D. Kittelson, "A New Electrical Mobility Particle Sizer Spectrometer for Engine Exhaust Particle Measurements," SAE Paper 2004-01-1341, 2004.
5- Lehmann, U, V. Niemela, and M. Mohr,"New Method for Time-Resolved Diesel Engine Exhaust Particle Mass Measurement," Environ. Sci. Technol., 38 (21), 5704-5711, 2004.